



Research Article pubs.acs.org/journal/ascecg

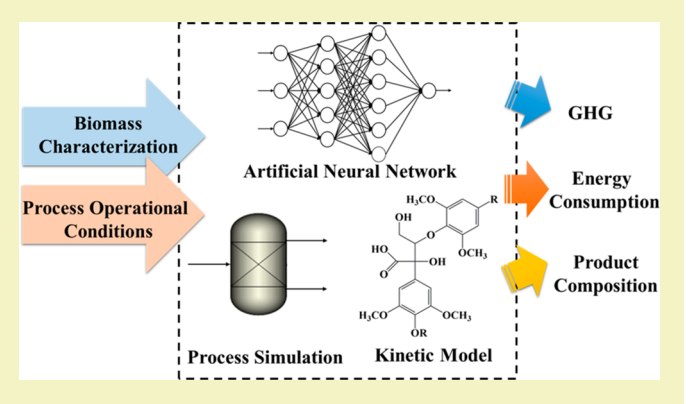
## Generating Energy and Greenhouse Gas Inventory Data of Activated Carbon Production Using Machine Learning and Kinetic Based **Process Simulation**

Mochen Liao, Stephen Kelley, and Yuan Yao\*

Department of Forest Biomaterials, North Carolina State University, Raleigh, North Carolina 27695, United States

Supporting Information

**ABSTRACT:** Understanding the environmental implications of activated carbon (AC) produced from diverse biomass feedstocks is critical for biomass screening and process optimization for sustainability. Many studies have developed Life Cycle Assessment (LCA) for biomass-derived AC. However, most of them either focused on individual biomass species with differing process conditions or compared multiple biomass feedstocks without investigating the impacts of feedstocks and process variations. Developing LCA for AC from diverse biomass is time-consuming and challenging due to the lack of process data (e.g., energy and mass balance). This study addresses these knowledge gaps by developing a modeling framework that integrates artificial neural network



(ANN), a machine learning approach, and kinetic-based process simulation. The integrated framework is able to generate Life Cycle Inventory data of AC produced from 73 different types of woody biomass with 250 characterization data samples. The results show large variations in energy consumption and GHG emissions across different biomass species (43.4-277 MJ/kg AC and 3.96-22.0 kg CO<sub>2</sub>-eq/kg AC). The sensitivity analysis indicates that biomass composition (e.g., hydrogen and oxygen content) and process operational conditions (e.g., activation temperature) have large impacts on energy consumption and GHG emissions associated with AC production.

KEYWORDS: Activated carbon, Biomass, Life Cycle Assessment, Machine learning, Artificial neural network, Kinetics, Process simulation

#### ■ INTRODUCTION

Activated carbon (AC) is a carbonaceous material with high porosity, absorptivity, and surface reactivity and has high valueadded applications in water purification, industrial processes, and flue gas cleanup. 1,2 AC also has many emerging applications such as functional materials used for electrode, catalyst, and carbon capture.<sup>3</sup> The worldwide consumption of AC was 12.8 million metric tons in 2015,4 and the annual growth rate of the AC market was projected as 6.31% from 2019 to 2024.5 AC can be produced from diverse carbonaceous sources such as coal (the main current source of commercial AC) and biomass (e.g., agricultural waste, wood, and herbaceous plants).3,6 Given a large number of potential feedstocks for AC production and rapid growth of AC demand, it is critical to understand the environmental implications of producing AC from alternative biomass feedstocks, especially given that AC production is one of the largest contributors to the overall environmental impacts of relevant technologies such as wastewater treatment based on previous Life Cycle Assessment (LCA) studies. 7-10 This understanding will enable more informed decision-making related to biomass selection, technology investment, process design, and optimization.

Many LCA studies evaluated the environmental implications of AC produced from diverse sources. A comprehensive literature review of previous studies is provided in Supporting Information (SI), section 1. The review indicates large variations in the environmental burdens associated with AC production from different biomass feedstocks (see Table S1). Given that most previous studies focused on a specific biomass feedstock, it is difficult to apply their results for other biomass feedstocks or make generic comparisons. 11-13 Developing LCAs for AC produced from a variety of biomass is challenging due to the lack of Life Cycle Inventory (LCI) data. Rapid and reliable estimation of LCI data for AC produced from diverse biomass sources is essential to screen different types of biomass feedstock and support early stage technology development and process design for sustainable AC production. It also significantly reduces the time and efforts needed for the gateto-gate LCI data collection for manufacturing processes that is usually the most time-consuming phase for LCA.<sup>14</sup> A few

Received: November 1, 2019 Revised: December 15, 2019 Published: December 17, 2019



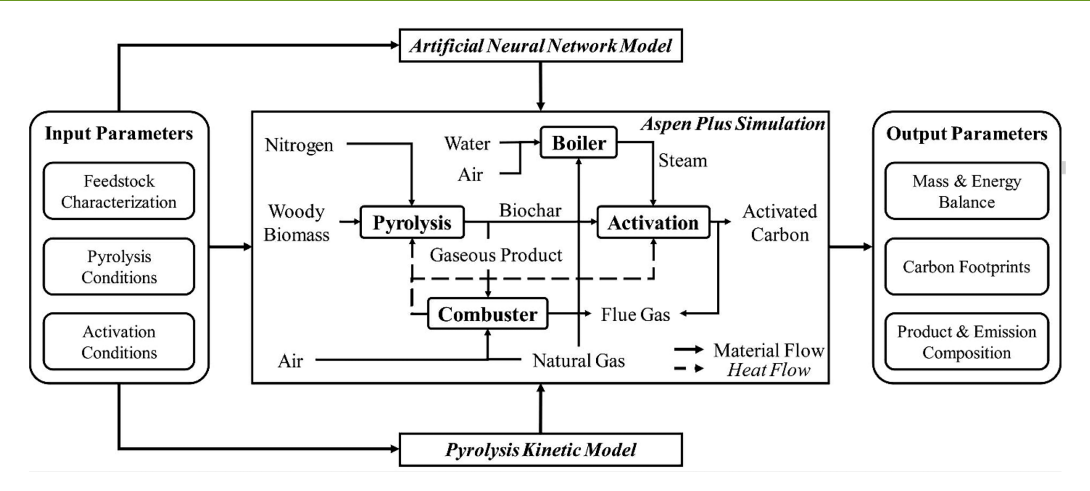


Figure 1. Schematic diagram of the integrated modeling framework in this study.

previous studies have investigated different approaches for the rapid generation of LCI data of production processes. For example, Parvatker and Eckelman<sup>15</sup> reviewed different methods that have been used for LCI estimation, such as process simulation tools, <sup>16,17</sup> process design calculations, <sup>18,19</sup> stoichiometry, proxy method, 20 molecular structure-based models,<sup>21</sup> and hybrid LCI.<sup>22,23</sup> Other studies have used other process simulations in conjunction with other techniques such as dynamic model,<sup>24</sup> kinetic model,<sup>25</sup> network approaches,<sup>26</sup> and knowledge-based models.<sup>27</sup> Applying previous approaches to estimate LCI for AC produced from diverse biomass feedstocks is challenging due to the lack of quantitative understandings of the relationships between LCI and large variations in biomass compositions and process operations, which are further discussed in the following two paragraphs. A few studies have tried to use machine learning (ML), a technique that does not rely on preknown knowledge, to directly generate LCI data<sup>21</sup> or environmental impacts.<sup>2</sup> However, these applications of ML techniques are limited to commercialized chemicals/products with abundant LCI data. Thus, it is challenging to apply ML alone to AC production that lacks LCI data for different biomass feedstocks.

Previous studies indicate that energy consumptions and greenhouse gas (GHG) emissions are mainly driven by the AC production stage that usually has large variations due to differences in the types and composition of biomass, process operational conditions, and sources of energy. 9,13 A few studies have tried to explore such variations by investigating AC production scenarios by varying process parameters. For example, Sepúlveda-Cervantes et al. conducted a gate-to-gate LCA of soybean shell-based AC production using zinc chloride activation.<sup>31</sup> By varying the operational conditions (i.e., activation temperature, time, and impregnation ratio), the electricity consumption of AC production changed from 17 to 50 MJ/kg AC, and the GHG emissions varied between 5.86 to 47.2 kg CO<sub>2</sub>-eq/kg AC.<sup>31</sup> Arena et al. analyzed the impacts of different energy sources on the environmental footprints of coconut shell AC, which showed a significant reduction of most environmental impact categories (60-80%) by using electricity from renewable sources. 12 For feedstock variations, most studies 13,32,33 developed LCA for individual biomass with a limited set of operational conditions then made a comparative analysis. To the best of the authors' knowledge, none of the previous studies have correlated LCA results with parameters related to biomass characteristics and process

operations. Thus, it is challenging to use previously developed LCA models to obtain quantitative understandings of the impacts of feedstocks and process variations or screen biomass and perform process optimization for AC production from an environmental perspective.

One additional, and significant, liability of many studies is that they have assumed a fixed composition for the gas and vapor product generated by the activation process, 11,12,31 whose accuracy cannot be ensured in the scenarios with varying feedstocks and operating conditions. The composition of these gas and vapor can have a significant effect on LCI. 11,12,31 The composition of gases and vapors will vary depending on both the composition of the starting biomass and operational conditions. 31,34

To address the gaps discussed above, this study integrated kinetic-based process simulation and artificial neural network (ANN), a machine learning approach, to estimate environmental footprints of AC produced from a variety of biomass feedstocks. Specifically, primary energy consumption and GHG emissions of AC production, two most commonly used indicators in previous LCAs for AC production, 11-13 were parametrized by process models that used large data sets collected from literature (e.g., ultimate analysis of biomass, in total 250 data samples) and predicted by ANN (e.g., total AC yield). As the focus is to demonstrate the functionality of the integrated framework in generating the LCI data for AC produced from different biomass, the system boundary of this work is gate-to-gate. This system boundary is also consistent with most of the previous LCAs of AC. 9-12,31-33,35-42 The influences of biomass feedstock characteristics were investigated by correlating the feedstock compositions with energy consumption and GHG emissions.

This study can be used for screening a diverse array of biomass feedstocks useful for AC production, enhancing options for feedstock selection, process design, and process optimization. Although this work focuses on AC production, the integration of ANN and kinetic-based based simulation can be applied to other production systems to generate LCI data for rapid LCA analysis, especially for emerging technologies whose LCI data is not available. These combined models will allow future research and production on biomass-based AC to clearly understand the environmental sustainability implications of their process choices. Furthermore, the sensitivity analysis was constructed to identify the key biomass properties and operational parameters driving the energy and GHG

emissions, which are valuable information for future process optimization and improvement.

#### MATERIALS AND METHODS

This study focuses on steam activation, a common technology for AC production.<sup>3</sup> The steam AC production process consists of two steps. In the first step, dried biomass is treated at high temperature (400-850 °C) and inert atmosphere in a slow pyrolysis process that produces solid biochar, syngas, and condensable bio-oil.<sup>2</sup> In the second step, the biochar is placed in a high-temperature reactor without air, and superheated steam is injected to activate the biochar. A series of complex chemical reactions are involved in both steps, and it is challenging to directly determine the yields and composition of the products of each step. Yet the yield and composition of the gases and vapors are required to estimate the energy consumption and GHG emissions of AC production.<sup>43</sup> To address this challenge, previous studies used either experiments or literature data for specific feedstocks with a limited set of activation conditions. 12,11 However, such data cannot be accurately extended to a broad array of different feedstocks. Although some recent studies tried to use ANN models to predict the LCI data or LCIA (life cycle impact assessment) results, <sup>21,28–30</sup> it is very challenging to use ANN alone to estimate the environmental burdens of AC production that does not have sufficient data samples for different biomass feedstocks and process operational conditions. This work addressed this challenge by first using kinetic-based process models to estimate pyrolysis yield and gas composition and then using trained ANN models to predict the activation yield, and Aspen Plus process simulation to generate gateto-gate LCI data such as energy consumption and air emissions (see Figure 1).45,

Three types of input parameters were used in this modeling framework, including biomass characterization (i.e., ultimate analysis data), pyrolysis conditions (i.e., temperature and reaction time), and activation conditions (i.e., steam to biochar mass ratio, activation time, and temperature). These data were used as the input of the ANN model to predict the total yield of AC production. The training process is detailed in our prior work.<sup>45</sup> This study focuses on woody biomass, given that it is one of the most abundant biomass resources in the world.<sup>47</sup> This also has the practical advantage of limiting the effects of ash, in particular active alkali, which can have a significant impact on the initial slow pyrolysis reactions and be significant in herbaceous or agricultural feedstocks. The data of ultimate analysis (a type of chemical analysis commonly used for biomass and fuels, it provides composition information such as the contents of carbon, hydrogen, and oxygen)<sup>48</sup> combined with the pyrolysis time and temperature were then used as the inputs to the pyrolysis kinetic model adapted from the previous study, 46 producing data on the quantity and composition of pyrolysis products. Both ANN and kinetic models were run independently, although they used the same data sets for biomass characterization and operational conditions. Then the data generated by the kinetic model (gas and solid products from pyrolysis) and ANN model (total AC yield) were used in an Aspen Plus process simulation that ultimately provided the energy and mass balance data needed to estimate the environmental burdens of AC. <sup>49</sup> A list of input and output parameters is provided in Table S2. As this study mainly focused on energy and GHG emissions, energy consumption and GHG in the gas products were mainly tracked for the process simulation. However, the integrated modeling framework is capable to provide the full list of inputs and outputs that can be used as LCI to estimate other environmental impact categories such as acidification and eutrophication that other researchers may be

**Pyrolysis Kinetic Model.** Many mechanistic studies have attempted to investigate biomass thermochemical conversion processes. Four types of mechanisms were commonly used, including (1) three-step reaction mechanism, (2) two-stage semiglobal reaction mechanism, (3) Broido-Shafizadeh reaction mechanism, and (4) multistep reaction mechanism (MSRM).<sup>50</sup> The MSRM framework was chosen in this study given its capability of predicting the

composition of the biochar solid and the product gases and vapors. <sup>50,51</sup> MSRM assumes that biomass is composed of the lignocellulosic components (i.e., cellulose, hemicellulose, and lignin) and thermal degradations happen on these components and derived products. Then the MSRM based model suggests a series of reactions, related to the decomposition of the individual biomass components, where the overall reaction rate can be determined by the kinetic equation shown in eq 1:

$$r = kT^n e^{-E/RT} (1)$$

where r is the rate of reaction, k is the pre-exponential factor, T is the reaction temperature, n is the exponential factor of temperature, E is the activation energy of the reaction, and E is the ideal gas constant. The E, E, and E are given for each reaction included in the MSRM model, E and thus the product compositions can be calculated based on a given combination of temperature, time and starting biomass composition. See Table S3 for parameter values associated with each reaction included in this model. In total, the kinetic model includes 5 reactions for cellulose, 10 for hemicellulose, 12 for lignin, 8 for metaplastic compounds, and 13 for gas-phase tar cracking.

In this study, the pyrolysis kinetic model was developed based on the MSRM model published in 2017. 46 Modifications were made by considering gas-phase tar cracking reactions and the differences between softwood and hardwood. 53,54 Extractive components of biomass were not considered in this study as previous studies indicated that the extractive content of woody biomass is generally low (1-5% for softwood and 2-8% for hardwood), and there is limited interaction between the reactions of these extractives and the bulk of the biomass.  $^{55-58}$  The triangulation method (see eqs 1–5 in the SI) was used to estimate the lignocellulosic composition of biomass (used as the inputs of MSRM) from the ultimate analysis data of biomass.<sup>58</sup> This method was used due to the lack of lignocellulosic composition data from the literature and database. It is recognized that the use of triangulation method may lead to some deviations, for example, the cellulose and hemicellulose in woody biomass perform similar elemental composition but different decomposition pathways.<sup>59</sup> This limitation can be addressed in the future when more lignocellulosic composition data is available. Even with this limitation, the pyrolysis yield of biochar generated by the kinetic model ranges from 20.8 to 39.1% that is well-aligned with industrial pyrolysis operations. 60,61

**Artificial Neural Network.** A key parameter needed by the Aspen Plus process simulation is the yield of AC. The MSRM kinetic model provides the yield of the intermediate biochar (pyrolysis yield), but it does not provide the final yield of AC from biochar (activation yield). In this study, the yield of the final AC product from the starting biomass (biomass yield) was estimated by using ANN as outlined in our prior work. The ANN model was trained using eight input variables, including five process variables (i.e., pyrolysis time, pyrolysis temperature, activation time, activation temperature, and steam to biochar ratio) and three biomass characterization variables (i.e., biomass carbon content, hydrogen content, and oxygen content). The output variable is the total AC yield based on the total biomass input of the entire AC production process. The ANN model demonstrated a high accuracy ( $R^2 = 0.971$ ) and showed high consistency with independent experimental data through an additional model validation step.

Aspen Plus Process Simulation. In this study, the process simulation model was developed using Aspen Plus (Aspen Plus V10) to generate energy and mass balances. The process flowsheets of pyrolysis and steam activation are provided in Figure S3 and S4, and the detailed model is shown in SI, section 2.3. One key parameter needed for the process simulation of steam activation is the activation yield that is defined as the AC produced divided by the total biochar input to the activation process. The activation yield could have large variations depending on the quantity and quality of biochar (that are driven by pyrolysis process and biomass feedstock) and process operational conditions. To take such variations into consideration, this study calculated the activation yield using eq 2, where the total AC yield is given by the ANN model and the pyrolysis yield of

biochar was provided by the kinetic model. The calculated activation yields range from 29.0 to 94.8%, which is consistent with the activation yields derived from literature. <sup>63</sup>

activation yield = 
$$\frac{\text{total AC yield}}{\text{pyrolysis yield of biochar}} \times 100\%$$
 (2)

In addition to the data provided by the ANN and kinetic models discussed previously, another key piece of information is the composition of flue gas coming from the steam activation. This gas needs to be counted as an air emission. Previous LCA studies have assumed that the only steam-carbon reaction occurs without  $\rm CO_2$  generation, which is not consistent with experimental measurements. Other reactions such as the water—gas shift reaction, methanation reactions, steam-reforming reactions, and the Boudouard reaction also occur. In this study, those reactions were considered by using the model from Martín-Gullón et al.  $^{66}$  as shown in eq 3.

$$C + \alpha H_2 O \rightarrow (2 - \alpha)CO + (\alpha - 1)CO_2 + \alpha H_2,$$
  
 $\alpha = 3.4690 - 0.0019T(K)$  (3)

The Aspen Plus database has property data, which can be used to model gas-phase reactions and estimate the reaction products including gases (e.g., hydrogen, methane, carbon monoxide and carbon dioxide) and vapors (e.g., alkanes, alkenes and oxygenates). <sup>67,68</sup> However, the property data for solid components (e.g., woody biomass, biochar, and AC), lignocellulosic components (e.g., cellulose, hemicellulose and lignin) and monosaccharides (e.g., glucose and xylose) are not included in Aspen databases. The relevant physical property parameters for lignocellulosic components and monosaccharides were collected from the literature. <sup>69</sup> For solid components, the thermodynamic data was calculated based on previous studies <sup>54,70</sup> and documented in SI, section 2.4. Key process parameters used in the Aspen Plus simulation are listed in Table 1.

Table 1. Key Process Parameters Used in the Process Simulation Model

parameter	value	ref
heat capacity of biomass feedstock $(J/(kg K))$	$1500 + T^a$	71
heat capacity of biochar and AC $(J/(kg K))$	$420 + 2.09T - 6.85 \times 10^{-4} T^{2a}$	71
pyrolysis gas residence time (s)	2	52
pyrolysis nitrogen gas mass flow	1/6 of feedstock mass flow	44
pyrolysis thermal efficiency (%)	90	72
combustor excess air rate (%)	30	12
pyrolysis nonsolid product combustion rate (%)	80	73
steam boiler thermal efficiency (%)	82	74
activation furnace thermal efficiency (%)	90	72
pyrolysis temperature (K) <sup>b</sup>	773	
pyrolysis time $(min)^b$	60	
activation temperature (K) <sup>b</sup>	1073	
activation time $(min)^b$	60	
steam to biochar ratio (kg/kg) <sup>b</sup>	2	

<sup>a</sup>T represents the absolute temperature in Kelvin. <sup>b</sup>These parameters were used in the sensitivity analysis with ranges provided in Table S5.

In this study, the natural gas was combusted in the combuster to provide the heat for pyrolysis and activation, given that natural gas is the most commonly used fuel type to supply heat in the U.S. manufacturing industry. A few studies used electricity to supply heat, but all of them were based on lab-scale AC production/experiments. II,31,36,39 Electricity could be used for ancillary facilities or purposes (e.g., process monitoring and control), but the electricity consumption for those purposes is generally negligible I3,33,35 and

needs to be assessed on a case-by-case basis given the specific equipment used. Thus, this study does not include ancillary electricity consumption and the primary energy consumption is reported in the form of natural gas. Meanwhile, all of the gaseous byproducts from the initial pyrolysis process were combusted with an 80% combustion rate to produce process energy. The combustion rate is the ratio of pyrolysis products that can be fully combusted, and 80% was used based on the ratio of unidentified and hard-to-combust substances of nonsolid pyrolysis products.<sup>73</sup> The energy content in the flue gases from the activation process are estimated to be minor, <sup>13</sup> so they were not combusted. To understand the impacts of energy recovery, scenarios with and without burning gas products were evaluated using energy recovery ratio (ERR) calculated by eq 4:

$$ERR = \frac{energy \, recovered}{total \, energy \, consumption} \times 100\% \tag{4}$$

Understanding the Impacts of Biomass Feedstock. To investigate the impact of the composition of the woody biomass feedstock, a large data set (250 data samples) containing the characterization data of woody biomass feedstocks was collected from Bioenergy Feedstock Library, <sup>76</sup> Phyllis2 database, <sup>77</sup> and the literature. <sup>78–112</sup> The entire data set is provided in Table S6. The Aspen Plus process simulation was run for each sample with the fixed operational conditions shown in Table 1, allowing for comparisons among different feedstocks, as well as an initial quantification of the variations in energy and GHG emissions for individual species of biomass sources. In addition, the sensitivity analysis was conducted to understand the impacts of varied biomass composition and operational conditions on the energy and GHG emissions of AC. The typical value and upper/lower bounds of all parameters were determined by the literature review and documented in Table S5. <sup>45,63,113–115</sup>

Fossil-based and biogenic GHG were tracked separately in this study given the debate of accounting biogenic GHG.  $^{116}$  Some studies set the characterization factor of biogenic CO $_2$  as zero according to the carbon-neutral assumption.  $^{13,117,118}$  Fossil-based GHG emissions were generated from burning natural gas that was assumed to be the sole fossil fuel used in the AC production.  $^{119}$  Biogenic GHG emissions were generated from both energy recovery (burning pyrolysis gas products) and the activation process (GHG as byproducts). Both fossil-based and biogenic GHGs were converted to the same unit (kg CO $_2$  eq/kg AC) by applying the latest 100-year Global Warming Potential (GWP) conversion factors from IPCC, which distinguishes methane from biogenic and fossil sources (the GWP conversion factor is 30 for fossil methane and 28 for biogenic methane).  $^{120}$ 

## ■ RESULTS AND DISCUSSION

Table 2 lists the average, minimum, maximum, and standard deviation (STD) for 250 data samples of different biomass feedstocks. These ranges are consistent with the results of previous LCA studies using woody biomass (Table S1). Some observations can be identified in Table 2. First, there are large variations in energy consumption and fossil-based/biogenic GHG emissions of steam AC production across different types of biomass. Second, although the average energy consumption and GHG emissions of softwood are higher than that of hardwood, there are large overlaps between the softwood and hardwood for the min-max results across all categories. The differences between hardwood and softwood could be more remarkable if more characterization data is available (e.g., textural properties, lignocellulose composition, morphology). Third, energy recovery reduces the primary energy consumption and fossil-based GHG emissions by burning gas byproducts as biogenic fuel sources (and as a result biogenic GHG emissions increase). The detailed LCI generated by this

Table 2. Variability in Primary Energy Consumption, Fossil-Based and Biogenic GHG Emissions

	softwood		hardwood		total		
	average (min-max)	STD <sup>a</sup>	average (min-max)	STD <sup>a</sup>	average (min-max)	STD <sup>a</sup>	
$E_{\rm NRE}$ (MJ/kg AC)	101(43-224)	32	88(43-277)	32	93(43-277)	33	
$E_{RE}$ (MJ/kg AC)	65(25-155)	23	57(23-208)	24	60(23-207)	24	
fossil GHG <sub>NRE</sub> (kg CO <sub>2</sub> -eq/kg AC)	8.7(4.2-18.8)	2.6	7.4(4.0-22)	2.4	7.9(4.0-22)	2.6	
fossil GHG <sub>RE</sub> (kg CO <sub>2</sub> -eq/kg AC)	4.0(1.7-9.3)	1.4	3.5(1.5-12)	1.4	3.7(1.5-12)	1.4	
biogenic GHG <sub>NRE</sub> (kg CO <sub>2</sub> -eq/kg AC)	5.1(2.7-12)	1.5	4.3(2.4-13)	1.4	4.6(2.4-13)	1.5	
biogenic $GHG_{RE}$ (kg $CO_2$ -eq/kg AC)	6.7(3.4-14)	1.9	5.9(3.4-16)	1.8	6.2(3.4-16)	1.9	

<sup>a</sup>STD: Standard deviation; RE: with energy recovery; NRE: without energy recovery.

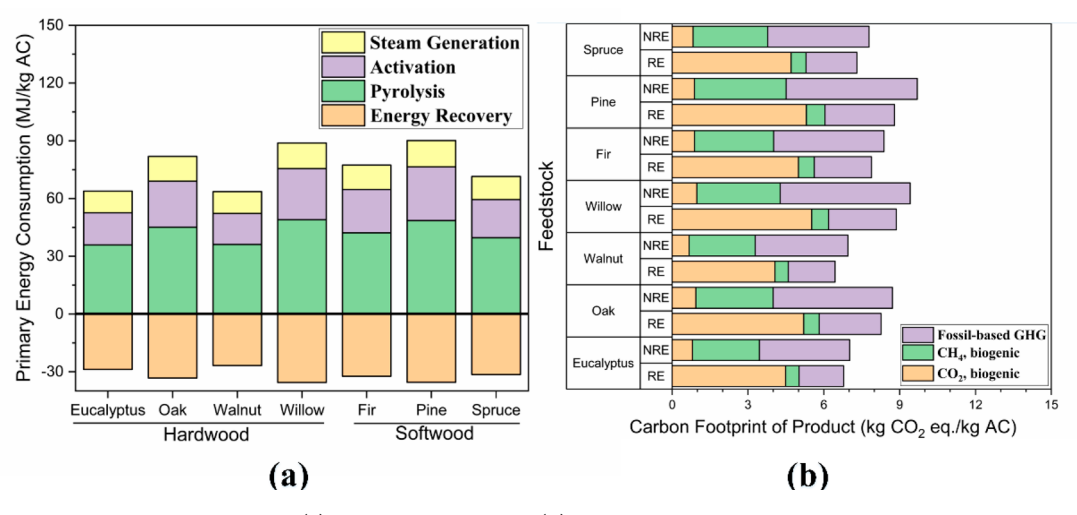


Figure 2. Average primary energy consumption (a) and carbon footprint (b) of steam AC production from different woody biomass species.

study for each of the 250 data samples were provided in the EXCEL file supplemented as one of the SI documents.

To understand the major contributors to both energy and GHG emissions results, the breakdown results of four types of common hardwood (i.e., eucalyptus, oak, walnut, and willow) and three types of common softwood (i.e., fir, pine, and spruce) were shown in Figure 2. Because more than one data sample of biomass characterization was collected from the literature, the average values of the results for each type of wood were shown.

In Figure 2a, the energy demand by different unit processes in the AC production is shown as positive and the energy recovered by burning flue gas is shown as negative. Figure 2a shows that across all different biomass species, pyrolysis has the largest energy demand (53–57% without energy recovery), which is consistent with the literature. <sup>33,38,44</sup> Across seven feedstocks, 72–80% of the pyrolysis energy consumption can be supplied by the energy recovered from flue gas, which is also consistent with the previous study (~75%). <sup>67</sup> For the entire AC production process, at most 45% of the primary energy consumption can be recovered by burning flue gas from pyrolysis, indicating the importance of including energy recovery in AC production.

Figure 2b shows the average results of the carbon footprint of AC production from seven types of woody biomass. The  ${\rm CO_2}$  and  ${\rm CH_4}$  from pyrolysis and steam activation as byproducts, and in the case of energy recovery from flue gas combustion of the pyrolysis gases, are considered as biogenic as the carbon is originally from biomass. Figure 2b shows that without energy recovery most of the GHG emissions were from natural gas combustion. When energy recovery from

pyrolysis gas combustion is included most of the GHG emissions come from biogenic sources. The biogenic carbon emission can be sequestrated by the regrowth of the plant, which was not included in this study as the carbon sequestration capacity of different wood species is highly variable and depends on regional climate and forest management practices. However, carbon sequestration could be easily incorporated into this framework in future work. Given the large contribution of biogenic carbon in the results (69–74%) it is clear that the GHG emissions of AC production with energy recovery will be much lower if carbon sequestration from biomass is included.

To further understand the impacts of biomass feedstocks on AC production energy and carbon footprints, the results of 250 data samples were plotted with different biomass compositions (see Table S6). The results indicated that hydrogen content and hydrogen/carbon ratio (H/C ratio) are two parameters strongly correlated with GHG emissions (Figures S6-S7) and primary energy consumption as shown in Figure 3a,b. For both softwood and hardwood, increasing the hydrogen content increases the primary energy consumption, except for a few samples that show decreased energy consumption with hydrogen content higher than 6.5%. Since the carbon contents for these outliers are relatively higher than other data samples, Figure 3b plots energy consumption and H/C ratio to eliminate the influence of the carbon content, which shows similar trends as Figure 3a but with a more scattered distribution of results. The results of the scenario without energy recovery have similar trends and shown in Figure S7.

The large impacts of hydrogen and H/C ratios can be explained by their impacts on the AC yields. A high H/C ratio

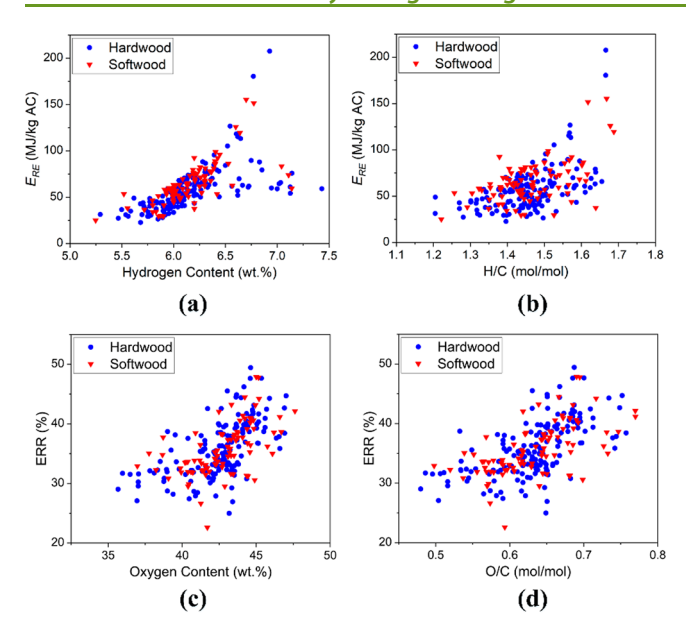


Figure 3. Impacts of feedstock characteristics on the primary energy consumption ((a) hydrogen content and (b) hydrogen to carbon ratio) and energy recovery ratio ((c) oxygen content and (d) oxygen to carbon ratio).

in biomass feedstock usually indicates a lower percentage of aromatic carbon, which may lead to low AC yields given the important role of aromatic carbon in steam activation. <sup>2,121</sup> Such information could be helpful for future biomass selection and process design, it also demonstrates the unique capability of the modeling framework presented in this study.

A similar approach was applied to ERR, the indicator of energy recovery (see Figure S9). Two parameters, oxygen content and O/C ratio, show correlations with ERR as shown in Figure 3c,d. For both hardwood and softwood, the higher oxygen content of biomass or atomic O/C ratio, the higher ERR in the steam AC production process. This higher O/C ratio is indicative of higher carbohydrate content, and hemicellulose in particular are known to be less stable and generate more gas and vapor products under pyrolysis conditions. Thus, feedstocks with higher O/C ratios will produce more gases and vapors that are important for energy recovery. Based on the discussion above, one conclusion is that choosing biomass with lower hydrogen contents, H/C ratio, and higher oxygen contents, O/C ratio is beneficial from energy and GHG emissions perspectives.

In addition to biomass characteristics, another set of parameters that have large impacts on pyrolysis and steam activation processes are operational conditions. To understand the impacts of these parameters, a sensitivity analysis was performed using the ranges shown in Table S5 and the results for primary energy consumption and biogenic GHG emissions are shown in Figure 4 (see Figure S10 for the results without energy recovery and the results for fossil-based GHG emissions). Figure 4 indicates that among different biomass characteristics, hydrogen content and ash content are both important. The importance of hydrogen is already discussed previously. The effects of ash are complex. Active alkali ash species (e.g., sodium, potassium, calcium, etc.) can impact the decomposition of the biomass carbohydrate fraction in particular during the pyrolysis process, which in turn will affect the ratio of biochar to pyrolysis vapors and thus the final AC yield will also be affected. 123

Among different operating parameters, the activation temperature has the greatest impact. This is due to its large impact on the final AC yield, and associated heat duty on the furnace and boiler. In general, choosing biomass with low hydrogen contents and setting the low temperature for steam activation and pyrolysis processes are beneficial from energy and GHG emissions perspectives.

There are some limitations of the modeling framework presented in this study. While understanding the primary energy consumption and GHG emissions for AC production are useful, the AC product must meet a series of performance specifications demanded by the market. For example, the adsorption capacity of AC is a key parameter determining the effectiveness of applications such as contamination removal in water and associated prices. This parameter was not included in this study due to the lack of data. The authors previously published a study that used ANN to predict the BET surface area of AC, which could be used as an initial proxy of the adsorption capacity of AC.<sup>45</sup> In that study, a contribution analysis was conducted to understand the impacts of variations in feedstocks and process operations on the yields and BET surface area of AC produced. The results indicated that both yields and BET surface area of AC are highly driven by the variations of feedstock compositions (e.g., ash and carbon content) and operational conditions of steam activation (e.g., activation temperature and steam to carbon ratio). Depending on the applications, other performance specifications may be expected for AC such as iodine number and methylene blue index. 124 Previous literature indicated that these specifications are affected by process and feedstock variations, which could

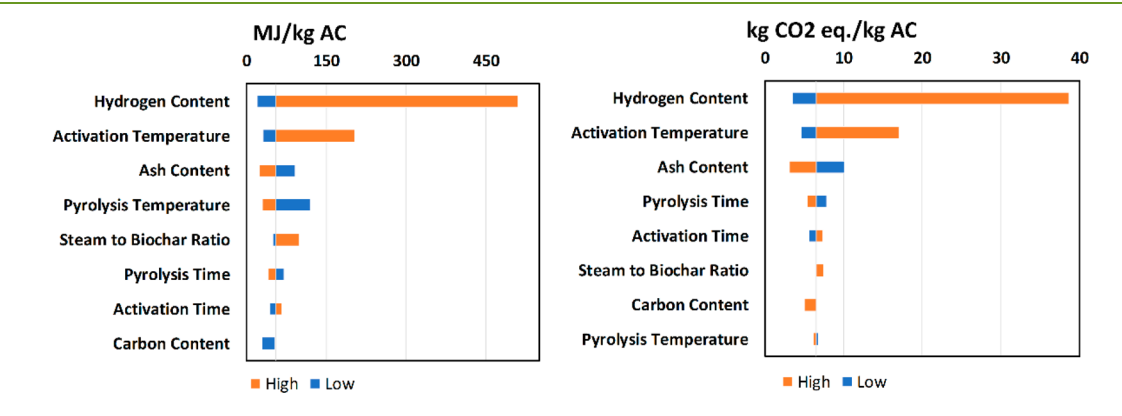


Figure 4. Sensitivity analysis for the energy consumption and biogenic GHG emissions (with energy recovery) of the steam AC production process

be the future research direction for the authors if sufficient experimental data are available. Another limitation is the procedure used to estimate the quality and heating value of the intermediate pyrolysis gases, which could be further improved with the improvement of pyrolysis kinetic models in the future. Finally, this study does not include other biomass-related parameters such as particle size due to their relative low impacts on the results based on previous studies. In addition, the oven-dried biomass used in the present study avoided the influence of the moisture content, which may have some impact and needs additional clarification when evaluating the cradle-to-gate AC production process that is a larger system boundary than this gate-to-gate study. This limitation can be addressed by adding additional drying processes in future work.

In conclusion, this work developed a modeling framework that integrates ANN and kinetic-based process simulation models to estimate the gate-to-gate primary energy consumption and GHG emissions across a variety of woody biomass. The LCI generated by the integrated models can be used as data sources for future LCAs of AC or industrial systems using AC materials. To understand opportunities for reducing energy consumption and GHG emissions from AC production, the key driving factors were identified and the impacts of variations were quantified. Furthermore, the results of this study indicated the importance of feedstock selection and operation of AC production from an environmental sustainability perspective. Both the results and modeling framework can be used by engineers and project managers to select biomass feedstocks and improve process operations. Although this study focused on woody biomass and AC production, the modeling framework can be applied to other types of biomass and other biomass utilization technologies. The ranges and distributions of the primary energy consumption and GHG emissions estimated in this study can also be used as transparent and reliable data sources for future LCA and Techno-Economic Assessment.

#### ASSOCIATED CONTENT

## **S** Supporting Information

The Supporting Information is available free of charge at https://pubs.acs.org/doi/10.1021/acssuschemeng.9b06522.

Detailed information on literature review, modeling framework and settings, feedstock data set, additional results, and references (PDF)

Detailed Life Cycle Inventory generated for AC production using different biomass species (XLSX)

## **■** AUTHOR INFORMATION

#### **Corresponding Author**

\*Phone: (919)-515-8957. E-mail: Yuan\_Yao@ncsu.edu.

ORCID

Yuan Yao: 0000-0001-9359-2030

Notes

The authors declare no competing financial interest.

#### ACKNOWLEDGMENTS

The authors thank the funding support from the Department of Forest Biomaterials at North Carolina State University and the U.S. National Science Foundation. This material is based upon work supported by the National Science Foundation under Grant No. (1847182). Any opinions, findings, and conclusions or recommendations expressed in this material are those of the author(s) and do not necessarily reflect the views of the National Science Foundation.

#### REFERENCES

- (1) Suhas; Gupta, V. K.; Carrott, P. J. M.; Singh, R.; Chaudhary, M.; Kushwaha, S. Cellulose: A Review as Natural, Modified and Activated Carbon Adsorbent. *Bioresour. Technol.* **2016**, 216, 1066–1076.
- (2) Yahya, M. A.; Al-Qodah, Z.; Ngah, C. W. Z. Agricultural Bio-Waste Materials as Potential Sustainable Precursors Used for Activated Carbon Production: A Review. *Renewable Sustainable Energy Rev.* **2015**, *46*, 218–235.
- (3) Tan, X.; Liu, S.; Liu, Y.; Gu, Y.; Zeng, G.; Hu, X.; Wang, X.; Liu, S.; Jiang, L. Biochar as Potential Sustainable Precursors for Activated Carbon Production: Multiple Applications in Environmental Protection and Energy Storage. *Bioresour. Technol.* **2017**, 227, 359–372
- (4) Transparency Market Research. Activated Carbon Market (Powdered, Granular) for Liquid Phase and Gas Phase Applications Global Industry Analysis, Size, Share, Growth, Trends and Forecast, 2013–2019; Albany, NY, 2013.
- (5) Mordor Intelligence. Activated Carbon Market Growth, Trends, and Forecast (2019–2024); Hyderabad, India, 2019.
- (6) Mohammad-Khah, A.; Ansari, R. Activated Charcoal: Preparation, Characterization and Applications: A Review Article. *Int. J. ChemTech Res.* **2009**, *1* (4), 859–864.
- (7) Thompson, K. A.; Shimabuku, K. K.; Kearns, J. P.; Knappe, D. R. U.; Summers, R. S.; Cook, S. M. Environmental Comparison of Biochar and Activated Carbon for Tertiary Wastewater Treatment. *Environ. Sci. Technol.* **2016**, *50* (20), 11253–11262.
- (8) Bonton, A.; Bouchard, C.; Barbeau, B.; Jedrzejak, S. Comparative Life Cycle Assessment of Water Treatment Plants. *Desalination* **2012**, 284, 42–54.
- (9) Jeswani, H. K.; Gujba, H.; Brown, N. W.; Roberts, E. P. L.; Azapagic, A. Removal of Organic Compounds from Water: Life Cycle Environmental Impacts and Economic Costs of the Arvia Process Compared to Granulated Activated Carbon. *J. Cleaner Prod.* **2015**, *89*, 203–213
- (10) Muñoz, I.; Peral, J.; Antonio Ayllón, J.; Malato, S.; José Martin, M.; Yves Perrot, J.; Vincent, M.; Domènech, X. Life-Cycle Assessment of a Coupled Advanced Oxidation-Biological Process for Wastewater Treatment: Comparison with Granular Activated Carbon Adsorption. *Environ. Eng. Sci.* **2007**, *24* (5), 638–651.
- (11) Hjaila, K.; Baccar, R.; Sarrà, M.; Gasol, C. M.; Blánquez, P. Environmental Impact Associated with Activated Carbon Preparation from Olive-Waste Cake via Life Cycle Assessment. *J. Environ. Manage.* **2013**, 130, 242–247.
- (12) Arena, N.; Lee, J.; Clift, R. Life Cycle Assessment of Activated Carbon Production from Coconut Shells. *J. Cleaner Prod.* **2016**, *125*, 68–77.
- (13) Gu, H.; Bergman, R.; Anderson, N.; Alanya-Rosenbaum, S. Life Cycle Assessment of Activated Carbon From Woody Biomass. *Wood Fiber Sci.* **2018**, *50* (3), 1–15.
- (14) Liu, Y.; Syberfeldt, A.; Strand, M. Review of Simulation-Based Life Cycle Assessment in Manufacturing Industry. *Prod. Manuf. Res.* **2019**, *7* (1), 490–502.
- (15) Parvatker, A. G.; Eckelman, M. J. Comparative Evaluation of Chemical Life Cycle Inventory Generation Methods and Implications for Life Cycle Assessment Results. *ACS Sustainable Chem. Eng.* **2019**, 7 (1), 350–367.
- (16) Montazeri, M.; Eckelman, M. J. Life Cycle Assessment of Catechols from Lignin Depolymerization. *ACS Sustainable Chem. Eng.* **2016**, *4* (3), 708–718.
- (17) Smith, R. L.; Ruiz-Mercado, G. J.; Meyer, D. E.; Gonzalez, M. A.; Abraham, J. P.; Barrett, W. M.; Randall, P. M. Coupling Computer-Aided Process Simulation and Estimations of Emissions

- and Land Use for Rapid Life Cycle Inventory Modeling. ACS Sustainable Chem. Eng. 2017, 5 (5), 3786–3794.
- (18) Parvatker, A. G.; Tunceroglu, H.; Sherman, J. D.; Coish, P.; Anastas, P.; Zimmerman, J. B.; Eckelman, M. J. Cradle-to-Gate Greenhouse Gas Emissions for Twenty Anesthetic Active Pharmaceutical Ingredients Based on Process Scale-Up and Process Design Calculations. ACS Sustainable Chem. Eng. 2019, 7 (7), 6580–6591.
- (19) Yao, Y.; Masanet, E. Life-Cycle Modeling Framework for Generating Energy and Greenhouse Gas Emissions Inventory of Emerging Technologies in the Chemical Industry. *J. Cleaner Prod.* **2018**, *172*, 768–777.
- (20) Song, R.; Keller, A. A.; Suh, S. Rapid Life-Cycle Impact Screening Using Artificial Neural Networks. *Environ. Sci. Technol.* **2017**, *51* (18), 10777–10785.
- (21) Wernet, G.; Hellweg, S.; Fischer, U.; Papadokonstantakis, S.; Hungerbühler, K. Molecular-Structure-Based Models of Chemical Inventories Using Neural Networks. *Environ. Sci. Technol.* **2008**, 42 (17), 6717–6722.
- (22) Crawford, R. H.; Bontinck, P. A.; Stephan, A.; Wiedmann, T.; Yu, M. Hybrid Life Cycle Inventory Methods A Review. *J. Cleaner Prod.* **2018**, *172*, 1273—1288.
- (23) Suh, S.; Huppes, G. Missing Inventory Estimation Tool Using Extended Input-Output Analysis. *Int. J. Life Cycle Assess.* **2002**, *7* (3), 134–140.
- (24) Bisinella de Faria, A. B.; Spérandio, M.; Ahmadi, A.; Tiruta-Barna, L. Evaluation of New Alternatives in Wastewater Treatment Plants Based on Dynamic Modelling and Life Cycle Assessment (DM-LCA). *Water Res.* **2015**, *84*, 99–111.
- (25) De Oliveira, L. P.; Hudebine, D.; Guillaume, D.; Verstraete, J. J. A Review of Kinetic Modeling Methodologies for Complex Processes. *Oil Gas Sci. Technol.* **2016**, *71* (3), 45.
- (26) Fahmi, I.; Cremaschi, S. Process Synthesis of Biodiesel Production Plant Using Artificial Neural Networks as the Surrogate Models. *Comput. Chem. Eng.* **2012**, *46*, 105–123.
- (27) Bugaeva, L. N.; Beznosik, Y. A.; Statjukha, G. A.; Kvitka, A. A. An Application of Expert System to Choice, Simulation and Development of Gases Purification Processes. *Comput. Chem. Eng.* 1996, 20 (S1), S401–S406.
- (28) Nabavi-Pelesaraei, A.; Rafiee, S.; Mohtasebi, S. S.; Hosseinzadeh-Bandbafha, H.; Chau, K.-w. Integration of Artificial Intelligence Methods and Life Cycle Assessment to Predict Energy Output and Environmental Impacts of Paddy Production. *Sci. Total Environ.* **2018**, 631–632, 1279–1294.
- (29) Kaab, A.; Sharifi, M.; Mobli, H.; Nabavi-Pelesaraei, A.; Chau, K.-w. Combined Life Cycle Assessment and Artificial Intelligence for Prediction of Output Energy and Environmental Impacts of Sugarcane Production. *Sci. Total Environ.* **2019**, *664*, 1005–1019.
- (30) Song, R. Machine Learning for Addressing Data Deficiencies in Life Cycle Assessment, University of Santa Barbara: Santa Barbara, CA, 2019.
- (31) Sepúlveda-Cervantes, C. V.; Soto-Regalado, E.; Rivas-García, P.; Loredo-Cancino, M.; Cerino-Córdova, F. d. J.; García Reyes, R. B. Technical-Environmental Optimisation of the Activated Carbon Production of an Agroindustrial Waste by Means Response Surface and Life Cycle Assessment. *Waste Manage. Res.* **2018**, 36 (2), 121–130
- (32) Manda, B. M. K.; Worrell, E.; Patel, M. K. Innovative Membrane Filtration System for Micropollutant Removal from Drinking Water Prospective Environmental LCA and Its Integration in Business Decisions. *J. Cleaner Prod.* **2014**, *72*, 153–166.
- (33) Kim, M. H.; Jeong, I. T.; Park, S. B.; Kim, J. W. Analysis of Environmental Impact of Activated Carbon Production from Wood Waste. *Environ. Eng. Res.* **2019**, 24 (1), 117–126.
- (34) Loya-González, D.; Loredo-Cancino, M.; Soto-Regalado, E.; Rivas-García, P.; Cerino-Córdova, F. de J.; García-Reyes, R. B.; Bustos-Martínez, D.; Estrada-Baltazar, A. Optimal Activated Carbon Production from Corn Pericarp: A Life Cycle Assessment Approach. *J. Cleaner Prod.* **2019**, 219, 316–325.

- (35) Kim, M.; Kim, G. Life Cycle Assessment of Activated Carbon Production System by Using Poplar. *J. Korean Soc. Environ. Eng.* **2014**, 36 (11), 725–732.
- (36) Sharifan, S. A Comparative Optimization Study of Activated Carbon Production from Hazelnut Shells by Thermal and Microwave Heating Methods, Imperial College London, 2013.
- (37) Joy Hung, J. The Production of Activated Carbon from Coconut Shells Using Pyrolysis and Fluidized Bed Reactors. 2012.
- (38) Campo, B. G. Production of Activated Carbon from Fast Pyrolysis Biochar and the Detoxification of Pyrolytic Sugars for Ethanol Fermentation, Iowa State University, 2015.
- (39) Heidari, A.; Khaki, E.; Younesi, H.; Ray, H. Evaluation of Fast and Slow Pyrolysis Methods for Bio-Oil and Activated Carbon Production from Eucalyptus Wastes Using a Life Cycle Assessment Approach. *J. Cleaner Prod.* **2019**, 241, 118394.
- (40) Bayer, P.; Heuer, E.; Karl, U.; Finkel, M. Economical and Ecological Comparison of Granular Activated Carbon (GAC) Adsorber Refill Strategies. *Water Res.* **2005**, *39* (9), 1719–1728.
- (41) Markus Andreas, M. Eco-Efficiency Evaluation of Waste Gas Purification Systems in the Chemical Industry; Swiss Federal Institute of Technology Zurich, 1997.
- (42) Gabarrell, X.; Font, M.; Vicent, T.; Caminal, G.; Sarrà, M.; Blánquez, P. A Comparative Life Cycle Assessment of Two Treatment Technologies for the Grey Lanaset G Textile Dye: Biodegradation by Trametes Versicolor and Granular Activated Carbon Adsorption. *Int. J. Life Cycle Assess.* 2012, 17 (5), 613–624.
- (43) Kodera, Y.; Kiho, M. Model Calculation of Heat Balance of Wood Pyrolysis. *J. Inst. Energy* **2016**, *95*, 881–889.
- (44) Hung, J. J. The Production of Activated Carbon from Coconut Shells Using Pyrolysis and Fluidized Bed Reactors, The University of Arizona, 2012.
- (45) Liao, M.; Kelley, S. S.; Yao, Y. Artificial Neural Network Based Modeling for the Prediction of Yield and Surface Area of Activated Carbon from Biomass. *Biofuels, Bioprod. Biorefin.* **2019**, *13*, 1015–1027.
- (46) Anca-Couce, A.; Scharler, R. Modelling Heat of Reaction in Biomass Pyrolysis with Detailed Reaction Schemes. *Fuel* **2017**, *206*, 572–579.
- (47) 2016 Billion-Ton Report: Advancing Domestic Resources for a Thriving Bioeconomy, Vol. 1: Economic Availability of Feedstocks; U.S. Department of Energy: Oak Ridge, TN, 2016; Vol. 1160.
- (48) Cai, J.; He, Y.; Yu, X.; Banks, S. W.; Yang, Y.; Zhang, X.; Yu, Y.; Liu, R.; Bridgwater, A. V. Review of Physicochemical Properties and Analytical Characterization of Lignocellulosic Biomass. *Renewable Sustainable Energy Rev.* **2017**, *76*, 309–322.
- (49) Aspen Plus User Guide; AspenTech: Cambridge, 2000.
- (50) Choi, M. k.; Park, H. C.; Choi, H. S. Comprehensive Evaluation of Various Pyrolysis Reaction Mechanisms for Pyrolysis Process Simulation. *Chem. Eng. Process.* **2018**, *130*, 19–35.
- (51) Ranzi, E.; Cuoci, A.; Faravelli, T.; Frassoldati, A.; Migliavacca, G.; Pierucci, S.; Sommariva, S. Chemical Kinetics of Biomass Pyrolysis. *Energy Fuels* **2008**, 22 (6), 4292–4300.
- (52) Ferreiro, A. I.; Giudicianni, P.; Grottola, C. M.; Rabaçal, M.; Costa, M.; Ragucci, R. Unresolved Issues on the Kinetic Modeling of Pyrolysis of Woody and Nonwoody Biomass Fuels. *Energy Fuels* **2017**, 31 (4), 4035–4044.
- (53) Anca-Couce, A.; Sommersacher, P.; Scharler, R. Online Experiments and Modelling with a Detailed Reaction Scheme of Single Particle Biomass Pyrolysis. *J. Anal. Appl. Pyrolysis* **2017**, 127, 411–425.
- (54) Debiagi, P.; Gentile, G.; Cuoci, A.; Frassoldati, A.; Ranzi, E.; Faravelli, T. A Predictive Model of Biochar Formation and Characterization. *J. Anal. Appl. Pyrolysis* **2018**, *134*, 326–335.
- (55) Blondeau, J.; Jeanmart, H. Biomass Pyrolysis at High Temperatures: Prediction of Gaseous Species Yields from an Anisotropic Particle. *Biomass Bioenergy* **2012**, *41*, 107–121.
- (56) Rowell, R. M. Handbook of Wood Chemistry and Wood Composites; Rowell, R. M., Ed.; CRC Press: Madison, WI, 2005.

- (57) Smook, G. A. Handbook for Pulp and Paper Technologists, Third ed., 3rd ed.; Kocurek, M. J., Ed.; Angus Wilde Publications, Inc.: Vancouver, Canada, 2003.
- (58) Debiagi, P. E. A.; Pecchi, C.; Gentile, G.; Frassoldati, A.; Cuoci, A.; Faravelli, T.; Ranzi, E. Extractives Extend the Applicability of Multistep Kinetic Scheme of Biomass Pyrolysis. *Energy Fuels* **2015**, 29 (10), 6544–6555.
- (59) Collard, F. X.; Blin, J. A Review on Pyrolysis of Biomass Constituents: Mechanisms and Composition of the Products Obtained from the Conversion of Cellulose, Hemicelluloses and Lignin. *Renewable Sustainable Energy Rev.* **2014**, 38, 594–608.
- (60) Wiedner, K.; Rumpel, C.; Steiner, C.; Pozzi, A.; Maas, R.; Glaser, B. Chemical Evaluation of Chars Produced by Thermochemical Conversion (Gasification, Pyrolysis and Hydrothermal Carbonization) of Agro-Industrial Biomass on a Commercial Scale. *Biomass Bioenergy* 2013, 59, 264–278.
- (61) Khor, K. H.; Lim, K. O.; Zainal, Z. A.; Mah, K. F. Small Industrial Scale Pyrolysis of Oil Palm Shells and Characterizations of Their Products. *Int. Energy J.* **2008**, 9 (4), 251–258.
- (62) Cagnon, B.; Py, X.; Guillot, A.; Stoeckli, F.; Chambat, G. Contributions of Hemicellulose, Cellulose and Lignin to the Mass and the Porous Properties of Chars and Steam Activated Carbons from Various Lignocellulosic Precursors. *Bioresour. Technol.* **2009**, *100* (1), 292–298.
- (63) Li, W.; Yang, K.; Peng, J.; Zhang, L.; Guo, S.; Xia, H. Effects of Carbonization Temperatures on Characteristics of Porosity in Coconut Shell Chars and Activated Carbons Derived from Carbonized Coconut Shell Chars. *Ind. Crops Prod.* **2008**, 28 (2), 190–198.
- (64) Liu, W. J.; Jiang, H.; Yu, H. Q. Development of Biochar-Based Functional Materials: Toward a Sustainable Platform Carbon Material. *Chem. Rev.* **2015**, *115* (22), 12251–12285.
- (65) Aguda, R. Preparation and Characterization of Modified Biomass as Functional Carbon-Based Materials, North Carolina State University, 2017.
- (66) Martín-Gullón, I.; Asensio, M.; Marcilla, A.; Font, R. Steam Activation of a Bituminous Coal in a Multistage Fluidized Bed Pilot Plant: Operation and Simulation Model. *Ind. Eng. Chem. Res.* **1996**, 35 (11), 4139–4146.
- (67) Klinar, D. Universal Model of Slow Pyrolysis Technology Producing Biochar and Heat from Standard Biomass Needed for the Techno-Economic Assessment. *Bioresour. Technol.* **2016**, 206, 112–120.
- (68) Gu, H.; Bergman, R. Life-Cycle Assessment of a Distributed-Scale Thermochemical Bioenergy Conversion System. *Wood Fiber Sci.* **2016**, 48 (2), 129–141.
- (69) Wooley, R. J.; Putsche, V. Development of an ASPEN PLUS Physical Property Database for Biofuels Components; Golden, Colorado, 1996.
- (70) Yang, H.; Kudo, S.; Kuo, H. P.; Norinaga, K.; Mori, A.; Mašek, O.; Hayashi, J. I. Estimation of Enthalpy of Bio-Oil Vapor and Heat Required for Pyrolysis of Biomass. *Energy Fuels* **2013**, *27* (5), 2675–2686.
- (71) Anca-Couce, A.; Zobel, N. Numerical Analysis of a Biomass Pyrolysis Particle Model: Solution Method Optimized for the Coupling to Reactor Models. *Fuel* **2012**, *97*, 80–88.
- (72) Dornburg, V.; Faaij, A. P. C. Efficiency and Economy of Wood-Fired Biomass Energy Systems in Relation to Scale Regarding Heat and Power Generation Using Combustion and Gasification Technologies. *Biomass Bioenergy* **2001**, *21* (2), 91–108.
- (73) Peters, J. F.; Banks, S. W.; Bridgwater, A. V.; Dufour, J. A Kinetic Reaction Model for Biomass Pyrolysis Processes in Aspen Plus. *Appl. Energy* **2017**, *188*, 595–603.
- (74) U.S. DOE-OIT. Steam System Opportunity Assessment for the Pulp and Paper, Chemical Manufacturing, and Petroleum Refining Industries. United States Department of Energy Office of Energy Efficiency and Renewable Energy: Washington, DC, 2002; pp 1–87.

- (75) U.S. Energy Information Administration. Natural gas explained Use of natural gas https://www.eia.gov/energyexplained/natural-gas/use-of-natural-gas.php (accessed Dec 14, 2019).
- (76) U.S. Department of Energy; Idaho National Laboratory. Bioenergy Feedstock Library bioenergylibrary.inl.gov (accessed Mar 13, 2019).
- (77) ECN.TNO. Phyllis2, database for biomass and waste https://phyllis.nl/ (accessed Mar 13, 2019).
- (78) González, J. F.; Román, S.; Encinar, J. M.; Martínez, G. Pyrolysis of Various Biomass Residues and Char Utilization for the Production of Activated Carbons. *J. Anal. Appl. Pyrolysis* **2009**, 85 (1–2), 134–141.
- (79) Garcìa-Pérez, M.; Chaala, A.; Pakdel, H.; Kretschmer, D.; Roy, C. Vacuum Pyrolysis of Softwood and Hardwood Biomass. Comparison between Product Yields and Bio-Oil Properties. *J. Anal. Appl. Pyrolysis* **2007**, 78 (1), 104–116.
- (80) Salinas-Martínez de Lecea, C.; Linares-Solano, A.; Garcia, P.; Molina, A.; Ruiz-Colorado, A. A.; Romero-Anaya, A. J. Phosphoric Acid Activation of Recalcitrant Biomass Originated in Ethanol Production from Banana Plants. *Biomass Bioenergy* **2011**, *35* (3), 1196–1204.
- (81) Gueye, M.; Richardson, Y.; Kafack, F. T.; Blin, J. High Efficiency Activated Carbons from African Biomass Residues for the Removal of Chromium(VI) from Wastewater. *J. Environ. Chem. Eng.* **2014**, 2 (1), 273–281.
- (82) Güngör, A.; Önenç, S.; Uçar, S.; Yanik, J. Comparison between the "One-Step" and "Two-Step" Catalytic Pyrolysis of Pine Bark. *J. Anal. Appl. Pyrolysis* **2012**, *97*, 39–48.
- (83) Rambo, M. K. D.; Schmidt, F. L.; Ferreira, M. M. C. Analysis of the Lignocellulosic Components of Biomass Residues for Biorefinery Opportunities. *Talanta* **2015**, *144*, 696–703.
- (84) Sasmal, S.; Goud, V. V.; Mohanty, K. Characterization of Biomasses Available in the Region of North-East India for Production of Biofuels. *Biomass Bioenergy* **2012**, *45*, 212–220.
- (85) Wei, L.; Xu, S.; Zhang, L.; Zhang, H.; Liu, C.; Zhu, H.; Liu, S. Characteristics of Fast Pyrolysis of Biomass in a Free Fall Reactor. *Fuel Process. Technol.* **2006**, *87* (10), 863–871.
- (86) Mun, T. Y.; Seon, P. G.; Kim, J. S. Production of a Producer Gas from Woody Waste via Air Gasification Using Activated Carbon and a Two-Stage Gasifier and Characterization of Tar. *Fuel* **2010**, *89* (11), 3226–3234.
- (87) Jung, S. H.; Kim, S. J.; Kim, J. S. Characteristics of Products from Fast Pyrolysis of Fractions of Waste Square Timber and Ordinary Plywood Using a Fluidized Bed Reactor. *Bioresour. Technol.* **2012**, *114*, 670–676.
- (88) Lyu, G.; Wu, S.; Zhang, H. Estimation and Comparison of Bio-Oil Components from Different Pyrolysis Conditions. *Front. Energy Res.* **2015**, 3 (June), 1–11.
- (89) Grnli, M. A Theoretical and Experimental Study of the Thermal Degradation of Biomass; Norwegian University of Science and Technology, 1996.
- (90) Demirbaş, A. Calculation of Higher Heating Values of Biomass Fuels. *Fuel* **1997**, *76* (5), 431–434.
- (91) Janković, B. The Pyrolysis Process of Wood Biomass Samples under Isothermal Experimental Conditions-Energy Density Considerations: Application of the Distributed Apparent Activation Energy Model with a Mixture of Distribution Functions. *Cellulose* **2014**, *21* (4), 2285–2314.
- (92) Shen, D. K.; Gu, S.; Luo, K. H.; Bridgwater, A. V.; Fang, M. X. Kinetic Study on Thermal Decomposition of Woods in Oxidative Environment. *Fuel* **2009**, 88 (6), 1024–1030.
- (93) Chen, Z.; Hu, M.; Zhu, X.; Guo, D.; Liu, S.; Hu, Z.; Xiao, B.; Wang, J.; Laghari, M. Characteristics and Kinetic Study on Pyrolysis of Five Lignocellulosic Biomass via Thermogravimetric Analysis. *Bioresour. Technol.* **2015**, *192*, 441–450.
- (94) Butler, E.; Devlin, G.; Meier, D.; McDonnell, K. Characterisation of Spruce, Salix, Miscanthus and Wheat Straw for Pyrolysis Applications. *Bioresour. Technol.* **2013**, *131*, 202–209.

- (95) Burhenne, L.; Messmer, J.; Aicher, T.; Laborie, M. P. The Effect of the Biomass Components Lignin, Cellulose and Hemicellulose on TGA and Fixed Bed Pyrolysis. *J. Anal. Appl. Pyrolysis* **2013**, *101*, 177–184.
- (96) Xu, J.; Elkamel, A.; Taqvi, S. T. H.; Liu, C.-G.; Rahimuddin, S. A.; Gull, M.; Mehmood, M. A.; Ahmad, M. S. Pyrolysis, Kinetics Analysis, Thermodynamics Parameters and Reaction Mechanism of Typha Latifolia to Evaluate Its Bioenergy Potential. *Bioresour. Technol.* **2017**, 245, 491–501.
- (97) Chen, Z.; Zhu, Q.; Wang, X.; Xiao, B.; Liu, S. Pyrolysis Behaviors and Kinetic Studies on Eucalyptus Residues Using Thermogravimetric Analysis. *Energy Convers. Manage.* **2015**, *105*, 251–259.
- (98) Williams, C. L.; Westover, T. L.; Emerson, R. M.; Tumuluru, J. S.; Li, C. Sources of Biomass Feedstock Variability and the Potential Impact on Biofuels Production. *BioEnergy Res.* **2016**, *9* (1), 1–14.
- (99) Raveendran, K.; Ganesh, A.; Khilar, K. C. Influence of Mineral Matter on Biomass Pyrolysis Characteristics. *Fuel* **1995**, 74 (12), 1812–1822.
- (100) Phanphanich, M.; Mani, S. Impact of Torrefaction on the Grindability and Fuel Characteristics of Forest Biomass. *Bioresour. Technol.* **2011**, *102* (2), 1246–1253.
- (101) Kataki, R.; Konwer, D. Fuelwood Characteristics of Some Indigenous Woody Species of North-East India. *Biomass Bioenergy* **2001**, 20 (1), 17–23.
- (102) López-González, D.; Fernandez-Lopez, M.; Valverde, J. L.; Sanchez-Silva, L. Thermogravimetric-Mass Spectrometric Analysis on Combustion of Lignocellulosic Biomass. *Bioresour. Technol.* **2013**, 143, 562–574.
- (103) Rousset, P.; Aguiar, C.; Labbé, N.; Commandré, J. M. Enhancing the Combustible Properties of Bamboo by Torrefaction. *Bioresour. Technol.* **2011**, *102* (17), 8225–8231.
- (104) Chen, W. H.; Hsu, H. C.; Lu, K. M.; Lee, W. J.; Lin, T. C. Thermal Pretreatment of Wood (Lauan) Block by Torrefaction and Its Influence on the Properties of the Biomass. *Energy* **2011**, *36* (5), 3012–3021.
- (105) Ramos-Carmona, S.; Martínez, J. D.; Pérez, J. F. Torrefaction of Patula Pine under Air Conditions: A Chemical and Structural Characterization. *Ind. Crops Prod.* **2018**, *118*, 302–310.
- (106) Zhou, C.; Liu, G.; Wang, X.; Qi, C. Co-Combustion of Bituminous Coal and Biomass Fuel Blends: Thermochemical Characterization, Potential Utilization and Environmental Advantage. *Bioresour. Technol.* **2016**, 218, 418–427.
- (107) Azeez, A. M.; Meier, D.; Odermatt, J.; Willner, T. Fast Pyrolysis of African and European Lignocellulosic Biomasses Using Py-GC/MS and Fluidized Bed Reactor. *Energy Fuels* **2010**, 24 (3), 2078–2085.
- (108) Jindal, M. K.; Jha, M. K. Catalytic Hydrothermal Liquefaction of Waste Furniture Sawdust to Bio-Oil. *Indian Chem. Eng.* **2016**, *58* (2), 157–171.
- (109) Di Blasi, C.; Signorelli, G.; Di Russo, C.; Rea, G. Product Distribution from Pyrolysis of Wood and Agricultural Residues. *Ind. Eng. Chem. Res.* **1999**, 38 (6), 2216–2224.
- (110) Luo, G.; Chandler, D. S.; Anjos, L. C. A.; Eng, R. J.; Jia, P.; Resende, F. L. P. Pyrolysis of Whole Wood Chips and Rods in a Novel Ablative Reactor. *Fuel* **2017**, *194*, 229–238.
- (111) Bridgeman, T. G.; Jones, J. M.; Shield, I.; Williams, P. T. Torrefaction of Reed Canary Grass, Wheat Straw and Willow to Enhance Solid Fuel Qualities and Combustion Properties. *Fuel* **2008**, 87 (6), 844–856.
- (112) López, F. A.; Centeno, T. A.; García-Díaz, I.; Alguacil, F. J. Textural and Fuel Characteristics of the Chars Produced by the Pyrolysis of Waste Wood, and the Properties of Activated Carbons Prepared from Them. J. Anal. Appl. Pyrolysis 2013, 104, 551–558.
- (113) Sajjadi, B.; Chen, W. Y.; Egiebor, N. O. A Comprehensive Review on Physical Activation of Biochar for Energy and Environmental Applications. *Rev. Chem. Eng.* **2019**, *35*, 735.

- (114) Demiral, H.; Demiral, I.; Karabacakoglu, B.; Tümsek, F. Production of Activated Carbon from Olive Bagasse by Physical Activation. *Chem. Eng. Res. Des.* **2011**, 89 (2), 206–213.
- (115) Zheng, Z.; Xia, H.; Srinivasakannan, C.; Peng, J.; Zhang, L. Steam Activation of Eupatorium Adenophorum for the Production of Porous Carbon and Hydrogen Rich Fuel Gas. *J. Anal. Appl. Pyrolysis* **2014**, *110* (1), 113–121.
- (116) Miner, R. A.; Abt, R. C.; Bowyer, J. L.; Buford, M. A.; Malmsheimer, R. W.; Laughlin, J. O.; Oneil, E. E.; Sedjo, R. A.; Skog, K. E. Forest Carbon Accounting Considerations in US Bioenergy Policy. *J. For.* **2014**, *112*, 591–606.
- (117) Ishikawa, S.; Hoshiba, S.; Hinata, T.; Hishinuma, T.; Morita, S. Evaluation of a Biogas Plant from Life Cycle Assessment (LCA). *Int. Congr. Ser.* **2006**, *1293*, 230–233.
- (118) Zhang, L. X.; Wang, C. B.; Song, B. Carbon Emission Reduction Potential of a Typical Household Biogas System in Rural China. *J. Cleaner Prod.* **2013**, *47*, 415–421.
- (119) Climate Change 2007: Synthesis Report; IPCC: Geneva, Switzerland, 2008.
- (120) Gunnar, M.; Shindell, D.; Bréon, F.-M.; Collins, W.; Fuglestvedt, J.; Huang, J.; Koch, D.; Lamarque, J.-F.; Lee, D.; Mendoza, B.; et al. Anthropogenic and Natural Radiative Forcing. In Climate change 2013: The physical science basis. Contribution of Working Group I to the Fifth Assessment Report of the Intergovernmental Panel on Climate Change; Jacob, D., Ravishankara, A. R., Shine, K., Eds.; Cambridge University Press: New York, 2013; pp 659–740.
- (121) Qiu, M.; Sun, K.; Jin, J.; Gao, B.; Yan, Y.; Han, L.; Wu, F.; Xing, B. Properties of the Plant- and Manure-Derived Biochars and Their Sorption of Dibutyl Phthalate and Phenanthrene. *Sci. Rep.* **2015**, *4*, 1–10.
- (122) Akhtar, J.; Saidina, N.; Wood, P. A Review on Operating Parameters for Optimum Liquid Oil Yield in Biomass Pyrolysis. *Renewable Sustainable Energy Rev.* **2012**, *16* (7), 5101–5109.
- (123) Edmunds, C. W.; Reyes Molina, E. A.; André, N.; Hamilton, C.; Park, S.; Fasina, O.; Adhikari, S.; Kelley, S. S.; Tumuluru, J. S.; Rials, T. G.; et al. Blended Feedstocks for Thermochemical Conversion: Biomass Characterization and Bio-Oil Production From Switchgrass-Pine Residues Blends. *Front. Energy Res.* **2018**, *6*, 1–16
- (124) González-García, P. Activated Carbon from Lignocellulosics Precursors: A Review of the Synthesis Methods, Characterization Techniques and Applications. *Renewable Sustainable Energy Rev.* **2018**, 82, 1393–1414.
- (125) Bergna, D.; Hu, T.; Prokkola, H.; Romar, H.; Lassi, U. Effect of Some Process Parameters on the Main Properties of Activated Carbon Produced from Peat in a Lab-Scale Process. *Waste Biomass Valorization* **2019**, 1–12.

CIDAN	Ganaratas	for AC By	aduction :	with Eng	one Pacou	

Mathematical
The column   The
1
1.00
1.00
1.60
1.00
1
1.00
1.   1.   1.   1.   1.   1.   1.   1.
1.00
1.00
Table   Tabl
18
18
1
1.
1
196   196
1.00
1.0
1.0
1.00
14
1.6
10
1
10
1
1
140
1.00
150
140
140
1.00
1.00
10
1.00
1.00
1.00
1.40
1.5
Map
1.00
1.00
1.50
1.1
## 1
140
140
140
1.00
1.00
\$2 No. 10
See
100
10   10   10   10   10   10   10   10
10   10   10   10   10   10   10   10
1.0
1,00
Mail
Mail
140
1.00
100   100
1.00
1.40
1.00
1.00
1.00
4.00
100
1.00
1.00
1
1
1
Alm   1.07   4.06   4.05   4.06   4
Natif   State   4900   1,000
Class 1470 2-077 25588 6580 6-270 12-067 12-067 13-069 15-069 25-

3 D	ata Generated for AC Producti	leasts Dry Homes	Recovery	Nitrona		Natural Con	Outsuts Region CO2	Name (NA	fuelent	G=2794	South W	Other Carre
1	Cisi Alashu Alashu	lig / lig AC product 7,8541 7,4566 4,3002 5,614	kg/ kg AC product 3.5300 3.5456	kg/kg AC product £1797 £260	kg / kg AC product 6.9700 7.7966	MI / kg AC product 79-4361 95-6000	kg / kg AC product 6.90% 1.2211	kg / kg AC product 0.0268 0.0272	kg / kg AC product 3.9940 4.9041	kg /kg AC product 7.536-05 6006-05	kg/kg AC product 7.59E-0s 9.89E-0s	kg / kg AC product 10,7002 11,4665
4	Alimond Alimond Alimond	4.202 5.010 5.000	2.385 2.566 2.622	67834 69738 63565	3.8605 5.7300 4.9294	30.604 56.904 42.302	3,6871 5,399 4,769	0.0139 0.0296 0.0179	1.5317 2.856 2.16%	2,965-05 5,165-05 4,056-05	2,865-0a 5,365-0a 6,055-0a	6.40% 9.000 3.369
2	Almond Almond Almond	5.645 5.456 4.4711	3.1417 3.1857 2.5000	6967 69627 6762	5.2653 5.1137 4.1916	60,7307 57,9662 37,4564	5,3126 5,0127 3,9125	0.6206 0.6200 0.8657	3.0509 2.9029 1.8023	5.19E-05 5.8E-05 3.59E-05	5.95-0s 5.65-0s 3.95-0s	8.4756 8.4756
10 11	Almond Almond Almond	5,639 4,609 4,605 4,797	3.790 2.909 2.460	6903 6460 6768	5.2344 3.87% 4.3%	65.5377 34.9528 37.3645	5 107 3.569 4 159	03145 03145	3 1005 1,7965 1,9029	3.36-65 3.36-65 3.56-65	6245-00 3.315-00 3.595-00	8.7974 6.3801 7.0881
12	Almond Two Promise American Arks (White Arks)	6.5549 13.3696	3.500 3.600 6.7349	6793 1169 2705	6.566 6.566 13.6528	56,5153 56,3600 307,5661	6.792 6.792 14.210	0.000 0.000	2,960 4,200 10,4007	5.16E-05 1.9E-05 1.9E-05	7.965-0s 7.965-0s 1.975-05	1,806 18,669 21,806
15	Apraid Bahassa Bamboo (Bambasa Valgarin)	4.067 6.647	2.049 3.369	1160 060 1060	3.4251 5.2297	\$6.3333 27.3907 63.3844	3.5924 6.2932	0336) 0336)	1,200 1,200 3,200	2.5%-05 5.0%-05	2.5%-0s 6.0%-0s	13,4669 21,806 13,666 4,267 8,4772
19 29	Rambor (Rambora volunia) - Middle Rambor (Rambora volunia) - Middle Rambor (Vandra volunia) - Ten	5.02 6.00 4.00	3,966 3,462 2,462	1196	7.600 6.7519 4.607	29.1309 63.2251 13.5599	5,006 6,709 4,700	0.600 0.000 0.000	3,9965 3,1702 1,4864	7.895-05 5.995-05 3.195-05	7.4% or 5.9% or 1.1% or	12.0599
22 29 28	Hamboo Sawakat Basak Basak	4.309 6.088 6.800	2 3059 2 6916 3 2054	6728 1609 1366	6.786 6.738 6.728	36.4157 50.7161 12.4008	3.701 5.8169 6.5875	03151 03213 0.037	1.1005 2.501 3.630	2.5(E-05 4.9(E-05 6.9(E-05	251E-04 4.81E-04 6.86E-04	6.1927 9.3683 18.3558
25 26 22	Result Ward Break Ward	5.290 5.295	2,659 2,679 2,679	1,0417 6/602 6/07	6.1410 5.3240 5.3490	62.388 61.379 52.680	5.580 5.580	03214 03210 03217	3.1301	5.90E-05 4.11E-05 4.96E-05	5.905-0s 4.115-0s 4.905-0s	9.4563 8.7276 8.0994
29 29 39	Mesh Mesh	5.460 7.462 5.969	2 4359 3 1743 3 2565 2 3989	1,0677 1,2440 6,9771	6.369 7.996 5.999	58,9995 13,6682 47,7890	5.90s 3.882 5.528	9336 9436 9310	2.669 2.964 3.639 2.1965	5.5%-05 6.925-05 4.526-05	5.995-0s 6.925-0s 4.925-0s	9.094 9.992 11.2130 9.92%
12 12 13	Bisch Beshagen Complex	11.256 4.96% 6.868	5.4002 2.3905 3.3082	1,8736 6,9000 1,1116	11,0977 4,760 6,500	251 6659 47.1466 33.4433	11.692 4.5102 6.4777	03428 03369 03253	2.600 2.560 3.607	1.65.00 4.65.00 6.96.00	1.665-01 6.675-04 6.965-04	16,9965 7,2645 18,1663
15 16	Oronina Ordar Ordar	5.566 8.366 5.368	2,665 3,663 3,269	1468 1468 6968	5.905 9.821 5.202	68,6560 92,309 69,6022	5.195 8.796 5.450	0335 0335 0336	2.600 4.607 3.5077	\$105.05 \$1%.05 \$445.05	6415-0s 8735-0s 6415-0s	8 507 1) 2652 8 2003
23 28	Chore tose Chory tose Chory tose	5.200 5.2156 5.600	2.405 2.405 3.3125	6360 6360 6903	5.000 5.000 5.0279	64.0029 64.0013 63.0005	4.891 4.891 5.391	03296 03288	2.299 3.254	5.79E-05 4.22E-05 6.06E-05	5.795-0s 4.225-0s 6.065-0s	1,909 1,909 8,469
6	Conne Conne Conne	4 101 3.750	2.5200 2.7357 2.9645 2.9777	0000 0000 0000	3.905 3.905 2.940	40.9454 43.4759 45.1755	3.000	03165 03162	2.879 2.676 2.198 2.362 2.360	198-6 116-6 417-6	186 oc 416 oc 475 oc	1.60% 8.46% 8.5902 6.40% 5.9024
65	Cocond Occord Occord	5.6000 3.7656 3.8560	2.004 2.090 2.203	6936 6606 6606	5.3666 3.4(39 3.573)	57,2710 31,4658 31,499	5.3054 3.2440 3.1535	03214 03117 0.007	2 9760 1 5622 1 5784	5.425.46 2.995.46 2.935.46	5.05 oc 2.95 oc 2.95 oc	8.507 5.605 6.1135
8	Colline Colline Colline	4.4637 3.999 6.201	2.405 2.008 3.206	6746 6698 1065	4.34% 3.77% 6.6402	32,5005 22,7519 66,4987	3,9090 3,4053 5,9592	03145 03127 03216	1.600 1.160 3.163	3.06-65 2.19-65 6.36-65	2155-04 6365-04	6.9074 6.0000 9.5547
53 51 52	Cottine Cypenes Decodes Fir	6.2607 4.5689 7.2881	3.264 2.836 3.962	1001 6315 1390	6.079 6.605 7.000	66, 6189 62,6800 82,7860	5,9935 4,5805 3,1360	03216 0.0368 03290	3.397 3.169 4.140	5.29E-05 5.99E-05 7.99E-05	5.5% 0c 5.5% 0c 7.8% 0c	9.5510 7.3629 38.9653
53 54 55	Dougles Fir Dougles Fir Wood Foobleck	5.306 5.306	3.3421 3.3471 3.865	1,0% 1,25% 6/95H	5.809 7.608 5.407	78.2363 78.6128 99.2355	5.1967 7.586 5.4055	03287 03368 03218	3.906 3.903 2.9%2	7.41E-05 7.39E-05 5.60E-05	7.41E-0s 7.36E-0s 5.61E-0s	9.4572 11.2980 8.4699
55 52 58	Die Die Encolptus	9.454 9.418 4.896	4.995 4.951 2.996	1500 1500 6506	9.902 9.6256 4.999	215,300 213,3300 30,7385	\$660 \$310 \$460	0.0342 0.0342	5.7965 5.6971 1.5967	1.0%-04 1.0%-04 2.9%-05	1.0%-01 1.0%-01 2.91E-01	14 1552 13.9654 7.1965
60	Faculation Faculation Faculation	5.1756 5.1607	2.892 2.892 2.425	5363 5363	5.100 5.100 5.1011	27.568 27.568 29.5628	4.728 4.728 4.737	0.01% 0.01% 0.01%	2,003 1,809 2,003	3.56E-65 3.76E-65	1.365-00 1.365-00 1.365-00	7.8670 7.8670
64	Escalatos Escalatos	6.1865 6.00%	1 265 1 2862	100H 10079	5.9550 5.7384 4.675	68,7811 66,005) 49,4700	5.996 5.927	03216 03219 0.0006	3.100	6.51E-05 6.25E-05	6.51E-0s 6.21E-0s	9,0009 9,0006 7,5746 2,1756 7,1750
8	Finaletic Sendet Fir	4.760 4.771 5.960	2.968 2.020 2.7540	6.7965 6.7962 6.9965	4.490 4.820 5.600	40 13157 29.4679 51.6727	42146 43227 5,662	0.0079 0.0066 0.0221	2.463 2.00% 1.4808 2.618	3,925-66 2,796-66 4,925-66	3 X25 0s 2 X6 0s 4 X25 0s	7,1756 7,1726 8,9546
69 29 71	6 6	5.890 6.879 6.806	2.947 3.962 3.698	1100 1100 1000	5.506 6.760 5.804	52 4840 71 7149 62 4250	5.540 6.700 5.60%	0.0218 0.0067 0.0241	2,665 3,604 3,1301	4.96-05 6.96-05 5.96-05	6.965-0s 5.965-0s	9.5560 98.4045 9.0026
72 79 74	For For Wood	5.5529 5.6555 5.9514	3.000 3.004 3.336	6905 6905 6902	5.362 5.362 5.5158	57.3625 59.9656 65.3999	5.294 5.350 5.500	0.6214 0.6229 0.8241	2.806 3.008 3.265	5.69E-05 5.69E-05 6.19E-05	5.05-to 5.05-to 6.76-to	2.4864 8.4359 9.2569 7.7645 5.9947
75 76 72	Chape Chape Chape	5.1014 3.6443 4.6009	2.4637 2.4172 2.4650	6350 6400 6700	5.6677 3.7921 4.5142	40.1216 29.5768 56.2116	4,643 3,0627 4,2198	0.0174 0.0125 0.0566	2.0563 1.4963 2.7284	3.90E-05 2.90E-05 5.13E-05	3.805-0s 2.805-0s 5.05-0s	7,7945 5,9007 7,2190
79 29	Chape Hardwood Hardwood rick in three	6.001 5.000	2.796 3.2405 3.1139	5916 1007 69211	5.9253 5.9268	94.993 30.3625 56.695	5.760 5.760	0.0240 0.0240 0.0000	3.5399 2.6392	6.135-05 6.66E-05 5.19E-05	6.03-0s 6.66-0s 5.16-0s	7,364 9,550 9,600
82 83	Harebet Harebet Harebet	4,610 4,620 4,361	2.364 2.566 2.652	6769 6474 6709	5.608 3.608 3.828	28,0008 36,969 42,974	1592 1592 1859	0.0054 0.0054 0.0071	1.890 1.890 2.192	2.6%-65 3.4%-65 4.062-65	2.6%-0: 3.6%-0: 4.0%-0:	6.364 6.692
85 86 97	Holin Oak Holin Oak Holini Paplar	4.939 4.7151	2.66 2.06	67677 6769	4.9727 4.6972 4.7995	35.3668 39.6127	4,000 4,000 4,000	0.0170 0.0177 0.0177	1.790 2.007	3.14E-05 3.79E-05	3.36-0: 3.36-0: 1.95-0:	7,1794 7,2266 7,1000
22 23	Innine Konaf (Inly) Kevi Branch	5.669 5.669 6.300	2.7188 2.905 2.6453	6706 69611 67182	3.992 4.923 3.926	89.9997 39.4429 89.7971	4,0757 4,56%	0.6251 0.6569 0.8179	2.50% 1.90% 2.00%	4.725-66 3.745-66 3.815-66	4.755-00 3.765-00 3.855-00	7,2296 7,1296 6,7065 7,7434 6,8766
90 90 90	Editor Lock Lock	4.965 7.960 8.260	2.5454 3.9304 3.9656	56%7 1307 1379	3.951 7.866 8.163	68,6570 95,9628 98,6118	3.760 8.150 8.150	0.8174 0.8145 0.8145	2.490 4.8294 4.904	1.66-65 1.06-65 1.13-65	9,005-0s 9,005-0s 9,315-0s	6 560 11.816 12.160
95 95 96	Longo Longo Polo Pino	13.1345 5.3430 5.4460	6,9642 2,964 2,987	2.189 6.970 6.982	12.6112 5.1112 5.403	260,4306 43,2360 53,3662	14.000 4.000 5.000	0.6955 0.0179 0.0320	9,0601 2,1709 2,6829	1.71E-04 4.18E-05 5.06E-05	1.765-00 4.105-00 5.062-00	19.4272 9.0924 9.2609
92 98 98	Logging Residue Chip Medican Mentanta	5.000 5.000 5.440	2.1122 2.513 2.566	89093 90924	5.5144 5.90% 5.2366	43.5124 44.7792 45.5854	5.409 5.109 4.8271	0.6245 0.6096 0.6086	2.3917 2.399 2.3984	4.15E-65 4.26E-65 4.15E-65	4.05-0s 4.36-0s 4.35-0s	8.800 8.4000 8.4000 9.0014
300 300 300	Magis Magis Manis	6.4300 6.6664 6.3660	2.136 3.369 1.369	10%0 10%0	5.909 5.909	32.6627 68.6565 66.2550	5.092 5.799	03234 03214 03210	3.490 3.196	6.58-65 6.28-65	6.965-0s 6.955-0s	9.8511 9.2571
304 305 306	Microl Microl	5.811 6.810 5.900	3.016 3.016 3.012	69752 19936 19936	5.5774 5.5774 5.9674	62.2551 59.5540 55.7647	5.948 5.739 5.631	0.005 0.005 0.021	3.126 3.009	5.90E-05 5.60E-05 5.70E-05	5.95 oc 5.95 oc 5.95 oc	9.1129 9.1602
307 308 309	Mitted Mitted Mitted	5.7139 5.963 5.7544	2.8543 3.896 2.7016	6903 6903 6903	5.5123 5.6650 5.6532	55.3662 59.5423 50.3696	5.638 5.619 5.790	0.0211 0.0219 0.0213	2.7722 3.0022 2.5963	5.226-65 5.666-65 4.826-65	5.235-0s 5.665-0s 4.825-0s	1.4533 1.9660 1.4235
12   12   13   13   13   13   13   13	Mitted Maj Mulharry	5.3456 6.071 6.690	2.965) 2.9900 3.9019	£3909 £0239 £0027	5.0219 6.0007 6.0008	58.3522 61.788 77.6532	5,969 5,969	9.6205 9.6254 9.6257	2.9023 3.1025 3.9791	5.5%-65 5.8%-65 7.10E-65	5.05 oc 5.05 oc 7.05 oc	9.20% 9.20% 9.900
11) 114 115	Norwe Serace Onli Onli	6.5673 5.3693 6.3651	3.496 2.715) 2.499	1140 6963 1606	6.6527 5.7351 6.2403	76 2602 68 6607 51 5840	6.70% 5.40% 5.768	0.0112 0.0212	3.1901 2.405 2.502	7.00E-05 4.60E-05 4.80E-05	1895-00 4,895-00	98.9500 8.7544 9.2768 9.2166 6.8967 8.4293
116 117 118	OME OME	6.360 4.500 5.516	2.7656 2.020 2.690	100% 67%2 6909	6.199 4.51% 5.398	54.6962 29.3834 46.5921	5.909 4.007 5.2128	93218 93363 9.8992	2.7154 1.436 2.1584	5.135-65 2.795-65 4.445-65	5125-0s 2765-0s 6.465-0s	9.21% 6.8967 8.4243
129	os os	5.539 7.612 5.539	2 9629 3 7359 2 8397	1220 1220 6956	7.088 5.665	60.7412 99.2460 53.2214	52HF 10ND 54R6	0.004 0.004 0.013	1.604 4.696 2.636	\$ 192-05 \$ 162-05 \$ 08-05	5.765-0s 5.865-0s 5.865-0s	9,3067 11,3077 8,6215
122 128 126	Chia Chia	5.956 9.5618	2.999 4.2955	1903 5909 1649	5.7410 5.7410 30.6412	58,4935 118,3154	5.660 10003	03256 03276 03270	2.964 5.964	5.9E-65 1.135-04	5.95-0: 1.05-0:	8,996 8,996 16,624
126 127 129	Out Out	5.890 6.594 5.194	3.2558 2.8602 2.8727	6903 6756 6909	5.5464 4.960 4.900	68.1721 68.6731 64.0678	3.505 4.169 4.899	0.0218	3.42% 2.2544 3.47%	6.46E-05 4.13E-05	6.45 to 41% to	9,1294 6,9690 7,66% 1,3272
126 127 128 129 130 131 132	Ulico Ulico	5.00 6350 4450	2.4907 3.4974 2.9618	6892 1169 6776	5.8977 6.7691	39.5641 15.6912 50.7000	4.670 6.685	0.074	1.992 3.992 3.699	3.790-05 3.130-05 4.790-05	3.79E-04 7.77E-04 4.79E-04	7.6272 18.6989 7.1897 18.0060
132 133 134	Olice Olice	5.942 5.942	3.166 3.366 3.600	1100 69049 1001	6.5332 6.9962 5.8771	79.5032 25.5094 26.6911	5.292 5.292	0.0241 0.0211 0.0302	3.982 3.8151 3.9213	7.5%-65 7.1%-65 7.3%-65	7.53E-0s 7.19E-0s 7.39E-0s	13.0360 3.5065 9.6002
110 134 135 136 138 139 140 140 140 140 140 140 140 140 140 140	Clino Clino	4.5726 4.5564 4.6519	3.892 2.799 2.564	67621 6399 6729	3.966 4.579 4.3005	54,5000 59,6095 56,5656	4.298 4.467 4.105	0.6218 0.6087 0.6099	2.796 3.001 2.95%	5.16E-05 5.6TE-05 5.16E-05	5.00E-00 5.00E-00 5.00E-00	7.0019 7.4907 7.1156
139 139 140	Clina Clina Clina	4.659 4.369 4.360	2.9546 2.9506 2.8481	6,7765 6,7169 6,7244	4.000 3.4272 3.769	\$4,905 99,030 46,1144	4.0211 3.8572	0.0010 0.0086 0.0082	2.1961 2.968 2.3134	5.66-65 5.66-65 4.3%-65	5 ME-0s 5 ME-0s 4 JTS-0s	7.607 7.1156 7.1969 6.5144 6.560 8.900 8.900
140 140	Palm. Palm.	5.400 5.300	3.000 3.200	6908 6908	5.003 4.023 1.055	61,990 65,5308 47,799	4305 4763	0.090	3.100 3.306	5.88E-05 6.28E-05	5 865 00 6245 00	8.554 8.656 6.400
145 146 147	Panis Pine Presis Presis	4.360 4.363 4.903	2.9965 3.3425 3.0172	6760 1090 6897	5.860 5.860 6.005	59.5779 71.5896 57.4058	6.000 6.000 6.000	0.6917 0.6254 0.6212	2,9999 3,6396 2,8962	5.66-05 6.90-05 5.66-05	5.66E-0s 6.90E-0s 5.46E-0s	7,3963 9,4225 7,5888
168 168 153	Promit Promit Promit	4.766 4.369 4.3627	2347 2462 2566	6.7977 6.7350 6.7971	4.962 4.9624 3.5486	99 5656 35 6734 33 5794	4.3031 3.8341 3.8138	0.0172 0.0150 0.0549	2,9750 1,7927 1,7925	5.60E-05 3.38E-05 3.22E-05	5 605 0s 3 305 0s 3 225 0s	3,299 6,795 6,594
151 152 153	Peer Pee	1,360 1,360 1,360	2.5412 3.666 3.356 2.467	67507 12040 1,3000	4.2018 7.5896 7.8985	37.3549 66.925 77.3400	1125 1664	0.6916 0.6916 0.6902	1.9872 3.1462 3.8365	3.565-65 5.365-65 7.315-65	1.355-0s 6.365-0s 7.355-0s	8,9687 38,954 11,7607
155	Fine Fine	5.874 7.568 5.600	2.9%	6909 12511	5.1347 7.2409 5.901	86,7698 85,6221 86,9617	5 067 1550	0.015	2.269 4.992	426-65 8.116-65	426 de 8.116 de 4.45 de	11.004 11.006
158 159 160	Pine Pine Pine	6.9272 5.761 6.465	3.3326 2.6650 3.4659	1156 6962 1000	6.992 5.992 6.099	36.5477 64.7296 15.4558	5556 5,566 6,169	0.000 0.0142 0.0279	3.867 3.866 3.768	7.290-05 5.990-05 7.190-05	7.255-0s 5.855-0s 7.255-0s	38.4266 8.7709 9.7127
162 162 163	Fee Fee	6.675 6.655 6.754	3.490 3.590 3.550	1109 1100 1100	6.3290 6.3715 6.4711	29.5308 \$1.3653 \$1.3094	6.45M 6.55M	0.6250 0.6250 0.6311	3,996 4,009 4,009	7.546-65 7.766-65 7.646-65	7.565-0x 7.565-0x 7.665-0x	10.0650 10.0651 0.00%
363 365 367 367 368 368 179	Fee Fee	6.000 6.00% 5.20%	3.207 2.800 3.3147	1.0085 1.1546 6.8796	5.760 7.042 6.760	69.7907 59.4652 67.6956	5.89d 6.767 5.000	0.0257 0.0256 0.0256	4.085 3.561 4.163 3.166	5.60E-05 7.90E-05 6.60E-05	6.605-00 7.905-00 6.605-00	9,000 9,101 10,002 9,1104 7,003 6,997 5,590 7,003
367 368 369	Piec Piec Berk	4.5348 4.4277 3.5906	2.9985 2.9983 2.2171	6,90% 6,736 6,766	4.1962 3.5547 3.7565	56.9812 53.1254 25.1363	4.004 4.000 1.000	0.6207 0.6566 0.6544	2.690 2.690 1.360	5.19E-05 5.00E-05 2.19E-05	5.86 m 5.86 m 2.86 m	7.4683 6.9997 5.9992
179 171 172	Fac Chip Fac Chip Fac Wood	11.6609 7.8779	4.8323 3.7779	1.842 1.928	3.565 11.2122 7.366	219.5648 229.5648 88.4655	114501 114501 1.5940	0.006	4.004 4.4677	1.1%-04 1.1%-04 1.4%-05	1.0540 8.05-0	16.416 12.1247
174 175 176	Papon Jusque Papon Pine Patoshio	4.902 4.902 4.968 5.304	2,586 2,586 2,580 2,690	0.686 0.798 0.896	3.6613 4.4684 5.3445	41.3714 54.9340 49.4714	3.7901 4.4693 4.9947	0.009 0.009 0.000 0.000	2,0760 2,7965 2,9667	3.192-05 5.196-05 4.696-44	3.95 to 3.95 to 3.96 to	12.000 9.2002 6.2007 7.3118 8.3004
122 178 179	Patada Patada Paplar	7,987 6,298 6,395	3,4658 3,2172 2,7566	1,266 1,050 1,064	7.460 6.005 6.3562	\$6,9340 65,7230 51,7350	3.4938 6.1239 6.0548	0.004 0.000 0.017	4.2651 3.3627 2.586	8.08-05 6.23-05 4.98-05	8.045-0s 6.235-0s 6.955-0s	1.1007 9.5144 9.655 3.9411 9.8061 8.2900 9.0072 18.650 19.0075 19.0075 18.650 19.0075 18.650 19.0075 1
190 191 192	Produc Produc Produc	5.229 6.525 5.801	2.4298 3.3155 3.3882	\$79.3 \$79.1 \$399.3	5.3002 6.3254 5.5600	39.3400 30.6640 69.3065	4792 5396 5.675	0.0179 0.0248 0.0218	1,9969 3,505 3,4758	3.79E-65 6.78E-65 6.54E-65	1.785-0s 6.785-0s 6.585-0s	7.9681 9.993 9.000
183 185 185	Papler - Heartmood Papler - Septemb	5.4067 9.5963 6.8665 7.6218	2.9900 3.9900 3.4379	1400 1100	5.000 3.900 6.047	56,3127 86,3479 13,7365	5.0%4 8.65% 6.6871	0.0211 0.0056 0.0280	2.009 5.298 3.7989	5.14E-05 9.94E-05 6.94E-05	5.36-0s 9.96-0s 6.96-0s	12.999 12.999 9.992
197	Prime Prime Primenson Claik	5.500 4.690 5.200	3.056 3.7118 2.6212 2.7145	1766 1068 6736	6.9852 6.966 4.9518 5.6823	36.933 99.8639 29.4639	4.960 4.190 4.199	0.0250 0.0260 0.000	3.892 4.4225 1.9933 2.4288	1.16-46 1.16-46 1.16-46 4.96-46	175 de 176 de 176 de 176 de	18.0057 18.0057
190 190 190	Present Oak Word (2) These dissector. De-	5.904 4.045 4.005	2.908 2.908 2.609	67997 67724 67724	5.8182 5.8182 6.4099 4.9953	60.8255 97.5752 45.7510	5.7%5 4.1622 4.2674	03345 03345 03344	3.0566 1.892 2.391	5.79E-65 3.79E-65 4.79E-65	5.76E-00 3.76E-00 4.76E-00	8.8582 3.1174 1.47%
199 198	Nalis Nacional	53897 63915 53015	2.5475 2.6697 3.6514	69799 100%	5.9365 5.930 4.6475	45,3907 60,5400 50,000	5.5308 5.800 5.000	03229 04210 04214	2.260 3.003 2.967	4305-05 5396-05	4365-04 5.795-04	9.3194 9.3184 9.1495
296 297 298	Inquis Inquis Short Willer	5.2207 5.1748 4.961	2.813 2.8158 2.5117	63706 63625 63039	4.3530 4.7628 4.3539	58.4150 58.6924 41.4927	4.998 4.690 4.670	0.0223 0.0222 0.0226	2,9983 2,9983 2,0921	5.5%-65 5.5%-65 3.9%-65	5.53E-0s 5.50E-0s 192E-0s	9.0005 7.4057 7.4968
299 200 200	More Fir Influent Influent help	6.961 7.6678 6.9562 6.9641	3.514 3.516 3.265	1,2746 1,0927 6,9274	7.6327 6.7896 4.3289	96.3055 79.6032 63.2300	7.6768 6.2954 4.6757	0.6962 0.6275 0.6237	4.986 4.098 3.1%5	3.18E-05 7.59E-05 5.99E-05	3.05-0: 7.35-0: 5.95-0:	11.4925 9.9029 7.4894
300 200 204	The bank of the color of the	1,366 4,896 1,475	3.660 2.028 3.602	1216 6398 1260	7.365 4.979 7.588	68: 992 30: 059 71:5221	3,186 4,369 7,469	03119 03179 0.601	3.656 1.516 3.590	5.86E-05 2.85E-05 5.73E-05	5.85 to 2.85 to 5.75 to	\$.300.5 9.2144 8.1905 9.2144 9.1905 9.005
205 205 207	Spece Spece	6.3621 4.3617 5.4413 5.665	2.6007 2.2143 2.8133 2.8133	1961 0163 2963	6.394 4.917 5.951 5.913	59.0008 34.2165 52.5366 55.9812	6,007 4,422 5,268 5,795	0.8237 0.8279 0.8238 0.8227	2,9981 1,796 2,661 2,910	\$ 600-46 3.240-46 4.960-45 5.340-46	5 ME 00 3.24E-00 4.96E-00 5 Vol. on	9.5942 7.3489 8.5971
209 233 231	larges Sprice	3.9855 4.7609 4.7603 5.75**	2.871 2.902 2.875 2.896	6795 6795 6797 63625	3.913 6.5432 4.6994 4.6994	55.9812 41.868 36.5527 45.699	5.796 4.169 4.373 4.885	0.0227 0.0277 0.0200 0.000	2.8132 2.0755 1.8369 2.3463	\$.165.45 3.465.45 3.465.45	5.000 oz 3.000 oz 3.000 oz 4.000 oz	7.565 7.565 7.296
212 213 214	Service Service	5.000 5.000 5.050 4.668	2,990 3,962 2,769 2,600	6963 6963 6968	5.865 4.796 4.317	63 5366 51 356 38 534	5.504 5.602 4.602 4.007	0.8227 0.8227 0.8295	3 1995 2 59% 1,900	4.89E-05 3.62E-05	435 m 436 m	1.000 1.000 1.004 6.014
215 216 217	Sprace Sprace Stark Sprace Ward	5.31% 1.365 6.368	3.2136 4.0058 3.1735	£9539 12190 11025	5.3440 6.5417 6.7905	64.6230 96.7667 62.2730	3,446 1166 6,759	0.0210 0.006 0.006	3,369 4,167 3,124	£125-05 £185-05 5.905-05	6.126-0s 9.196-0s 5.966-0s	8.7656 11.1656 18.1247
218 219 229	Sprace Wand Street Wand Street Page	6.400 5.708	1.000 1.300 1.000	1000 1008 6950	6.200 6.200 5.400	57.1757 74.9516 55.2716	6.28M 6.28M 5.4KS	0.004 0.004 0.004	3.766 3.776 2.77%	5.425-45 3.196-45 5.296-45	5.05 to 1.05 to 5.26 to	9.523 9.900 8.401
221 222 223	Easter Wood East Oak East	5.3345 6.0009 5.5009	2,679 2,792 3,298	6.9874 1.0047 6.9921	5.1916 6.1279 5.1667	44.379 50.4965 50.2089	5.7654 5.1760	0.097 0.039 0.0212	2.291 2.56% 3.501	4.29E-05 4.89E-05 6.69E-05	4.305-0s 4.805-0s 6.865-0s	8.1602 9.2904 8.7904
225 225 226	temporal Control of Con	5.600 6.2054 5.3000	2.5636 3.5803 3.6804	1090 1090 5386	5.7308 6.1117 4.9072	45.4127 66.7109 58.6549	5.4051 6.0768 4.9662	0.029 0.028 0.000	2.2851 3.1554 2.9054	4.315-05 6.325-05 5.495-05	4315-04 6325-04 5-865-04	8.690 9.556 8.1828
228 228 229 23P	Controlled Controlled Controlled	6.5800 6.1040 6.3090 5.6022	2.8564 2.8564 2.7962 3.2562	6.7567 1.6067 1.6052 6.9954	1 9907 6.8917 6.2113 5.7988	56 566) 57.1655 13.6608 67.7008	5.856 5.856 5.876 5.386	0.6179 0.0230 0.0226 0.0247	2.7901 2.8707 3.7902 3.4991	\$ 190-46 \$ 400-46 7.000-46 \$ 400-46	5.195-06 5.415-06 7.005-06 6.415-06	9.2006 9.2006 9.2006
230 232 233	Vine Walnut Walnut	4.3725 5.264 5.369	2.3641 2.5545 2.5600	6.7298 6.9674 6.9777	6.2516 5.1652 5.1658	29.4094 43.5033 44.2283	3849 4807 4807	0.6647 0.6685 0.3186	2.1961 2.22%	2.765.65 4.125.65 4.196.65	2.765-00 4.035-00 4.195-00	5.694 7.663 7.663
216 216 216	Walnut Walnut Walnut	6.4074 4.5087 4.7794	2.3925 2.3975 2.3629	6766 6754 6766	4.3655 4.4068 4.4638	31 3900 31 3400 34 3656	4.092 4.069 4.460	03157 03158 03179	1.504 1.539 1.700	2.962-05 2.976-05 3.246-05	295 m 295 m 336 m	6.9291 6.9870 7.1275
292 298 239	Nobel Walnut	5.6615 4.6955 4.6902	2.954 2.954 2.980	6/462 6/730	5.200 3.400 4.2251	64 3300 50 3665 62 5663	5.168 3.7974 4.1392	0.0210 0.0210 0.0210	3 592 2 592 3 192	6.095-05	47% or 53% or	\$ 5,021 \$ 5,001 \$ 6,000 \$ 1,000 \$ 1,00
260 260 261	Waste Ondeary Physical Waste Square Tender Willers	4.7058 4.9071 11.6402 6.7086	2.8983 2.8988 5.3616 3.0277	679-0 650-2 1,640 1,041	4.3464 4.5917 93.9985 6.4238	61.8542 37.4732 125.826 64.6239	4.462 4.550 11.6777	0.0227 0.0200 0.0099 0.0227	3.1133 1.890 4.320 3.2154	5.8%-05 3.5%-05 1.1%-04 6.0%-05	5.8%-0s 3.5%-0s 1.3%-0s 6.06-0s	7.1472 7.4549 16.4607
266 265 266	Vilor Vilor Vilor	5.595 5.368 5.368 5.901	2.5422 2.5422 2.5353 3.5543	2001 5973 5967 5969	5.6647 5.6500 5.7174	99.9677 54.3998 59.3663	5 1073 5 1073 5 1067 5 5001	0326 0326 0326 0326	2.005 2.726 2.726	5.68E-05 5.13E-05 5.63E-05	5.005 do 5.116 do 5.535 do	9.0799 9.0799 9.0799 9.0799
267 269 269	Widow Wood Back	8.009 6.000 4.500	3.4277 6.3447 2.2704	1,940 1,000 6,760	8.1251 5.6652 6.4627	99.5668 92.500	8.150 6.260 3.852	03319	4.500 4.604 1.461	1.46-05 1.76-05	3.465-0s 3.365-0s	11.9099

## Generating Energy and Greenhouse Gas Inventory Data of Activated Carbon Production Using Machine Learning and Kinetic Based Process Simulation

## **Supporting Information**

Mochen Liao<sup>†</sup>, Stephen Kelley<sup>†</sup>, Yuan Yao<sup>\*,†</sup>

† Department of Forest Biomaterials, North Carolina State University, Raleigh, North Carolina 27695, United States

\* Y. Yao. Phone: (919)-515-8957. E-mail: Yuan Yao@ncsu.edu

Number of pages: 40

Number of figures: 10

Number of tables: 6

## **Table of Contents**

- 1. Literature Review of LCA and Relevant Analysis of Activated Carbon Production
- 2. Modeling Framework Methods
  - 2.1. The Kinetic Model for Pyrolysis
  - 2.2. Artificial Neural Network
  - 2.3. Aspen Plus Simulation
  - 2.4. Other Assumptions
  - 2.5. Sensitivity Analysis
- 3. Woody Biomass Feedstock Characterization Dataset
- 4. Additional Results
  - 4.1. Correlations Between Simulation Results and Biomass Feedstock Properties
  - 4.2. Additional Sensitivity Analysis Results
- 5. References

# 1. Literature Review of LCA and Relevant Analysis for Activated Carbon Production

Previous studies have estimated the energy consumption and Global Warming Potential (GWP) of activated carbon (AC) produced from different feedstock and technological routes as shown in Table S1. All of these data were normalized to the functional unit as 1 kg of AC product. Since different energy sources are provided by different studies, the energy consumption from electricity was converted to primary energy consumption using the efficiency of 32.9%.

**Table S1** Primary Energy Consumption (PEC) and Global Warming Potential (GWP) of Activated Carbon Production (Functional Unit: 1 kg of AC)

Def	System	Eas data als	Activating	DEC (MI/I-a)	GWP	
Ref.	Boundaries	Feedstock	Agent	PEC (MJ/kg)	(kg CO <sub>2</sub> -eq./kg)	
2	Activation	Coal	Steam	30.71 <sup>a</sup>	5.321	
	Gate-to-gate	Coal	Steam	-	11.00	
3	Gate-to-gate	Coal	Steam	196.2ª	-	
4	Gate-to-gate	Coal	Steam	-	8.292	
5	Gate-to-gate	Coal	Steam	-	8.410	
6	Gate-to-gate	Coal	Steam	-	9.423	
7	Gate-to-gate	Coal	Steam	-	9.620	
	Gate-to-gate	Wood	Steam	-	1.790	
8	Drying	Olive Waste	$H_3PO_4$	47.47	2.777	
	Pyrolysis	Olive Waste	$H_3PO_4$	43.67	3.388	
	Impregnation	Olive Waste	H <sub>3</sub> PO <sub>4</sub>	52.15	3.317	
	Gate-to-gate	Olive Waste	$H_3PO_4$	167.6	11.10	
9	Gate-to-gate	Coconut shell	Steam	10.40-11.80 <sup>b</sup>	0.8752-1.000	
10	Drying	Soybean shell	$ZnCl_2$	0.3900 <sup>a</sup>	-	
	Pyrolysis	Soybean shell	$ZnCl_2$	7.560-10.25 <sup>a</sup>	-	
	Impregnation	Soybean shell	$ZnCl_2$	43.16-143.8 <sup>a</sup>	-	
	Gate-to-gate	Soybean shell	$ZnCl_2$	51.68-152.0 <sup>a</sup>	5.860-47.15	
11	Chipping	Wood waste	Steam	2.168	0.003246	
	Drying	Wood waste	Steam	1.252 <sup>a</sup>	0.05661	
	Pyrolysis	Wood waste	Steam	7.613	0.01136	
	Activation	Wood waste	Steam	2.271 <sup>a</sup>	0.01652	
	Gate-to-gate	Wood waste	Steam	13.30 <sup>a</sup>	0.08814	
	Gate-to-gate	Coconut shell	Steam	-	1.150	
12	Chipping	Poplar	Steam	0.2564	-	

Drying	Poplar	Steam	11.36	1.564
Pyrolysis	Poplar	Steam	1.325	0.1821
Activation	Poplar	Steam	0.7791	0.1092
Gate-to-gate	Poplar	Steam	13.72	1.853
Activation	Wood chip	Steam	106.4 <sup>a</sup>	-
Activation	Wood chip	Steam	73.50°	-
Activation	Coal	Steam	141.9 <sup>a</sup>	8.520
Cradle-to-gate	Wood chip	Steam	158.3	8.600
Cradle-to-gate	Coal	Steam	241.6	18.28
Pyrolysis	Hazelnut shell	Steam	23.18 <sup>d</sup>	-
Activation	Hazelnut shell	Steam	$20.00^{d}$	-
Pyrolysis	Coconut shell	Steam	85.64	-
Activation <sup>e</sup>	Coconut shell	Steam	-7.821	-
Drying	Corn stover	Steam	5.950	-
Pyrolysis <sup>f</sup>	Corn stover	Steam	18.45	-
Activation	Corn stover	Steam	11.90	-
Gate-to-gate	Eucalyptus wood	$ZnCl_2$	118.6	8.581
Gate-to-gate	Eucalyptus wood	H <sub>3</sub> PO <sub>4</sub>	153.8	5.575
	Pyrolysis Activation Gate-to-gate Activation Activation Activation Cradle-to-gate Cradle-to-gate Pyrolysis Activation Pyrolysis Activation  Pyrolysis Activation  Activation  Cradle-to-gate Activation  Cradle-to-gate	Pyrolysis Poplar Activation Poplar Gate-to-gate Poplar Activation Wood chip Activation Coal Cradle-to-gate Wood chip Cradle-to-gate Coal Pyrolysis Hazelnut shell Activation Hazelnut shell Pyrolysis Coconut shell Activation Corn stover Pyrolysis Corn stover Activation Corn stover Eucalyptus wood Gate-to-gate Eucalyptus wood	Pyrolysis Poplar Steam Activation Poplar Steam Gate-to-gate Poplar Steam Activation Wood chip Steam Activation Wood chip Steam Activation Coal Steam Cradle-to-gate Wood chip Steam Cradle-to-gate Coal Steam Pyrolysis Hazelnut shell Steam Activation Hazelnut shell Steam Pyrolysis Coconut shell Steam Activation Corn stover Steam Pyrolysis Corn stover Steam Activation Corn stover Steam Activation Corn stover Steam Activation Corn stover Steam Activation Corn stover Steam Gate-to-gate Eucalyptus wood Gate-to-gate Eucalyptus wood Gate-to-gate Eucalyptus wood Gate-to-gate Eucalyptus wood H3PO4	PyrolysisPoplarSteam1.325ActivationPoplarSteam0.7791Gate-to-gatePoplarSteam13.72ActivationWood chipSteam106.4aActivationWood chipSteam73.50cActivationCoalSteam141.9aCradle-to-gateWood chipSteam158.3Cradle-to-gateCoalSteam241.6PyrolysisHazelnut shellSteam23.18dActivationHazelnut shellSteam20.00dPyrolysisCoconut shellSteam85.64ActivationcCoconut shellSteam-7.821DryingCorn stoverSteam5.950PyrolysisfCorn stoverSteam18.45ActivationCorn stoverSteam11.90Gate-to-gateEucalyptus woodZnCl2118.6Gate-to-gateEucalyptus woodH3PO4153.8

<sup>&</sup>lt;sup>a</sup> Assume the electricity is purchased from the grid and the average energy efficiency is 32.9%<sup>1</sup>

Bayer et al. completed the first life cycle assessment (LCA) study of AC production from coal in 2005.<sup>2</sup> Steam activation was implemented to convert hard coal to granular activated carbon (GAC). In this study, 3 metric tons of hard coal and 1,600 kWh were needed to produce 1 ton of GAC. In addition, 330 m<sup>3</sup> of natural gas was combusted to provide 12 tons of steam as the activating agent for 1 ton GAC. The cradle-to-gate GWP of GAC production in this study was 11.0 kg CO<sub>2</sub> eq./kg AC.<sup>2</sup> However, if the GAC can be recycled and used as the feedstock of GAC production, the GWP of the process was reduced to 1.17 kg CO<sub>2</sub> eq./kg AC.<sup>2</sup>

<sup>&</sup>lt;sup>b</sup> The study assumed that flue gas is fully combusted to compensate the energy use

<sup>&</sup>lt;sup>c</sup> Activation in an upscaled reactor with a capacity of 33.3 kg biochar per hour, the result fixed the yield from the LCI of the present study<sup>13</sup>

<sup>&</sup>lt;sup>d</sup> The theoretical energy consumptions presented by the author are considered and normalized to the functional unit

<sup>&</sup>lt;sup>e</sup> The activation step was mixed with some oxygen to achieve partial oxidation

<sup>&</sup>lt;sup>f</sup> The carbonization step applied fast pyrolysis

Many studies then have developed LCA models for coal-based AC based on the process data by Bayer et al.<sup>2</sup> In these studies, the GWP of coal-based AC varied between 8.29-9.62 kg CO<sub>2</sub> eq./kg AC.<sup>4–7</sup> Manda et al. made a comparison between the coal-based GAC and wood-based GAC using the data from Azargohar.<sup>18</sup> The normalized results showed a significant reduction (81.4%) of GWP by changing the feedstock from coal to wood.<sup>7</sup>

A few studies have developed LCA models for AC from biomass. Hjaila et al. developed an LCA model for AC produced from olive waste cake using phosphoric acid as the activation agent. In this study, the system boundary is gate-to-gate, including all processes from the acquisition of olive waste cake to the production of AC. The LCI was developed based on the experimental data and the results were compared to coal-based AC. Arena et al. constructed the LCA of coconut shell based AC production via steam activation with the similar system boundary as Hjaila et al. Different scenarios were developed to compare different energy sources, coconut shell applications, and different byproduct disposal strategies. In this study, the life cycle inventory (LCI) data was developed based on the literature data. In this study highlighted the potential of low-carbon electricity energy sources and environmental management methods in reducing the environmental impact of AC production.

Some researchers have tried to generate detailed process data using experimental studies. Sepúlveda-Cervantes et al. developed an LCA for AC from soybean shell using zinc chloride activation, and the LCI data were developed based on the lab-scale experiments. The experiments and optimal operational conditions for high AC yields were determined by response surface methodology (RSM). A similar approach was used in another study for AC from corn pericarp by potassium hydroxide activation. The brew waste-based AC produced by sulfuric acid activation is also studied by the lab-scale experiments and LCA. In this study, it is

concluded that the impact of AC disposal is ignorable and the impact of untreated brew waste disposal is significant.<sup>21</sup> Gu et al. used steam to activate wood chip derived biochar in a pilot-scale test calciner (1.54 or 1.13 kg/h biochar precursor) and an upscaled commercial calciner (33.6 kg biochar precursor).<sup>13</sup> The cradle-to-gate LCA results demonstrate that the cumulative energy demand (CED) and GWP of wood chip-based AC production are 158.33 MJ/kg AC product and 8.60 kg CO<sub>2</sub> eq,/kg AC product, respectively.<sup>13</sup> The CED and GWP were higher for AC from hard coal.<sup>13</sup> A similar process was established by Kim et al. at a larger scale (4 tons a day).<sup>11</sup> In this study, the steam AC production from wood waste showed lower energy consumption and environmental impact compared with previous LCA studies.<sup>9,11,13</sup>

Some studies have used simulations and/or experiments to quantify the energy consumption of AC production. Hung simulated the AC production using coconut shell and steam activation processes by ChemCAD for an industrial-scale fluidized bed reactor (14.5 tons a day). Since the steam activation was implemented with high-pressure, the activation in the fluidized bed reactor was exothermic rather than endothermic. Another study simulated an industrial scale steam AC production using corn stover feedstock and fast pyrolysis. Sharifan used a lab-scale experiment to investigate the energy consumption of steam AC production from hazelnut shell.

production. These variations could be caused by different system boundaries, feedstock, and technologies (e,g., activation agent as shown in Table S1). Note that a few studies estimated energy consumption based on theoretical energy demand without considering the energy efficiency of energy end uses such as boilers. <sup>14</sup> In this study, the energy and mass balance was simulated in Aspen Plus based on the input variables collected either from literature or ANN models. The energy efficiency of different energy end uses was considered. The energy

Table S1 shows large variations for both primary energy consumption and GWP of AC

efficiency of the reactor was assumed to be 90%, the efficiency of the boiler was assumed to be 82%.  $^{22,23}$ 

## 2. Modeling Framework Methods

The input and output parameters of the modeling framework developed in this study are listed in Table S2.

Table S2 Model Input and Output Parameters

Inpu	t Parameters		
Parameters	Unit		
Feedstock Properties	·		
Carbon Content	wt%, dry basis		
Hydrogen Content	wt%, dry basis		
Oxygen Content	wt%, dry basis		
Ash Content	wt%, dry basis		
Pyrolysis			
Pyrolysis Time	minute		
Pyrolysis Temperature	K		
Activation			
Activation Time	minute		
Activation Temperature	K		
Steam to Biochar Mass Ratio	kg/kg		
Outpu	ıt Parameters		
Parameters	Unit		
Pyrolysis Reactor			
Feedstock – Woody Biomass	kg/kg AC		
Product – Biochar	kg/kg AC		
Syngas – Carbon Dioxide	kg/kg AC		
Syngas – Methane	kg/kg AC		
Thermal Energy Consumption	MJ/kg AC		
Combustor			
Flue Gas – Carbon Dioxide	kg/kg AC		
Flue Gas – Methane	kg/kg AC		
Thermal Energy Recovery	MJ/kg AC		
Steam Boiler			
Water Consumption	kg/kg AC		
Thermal Energy Consumption	MJ/kg AC		
Activation Furnace			
Flue Gas – Carbon Dioxide	kg/kg AC		

Thermal Energy Consumption	MJ/kg AC
Biochar Properties	
Carbon Content	wt%, dry basis
Hydrogen Content	wt%, dry basis
Oxygen Content	wt%, dry basis
Ash Content	wt%, dry basis
Activated Carbon Properties	
Carbon Content	wt%, dry basis
Hydrogen Content	wt%, dry basis
Oxygen Content	wt%, dry basis
Ash Content	wt%, dry basis

## 2.1 The Kinetic Model for Pyrolysis

The reactions in the slow pyrolysis stage were simulated by the multi-step reaction mechanism where biomass is decomposed to lignocellulosic components (cellulose, hemicellulose and lignin). Model compounds were chosen to represent major biomass lignocellulosic components based on literature.<sup>24</sup> Glucose (C<sub>6</sub>H<sub>10</sub>O<sub>5</sub>) was chosen to represent cellulose and xylose (C<sub>5</sub>H<sub>8</sub>O<sub>4</sub>) was chosen to represent hemicellulose. Given the complexity of lignin structure, three types of chemical compounds were chosen to present lignin: Lignin-C, lignin-O and lignin-H. The structures of these compounds are shown in Figure S1.

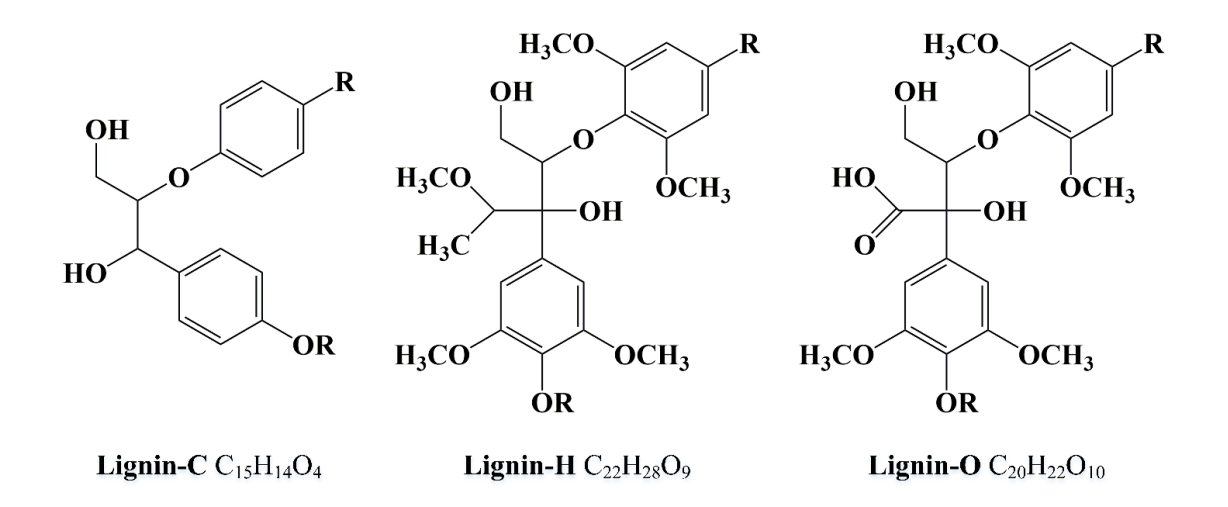


Figure S1 Structures and Chemical Formulas of lignin-C, lignin-O and lignin-H<sup>24</sup>

Since only ultimate analysis data were collected in the present study, the contents of these model compounds should be estimated by the ultimate analysis data. The triangle method developed by Debiagi et al. was used in this study as shown in Figure S2.<sup>25</sup> Considering the chemical composition of model compounds, the contents of different model compounds can be calculated by Equation 1-5. Then the triangle method was used to construct 3 reference components to replace 5 model compounds in order to reduce the degree of freedom in Equation 1-5 to be solvable.

$$x_{CELL}C_{CELL} + x_{HEMI}C_{HEMI} + x_{LIGC}C_{LIGC} + x_{LIGH}C_{LIGH} + x_{LIGO}C_{LIGO} = C_{BIOMASS}$$
 (1)

$$x_{CELL}H_{CELL} + x_{HEMI}H_{HEMI} + x_{LIGC}H_{LIGC} + x_{LIGH}H_{LIGH} + x_{LIGO}H_{LIGO} = H_{BIOMASS}$$
 (2)

$$x_{CELL}O_{CELL} + x_{HEMI}O_{HEMI} + x_{LIGC}O_{LIGC} + x_{LIGH}O_{LIGH} + x_{LIGO}O_{LIGO} = O_{BIOMASS}$$
(3)

$$x_{CELL} + x_{HEMI} + x_{LIGC} + x_{LIGH} + x_{LIGO} = 1 (4)$$

$$x_{CELL}, x_{HEMI}, x_{LIGC}, x_{LIGH}, x_{LIGO} \ge 0 \tag{5}$$

Note for equations:  $x_t$  – Mass fraction of compound t;  $C_t$  – Carbon content of compound t;  $H_t$  – Hydrogen content of compound t;  $O_t$  – Oxygen content of compound t; CELL – Cellulose; HEMI – Hemicellulose; LIGC – Lignin-C; LIGH – Lignin-H; LIGO – Lignin-O.

However, some biomass samples in Figure S2 are outside the model compounds. In this study, the components of model compounds in the samples outside the range were determined by fixing the variables in Equation 1-5 (fix  $x_{CELL}$  and  $x_{HEMI}$ ) by the experimental compositional analysis result of the corresponding biomass sample, and then solve the Equation 1-4. Since some solution may be negative when Equation 5 is not considered, these negative values are set as 0 and the remaining positive values are normalized to satisfy Equation 5.

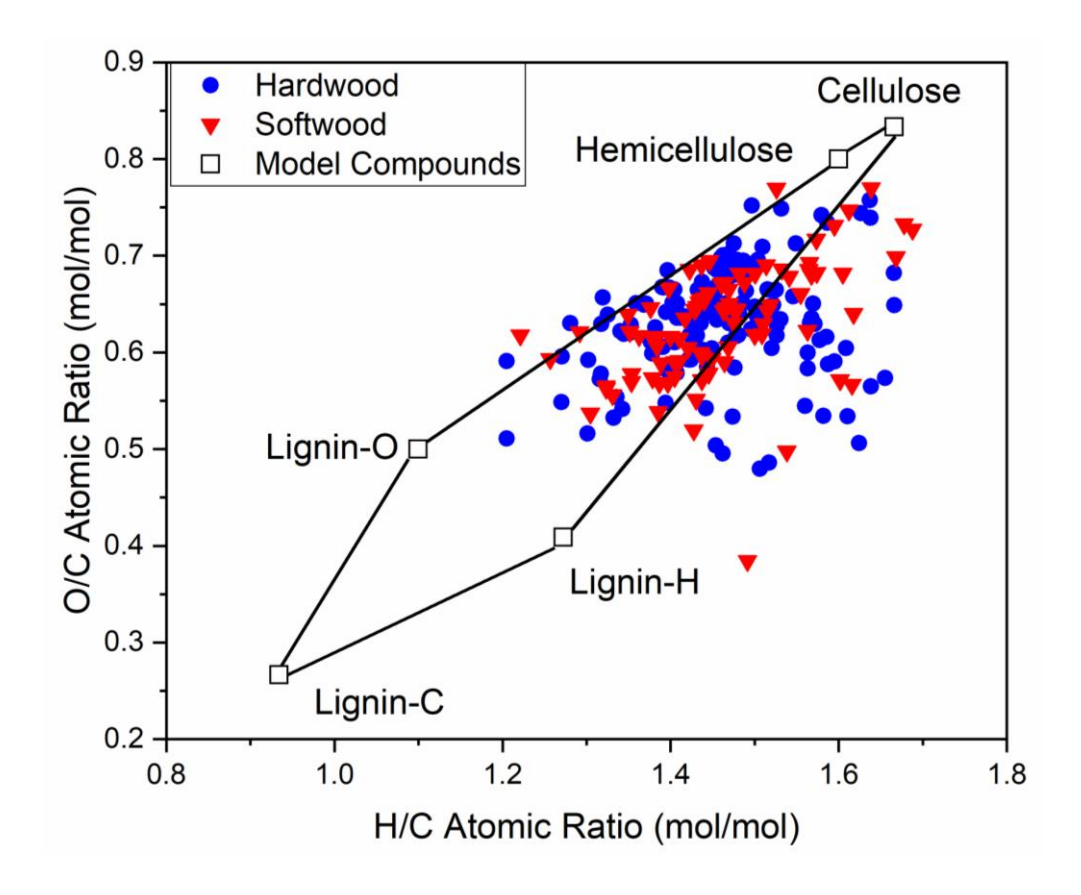


**Figure S2** Biomass characterization representation for model compounds and collected woody biomass samples by Krevelen diagram

After determining the model compounds of the woody biomass samples, the kinetic model was developed based on the multi-step reaction mechanism that provides a series of reactions. The reactants are model compounds and corresponding products. In this study, the pyrolysis kinetic model was based on the model developed by Anca-Couce et al.<sup>26</sup>, which was modified by adding gas-phase tar cracking reactions <sup>27</sup> and fitting the differences between different types of biomass.<sup>28</sup> The reactions, corresponding kinetic parameters, and other relevant parameters are listed in Table S3.

 Table S3 Pyrolysis Kinetic Model Reactions and Parameters<sup>26–28</sup>

Prin	nary	Kinetic Reactions (T = Pyrolysis Temperature	e, t = Pyroly	sis 7	Γime)
Reactions			$k(s^{-1})$	n	E (kJ/mol)
		Cellulose ( $x_{CELL} = 0.1$ )			
CELL	$\rightarrow$	CELLA	4×10 <sup>13</sup>	0	188.37
CELLA	$\rightarrow$	$(1-x_{CELL})*(0.45 \text{ HAA} + 0.2 \text{ GLYOX} + 0.3$	2×10 <sup>6</sup>	0	80.0
		$C_3H_6O + 0.25 \text{ HMFU} + 0.05 H_2 + 0.31 CO +$			
		$0.41 \text{ CO}_2 + 0.4 \text{ CH}_2\text{O} + 0.15 \text{ CH}_3\text{OH} + 0.1$			
		$CH_3CHO + 0.83 H_2O + 0.02 HCOOH + 0.05$			
		$G-H_2 + 0.2 G-CH_4 + 0.61 Char$			
CELLA	$\rightarrow$	$x_{CELL}*(5.5 Char + 4 H2O + 0.5 CO2 + H2)$	$2 \times 10^{6}$	0	80.0
CELLA	$\rightarrow$	$(1-x_{CELL})*(0.45 \text{ HAA} + 0.2 \text{ GLYOX} + 0.3$	4	1	41.86
		$C_3H_6O + 0.25 \text{ HMFU} + 0.05 H_2 + 0.31 \text{ CO} +$			
		$0.41 \text{ CO}_2 + 0.4 \text{ CH}_2\text{O} + 0.15 \text{ CH}_3\text{OH} + 0.1$			
		$CH_3CHO + 0.83 H_2O + 0.02 HCOOH + 0.05$			
		$G-H_2 + 0.2 G-CH_4 + 0.61 Char$			
CELLA	$\rightarrow$	$x_{CELL}*(5.5 \text{ Char} + 4 \text{ H}_2\text{O} + 0.5 \text{ CO}_2 + \text{H}_2)$	4	1	41.86
	Hemi	cellulose (XYHW for hardwood; GMSW for soft			<del></del>
GMSW	$\rightarrow$	0.7  HCE1 + 0.3  HCE2	1×10 <sup>10</sup>	0	129.70
XYHW	$\rightarrow$	0.35  HCE1 + 0.65  HCE2	$1.25 \times 10^{11}$	0	131.38
HCE1	$\rightarrow$	$(1-x_{HCE})*(0.5 CO + 0.5 CO_2 + 0.325 CH_4 +$	1.2×10 <sup>9</sup>	0	125.58
		$0.8 \text{ CH}_2\text{O} + 0.1 \text{ CH}_3\text{OH} + 0.25 \text{ C}_2\text{H}_4 + 0.125$			
		ETOH + $0.025 \text{ H}_2\text{O} + 0.025 \text{ HCOOH} +$			
		$0.275 \text{ G-CO}_2 + 0.4 \text{ G-COH}_2 + 0.125 \text{ G-H}_2 +$			
		0.45 G-CH <sub>3</sub> OH + 0.875 Char)	1.5.1.00		12.7.70
HCE1	$\rightarrow$	$x_{HCE}*(4.5 \text{ Char} + 3 \text{ H}_2\text{O} + 0.5 \text{ CO}_2 + \text{H}_2)$	1.2×10 <sup>9</sup>	0	125.58
HCE1	$\rightarrow$	( HeL) (	0.15	1	33.5
		$0.25 \text{ H}_2\text{O} + 0.05 \text{ HCOOH} + 0.15 \text{ G-CO}_2 +$			
		$0.15 \text{ G-CO} + 1.2 \text{ G-COH}_2 + 0.2 \text{ G-H}_2 +$			
HOE1		$0.625 \text{ G-CH}_4 + 0.375 \text{ G-C}_2\text{H}_4 + 0.875 \text{ Char}$	0.15		22.5
HCE1	$\rightarrow$	$x_{HCE}*(4.5 \text{ Char} + 3 \text{ H}_2\text{O} + 0.5 \text{ CO}_2 + \text{H}_2)$	0.15	1	33.5
HCE1	$\rightarrow$	$(1-x_{HCE})*(0.5 CO + 0.5 CO_2 + 0.325 CH_4 + 0.00 CH_2)*(0.5 CO + 0.5 CO_2 + 0.325 CH_4 + 0.00 CH_2)*(0.5 CO + 0.5 CO_2 + 0.325 CH_4 + 0.00 CH_2)*(0.5 CO + 0.5 CO_2 + 0.325 CH_4 + 0.00 CH_2)*(0.5 CO + 0.5 CO_2 + 0.325 CH_4 + 0.00 CH_2)*(0.5 CO + 0.5 CO_2 + 0.325 CH_4 + 0.00 CH_2)*(0.5 CO + 0.5 CO_2 + 0.325 CH_4 + 0.00 CH_2)*(0.5 CO + 0.5 CO_2 + 0.325 CH_4 + 0.00 CH_2)*(0.5 CO_2 + 0.325 CH_4)*(0.5 CO_2 + 0.32$	3	1	46.05
		$0.8 \text{ CH}_2\text{O} + 0.1 \text{ CH}_3\text{OH} + 0.25 \text{ C}_2\text{H}_4 + 0.125$			
		ETOH + $0.025 \text{ H}_2\text{O} + 0.025 \text{ HCOOH} +$			
		$0.275 \text{ G-CO}_2 + 0.4 \text{ G-COH}_2 + 0.125 \text{ G-H}_2 + 0.45 \text{ G-CH}_2 + 0.875 \text{ Ghar}$			
HCE1		$0.45 \text{ G-CH}_3\text{OH} + 0.875 \text{ Char}$	3	1	16.05
HCE1	<b>→</b>	$x_{HCE}*(4.5 \text{ Char} + 3 \text{ H}_2\text{O} + 0.5 \text{ CO}_2 + \text{H}_2)$			46.05
HCE2	$\rightarrow$	$(1-x_{HCE})^*(0.2 \text{ HAA} + 0.175 \text{ CO} + 0.275 \text{ CO}_2$	5×10 <sup>9</sup>	0	138.14
		$+0.5 \text{ CH}_2\text{O} + 0.1 \text{ ETOH} + 0.2 \text{ H}_2\text{O} + 0.025$			
		HCOOH + 0.4 G-CO <sub>2</sub> + 0.925 G-COH <sub>2</sub> + 0.25 G-CH <sub>4</sub> + 0.3 G+CH <sub>3</sub> OH + 0.275 G-			
		$0.23 \text{ G-CH}_4 + 0.3 \text{ G+CH}_3 \text{ OH} + 0.273 \text{ G-}$ $C_2H_4 + \text{Char}$			
HCE2	$\rightarrow$	$x_{HCE}*(4.5 \text{ Char} + 3 \text{ H}_2\text{O} + 0.5 \text{ CO}_2 + \text{H}_2)$	5×10 <sup>9</sup>	0	138.14
11002		AHOE (7.3 CHai + 3 1120 + 0.3 CO2 + 112)	510	U	130.17

		$Lignin (x_{LIG} = 0.3)$			
LIG-C	$\rightarrow$	0.35 LIG-CC + 0.1 pCoumaryl + 0.08 PHENOL +0.32 CO + 0.3 CH <sub>2</sub> O + H <sub>2</sub> O + 0.7 G-COH <sub>2</sub> + 0.495 G-CH <sub>4</sub> + 0.41 G-C <sub>2</sub> H <sub>4</sub> + 5.735 Char	1.33×10 <sup>15</sup>	0	203.02
LIG-H	$\rightarrow$	LIG-OH + 0.25 HAA + 0.5 C <sub>3</sub> H <sub>6</sub> O + 0.5 G- C <sub>2</sub> H <sub>4</sub>	6.7×10 <sup>12</sup>	0	156.97
LIG-O	$\rightarrow$	$LIG-OH + CO_2$	$3.3 \times 10^{8}$	0	106.74
LIG-CC	$\rightarrow$	(1-x <sub>LIG</sub> )*(0.35 HAA + 0.3 pCoumaryl + 0.2 PHENOL + 0.4 CO + 0.65 CH <sub>4</sub> + 0.6 C <sub>2</sub> H <sub>4</sub> + 0.7 H <sub>2</sub> O + 0.4 G-CO + G-COH <sub>2</sub> + 6.75 Char)	3×10 <sup>7</sup>	0	131.86
LIG-CC	$\rightarrow$	$x_{LIG}*(15 Char + 4 H2O + 3 H2)$	3×10 <sup>7</sup>	0	131.86
LIG-OH	$\rightarrow$	LIG + 0.55 CO + 0.05 CO <sub>2</sub> + 0.1 CH <sub>4</sub> + 0.6 CH <sub>3</sub> OH + 0.9 H <sub>2</sub> O + 0.05 HCOOH + 0.6 G- CO + 0.85 G-COH <sub>2</sub> + 0.1 G-H <sub>2</sub> + 0.35 G- CH <sub>4</sub> + 0.3 G-CH <sub>3</sub> OH + 0.2 G-C <sub>2</sub> H <sub>4</sub> + 4.15 Char	1×10 <sup>8</sup>	0	125.58
LIG	$\rightarrow$	(1-x <sub>LIG</sub> )*FE2MACR	4	1	50.2
LIG	$\rightarrow$	$x_{LIG}*(10.5 \text{ Char} + 3 \text{ H}_2\text{O} + 0.5 \text{ CO}_2 + 3 \text{ H}_2)$	4	1	50.2
LIG	$\rightarrow$	(1-x <sub>LIG</sub> )*(0.2 C3H6O + CO + 0.2 CH <sub>4</sub> + 0.2 CH <sub>2</sub> O + 0.4 CH <sub>3</sub> OH + 0.2 CH <sub>3</sub> CHO + 0.95 H <sub>2</sub> O + 0.05 HCOOH + 0.45 G-CO + 0.5 G- COH <sub>2</sub> + 0.4 CH <sub>4</sub> + 0.65 C <sub>2</sub> H <sub>4</sub> + 5.5 Char)	4×10 <sup>8</sup>	0	125.58
LIG	$\rightarrow$	$x_{LIG}*(10.5 \text{ Char} + 3 \text{ H}_2\text{O} + 0.5 \text{ CO}_2 + 3 \text{ H}_2)$	4×10 <sup>8</sup>	0	125.58
LIG	$\rightarrow$	(1-x <sub>LIG</sub> )*(0.4 CO + 0.2 CH <sub>4</sub> + 0.4 CH <sub>2</sub> O + 0.6 H <sub>2</sub> O + 0.2 G-CO + 2 G-COH <sub>2</sub> + 0.4 CH <sub>4</sub> + 0.4 G-CH <sub>3</sub> OH + 0.5 C <sub>2</sub> H <sub>4</sub> + 6 Char)	0.083	1	33.5
LIG	$\rightarrow$	$x_{LIG}*(10.5 \text{ Char} + 3 \text{ H}_2\text{O} + 0.5 \text{ CO}_2 + 3 \text{ H}_2)$	0.083	1	33.5
	1	$Metaplastic (x_G = 0.4)$	L		I.
G-CO <sub>2</sub>	$\rightarrow$	$CO_2$	4×10 <sup>5</sup>	0	100.46
G-CO	$\rightarrow$	$(1-x_G)*CO + x_G*(0.5 Char + 0.5 CO_2)$	3×10 <sup>13</sup>	0	209.3
G-COH <sub>2</sub>	$\rightarrow$	0.75 G2-COH <sub>2</sub> + 0.25*(H <sub>2</sub> + 0.5 CO + 0.25 CO <sub>2</sub> + 0.25 Char)	1×10 <sup>6</sup>	0	100.46
G-H <sub>2</sub>	$\rightarrow$	$H_2$	1×10 <sup>12</sup>	0	313.96
G-CH <sub>4</sub>	$\rightarrow$	CH <sub>4</sub>	2×10 <sup>13</sup>	0	300.0
G-CH <sub>3</sub> OH	$\rightarrow$	$(1-x_G)*CH_3OH + x_G*(Char + H_2O + H_2)$	1.2×10 <sup>13</sup>	0	209.3
G-C <sub>2</sub> H <sub>4</sub>	$\rightarrow$	$0.3 C_2H_4 + 0.7 CH_4 + 0.7 Char$	1×10 <sup>6</sup>	0	100.46
G2-COH <sub>2</sub>	$\rightarrow$	$0.2 \text{ G3-COH}_2 + 0.8*(\text{H}_2 + \text{CO})$	1.5×10 <sup>9</sup>	0	209.3
		Cracking Reactions (T = Pyrolysis Temperatu	re, t = Gas	 Resi	dence Time)
		$s = 3.08 \times 10^3 \text{ s}^{-1}, n = 0, E = 66.3 \text{ kJ/mol}$			
HAA	$\rightarrow$	$1.5 \text{ H}_2 + 1.5 \text{ CO} + 0.25 \text{ CO}_2 + 0.25 \text{ CH}_4$			
GLYOX	$\rightarrow$	$H_2 + 2CO$			

C <sub>3</sub> H <sub>6</sub> O	$\rightarrow$	$0.5 \text{ CO}_2 + \text{C}_2\text{H}_4 + 0.5 \text{ CH}_4$
C <sub>3</sub> H <sub>4</sub> O <sub>2</sub>	$\rightarrow$	$CO_2 + C_2H_4$
HMFU	$\rightarrow$	$3 \text{ CO} + 1.5 \text{ C}_2\text{H}_4$
pCoumaryl	$\rightarrow$	2 CO + 1.5 C <sub>2</sub> H <sub>4</sub> + CH <sub>4</sub> + 3 Char
PHENOL	$\rightarrow$	$CO + C_2H_4 + 0.5 CH_4 + 2.5 Char$
FE2MACR	$\rightarrow$	4 CO + C <sub>2</sub> H <sub>4</sub> + 2 CH <sub>4</sub> + 3 Char
CH <sub>2</sub> O	$\rightarrow$	$H_2 + CO$
CH <sub>3</sub> OH	$\rightarrow$	$1.5 \text{ H}_2 + 0.5 \text{ CO} + 0.25 \text{ CO}_2 + 0.25 \text{ CH}_4$
CH <sub>3</sub> CHO	$\rightarrow$	$CO + CH_4$
ЕТОН	$\rightarrow$	$H_2 + CO + CH_4$
НСООН	$\rightarrow$	$H_2 + CO_2$

Note1 (Solid): CELL – Cellulose; CELLA – Activated cellulose; XYHW – Hardwood hemicellulose; GMSW – Softwood hemicellulose; HCEA1 or HCEA2 – Activated hemicellulose 1 or 2; LIG-C – Carbon rich lignin (Lignin-C); LIG-H – Hydrogen rich lignin (Lignin-H); LIG-O – Oxygen rich lignin (Lignin-O); LIG-CC – Carbon rich lignin 2; LIG-OH – OH rich lignin; LIG – Intermediate lignin; G-X – Trapped substance X; Char – Biochar.

Note2 (Volatiles): HAA – Hydroxyacetaldehyde acid; HCOOH – Formic acid; GLYOX – Glyoxal; C<sub>3</sub>H<sub>6</sub>O – Acetone; C<sub>3</sub>H<sub>4</sub>O<sub>2</sub> – Propanedial; HMFU – 5-hydroxymethyl-furfural; pCoumaryl – Paracoumaryl alcohol; PHENOL – Phenol; FE2MACR – Sinapaldehyde; CH<sub>2</sub>O – Formaldehyde; ETOH – Ethanol.

#### 2.2 Artificial Neural Network

The integration of machine learning (ML) methods and LCA has been developed in recent years. Nabavi-Pelesaraei et al. integrated artificial neural network (ANN) models with LCA to estimate process energy output and environmental impacts of agricultural processes (e.g., paddy and sugarcane production).<sup>29,30</sup> However, this type of integration of LCA and ML is still limited by data availability. Therefore in this section, we coupled the ML with the simulation model to provide the required data for LCA, since the availability of the combination of ML and process simulation has been identified by the previous studies.<sup>31</sup>

In the presented study, ANN was used to predict the total yield of the overall steam AC production for different biomass feedstocks. The details of the trained ANN were documented in the authors' previous publication.<sup>32</sup> Then the yield of the biochar-to-AC process can be determined using Equation 6 and the biomass-to-biochar yield provided by the kinetic model. In

addition, it was assumed that the ash content from the biomass feedstock is retained in the biochar and the AC. Hence, the burn-off rate of organic components in biochar, which is the ratio of mass loss in the activation stage to the ash-free biochar mass, should be calculated by Equation 6.

$$Burn - off = (1 - \frac{Total\ AC\ Yield\ -\ Ash\ Content}{Pyrolysis\ Yield\ -\ Ash\ Content}) \times 100\% \tag{6}$$

The main reaction in the steam activation is shown in Equation 7:

$$C + H_2O \to H_2 + CO \tag{7}$$

Previous LCA of steam AC production assumed that only steam-carbon reaction exists in the activation process and as a result, the activation flue gas should not contain any CO<sub>2</sub>. However, experimental studies showed significant carbon dioxide content in the activation flue gas, which contradicts with this assumption. One study indicated that different types of reactions may happen in the steam activation process, including water-gas shift reaction (Equation 8), methanation reactions and steam-reforming reactions (Equation 9), and Boudouard reaction (Equation 10). However, the extent of these reactions in the specified temperature and time was hard to determine. Therefore, in this study, the reaction formula developed by Martín-Gullón et al. was used, which covered all products occurred in Equation 8-10. Even the aforementioned formula was established by fitting the data from bituminous coal-based AC production, it can be transferred to the biomass-based AC production due to the similar reaction mechanism of steam activation for coal and biochar.

$$CO + H_2O \to H_2 + CO_2$$
 (8)

$$C + 2H_2 \rightarrow CH_4; 2CO + 2H_2 \rightarrow CH_4 + CO_2; CO + 3H_2 \leftrightarrow CH_4 + H_2O; CO + 4H_2 \leftrightarrow CH_4 + 2H_2O \quad (9)$$

 $C + CO_2 \leftrightarrow 2CO \tag{10}$ 

## 2.3 Aspen Plus Simulation

The pyrolysis kinetic model and ANN provide essential data inputs of Aspen Plus process simulation models. Aspen Plus software provides different types of reactor, including RYield, RGibbs, RCSTIR, RStoic and RBatch.<sup>35</sup> In this study, RBatch is chosen as it is a common reactor type for pyrolysis simulations.<sup>36</sup> The process flowsheet of pyrolysis was shown in Figure S3.

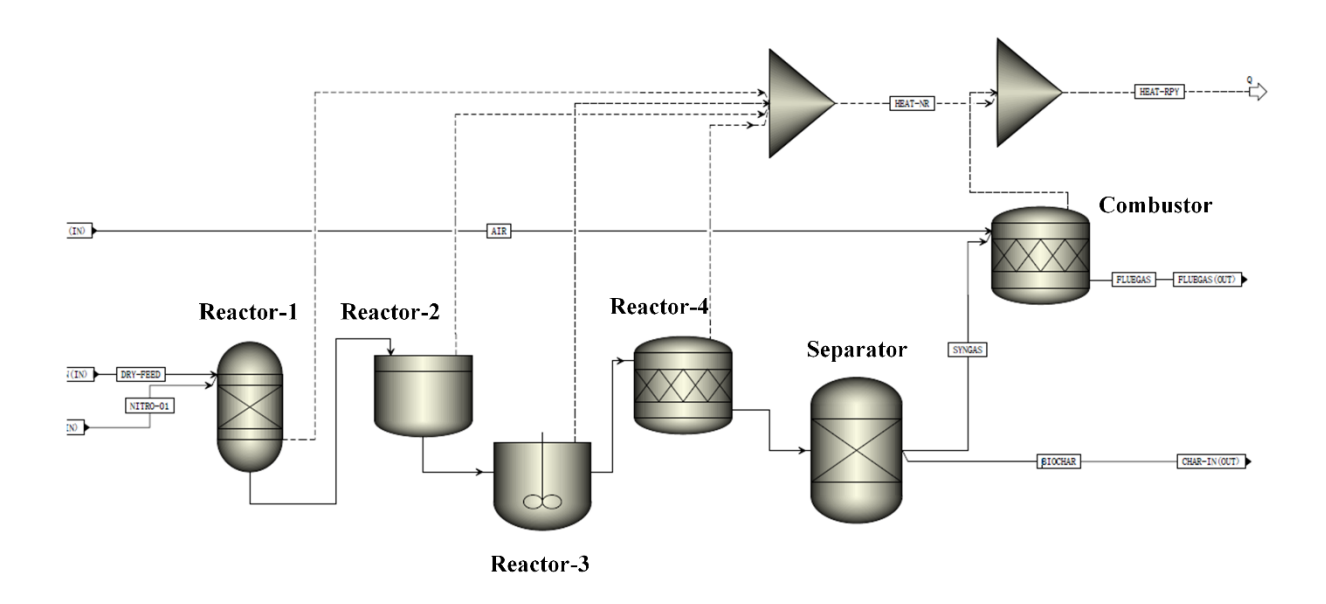


Figure S3 Process Flowsheet of Pyrolysis

The pyrolysis reaction process consists of four continuous sub-reactors. The Reactor-1, which is set as RYield reactor, decomposed the biomass feedstock into model compounds and ash content. Then the primary kinetic reactions mentioned in Table S3 were implemented in the Reactor-2 (RBatch). The Reactor-3 calculated gas-phase tar cracking reactions in Table S3.

Finally, the RStoic Reactor-4 converted the remaining metaplastic components into biochar. After the pyrolysis kinetic reactions, the Separator unit moved the solid components out and the hot volatiles was sent to the Combustor unit. The Combustor unit was set as RStoic, which oxidized all of the combustible components in the syngas with the burn-off rate of 80%. The heat generated from the Combustor unit was recovered to compensate for the energy consumption of Reactor units. The components of output flows from Separator and Combustor were tracked to generate the Life Cycle Inventory (LCI) data.

The assumed reaction provided by Martín-Gullón et al. can be directly simulated by the RStoic reactor in Aspen Plus, thus the process flowsheet of steam activation of biochar can be constructed, which is shown in Figure S4. The steam boiler rises the temperature of water from the room temperature to the desired temperature in order to generate the superheated steam. The Activation Reactor unit was set as the RStoic reactor, which implemented the reaction between water and biochar with the predefined reaction extent. Detailed information of the unit operations presented in Figure S3 and S4 are given in Table S4.

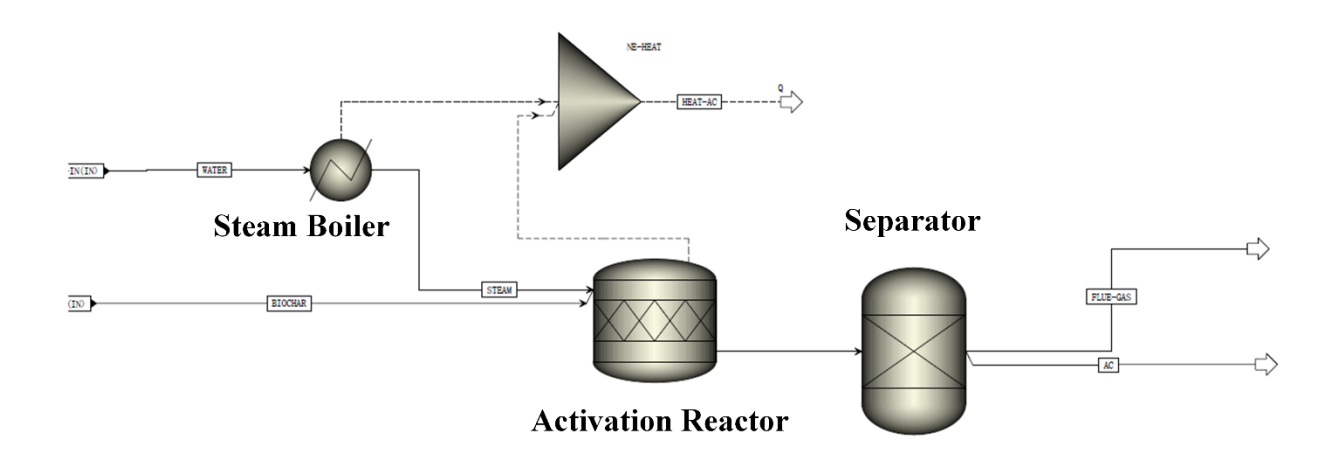


Figure S4 Process Flowsheet of Activation

Table S4 Parameter Settings for Unit Operators in the Aspen Process Simulation

Parameters	Values				
Figure S3 – Reactor-1					
Reactor Type	RYield				
Temperature <sup>a</sup>	773 K				
Pressure	1 atm				
Reactions	Conversion of biomass to lignocellulosic components and ash				
Figure S3 – Reactor-2	•				
Reactor Type	RBatch				
Temperature <sup>a</sup>	773 K				
Pressure	1 atm				
Catalyst Loading	0 kg				
Reaction time <sup>b</sup>	3600 s				
Reactions	Primary kinetic reactions in Table S3				
Figure S3 – Reactor-3					
Reactor Type	RCSTR				
Temperature <sup>a</sup>	773 K				
Pressure	1 atm				
Residence Time	2 s				
Reactions	Gas phase tar cracking reactions in Table S3				
Figure S3 – Reactor-4					
Reactor Type	RStoic				
Temperature <sup>a</sup>	773 K				
Pressure	1 atm				
Reactions	Conversion of trapped substances (see notes in Table S3) to biochar				
Figure S4 – Activation Reactor					
Temperature <sup>c</sup>	1073 K				
Pressure	1 atm				
Reactions	Activation reactions				
(B) 1 :	: T 11 C2 C 4 : : : : T 11 C2				

<sup>&</sup>lt;sup>a</sup> Pyrolysis temperature in Table S2; <sup>b</sup> Pyrolysis time in Table S2; <sup>c</sup> Activation temperature in Table S2. Note: The values for parameters that are indiced <sup>a,b,c</sup> are the default value.

The Aspen Simulation Workbook was used to automatically inputs the results of ANN models into the Aspen Plus simulation. Aspen Simulation Workbook was the plugin in the Microsoft excel which allows running simulations with different input parameters automatically. The thermal efficiencies of reactors and pyrolysis combustion rate can be seen in Table 1 in the manuscript. The combustion rate is set as 80% due to the heavy oil products from slow pyrolysis that is hard to combust. By fitting the characterization of products from slow pyrolysis of beech

at 500°C, around 20% of the non-solid products cannot be identified, which are considered as the heavy oil products.<sup>36</sup> Therefore the combustion rate is set as 80% in the present study.

When the simulation is finished, LCI of AC production can be established from the simulation results. An example AC production process material and energy flow chart that is generated from Aspen Plus simulation data is shown in Figure S5, and additional LCI information of the simulation scenarios are summarized in the attached excel file.

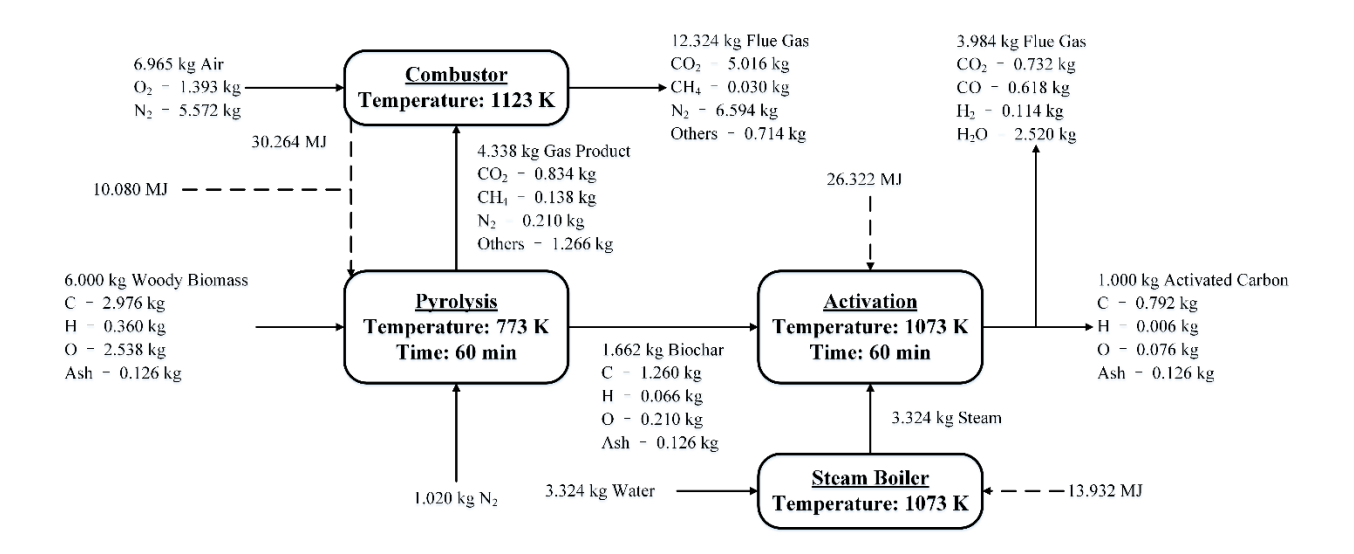


Figure S5 An Example of Material and Energy Flows of AC Production

## 2.4 Other Assumptions

The thermodynamic properties of the substances were collected from the Aspen Plus databank or the report from National Renewable Energy Laboratory (NREL).<sup>37,38</sup> The higher heating value (HHV) of solid compounds, a key parameter needed to calculate the DHSFRM parameters for process simulation<sup>39</sup>, was calculated by Dulong's equation (Equation 11), where  $m_C$ ,  $m_H$  and  $m_O$  represent the weight percentage (wt.%) of carbon, hydrogen, and oxygen in the biochar or AC.<sup>40</sup>

$$HHV(MJ/kg) = 0.338m_C + 1.442m_H - 0.182m_O$$
(11)

For the HHV of woody biomass, the equation was modified by Demirbaş in order to reflects the effect of considerable nitrogen content in the biomass.<sup>41</sup> The updated equation was shown in Equation 12:

$$HHV(MJ/kg) = 0.335m_C + 1.423m_H - 0.154m_O - 0.145m_N$$
(12)

Based on the previous equations, the ultimate analysis data of biochar and AC are needed. The pyrolysis kinetic model generates some metaplastic substances which trap the volatile components into the biochar. Therefore, based on the method developed by Debiagi et al., the carbon, hydrogen and oxygen content of biochar can be determined by normalizing the elemental composition of char (elemental carbon) and trapped substances (containing carbon, hydrogen, and oxygen).<sup>28</sup> In this study, the elemental compositions of AC were derived from the biochar by Equation 13-15, whose constants are fitted by the literature data.<sup>42</sup> All these data are in the dryash-free basis.

$$C_{AC} = 1.097 * C_{Biochar} \tag{13}$$

$$H_{AC} = 0.215 * H_{Biochar} \tag{14}$$

$$O_{AC} = 100 - C_{Biochar} - H_{Biochar} \tag{15}$$

With these equations, the produced AC contains higher carbon content and lower hydrogen content, which is consistent with the literature. One limitation is that Equation 13-15 were derived based on activation temperature – 1073K, activation time – 60 min, and steam to biochar ratio – 2 kg/kg. More experimental data are needed if the operational conditions are changed.

Besides, the Aspen Plus software also requires the parameters for the calculation of viscosity, which are categorized as VSPOLY parameters. In the present study, the VSPOLY parameters for

the substances were assumed to be either the default values in Aspen Plus database or from literature data. 37,38,43

## 2.5 Sensitivity Analysis

The sensitivity analysis was conducted in this study using the baseline and upper and lower bounds of parameters as shown in Table S5. For feedstock characteristics, the average value were used as baselines. For the operational conditions, the typical values used in literature were used. The upper and lower bound of biomass characteristics were determined based on the maximum and minimum value of feedstock datasets. The upper bound and lower bound of operational conditions were establish by referencing several literature conditions. 32,44–47

Table S5 The baseline and ranges of input parameters used in the sensitivity analysis

	Baseline	Lower Bound	Upper Bound	Ref.
Carbon Content (wt%)	49.59	42.55	55.52	а
Hydrogen Content (wt%)	6.02	5.05	7.19	а
Ash Content (wt%)	2.14	0.1	10.62	а
Pyrolysis Temperature (°C)	500	300	700	44
Pyrolysis Time (min)	60	10	120	32
Activation Temperature (°C)	800	750	900	45
Activation Time (min)	60	45	75	46
Steam to Biochar Ratio (kg/kg)	2	1.35	5.4	47

<sup>&</sup>lt;sup>a</sup> Based on the dataset

## 3. Woody Biomass Feedstock Characterization Dataset

In this study, large datasets of woody biomass characterization samples were collected from different databases and publications as shown in Table S6. The lignocellulosic components calculated based on ultimate analysis data and the triangle method were also presented in the

same table. There are four different data sources in this study: The biomass feedstock composition and property database from National Renewable Energy Laboratory<sup>48</sup>, the bioenergy feedstock library from Idaho National Laboratory<sup>49</sup>, the Phyllis2 database for biomass and waste from ECN<sup>50</sup>, and other literature references.<sup>25</sup> These data were used to create different simulation scenarios in order to understand the impacts of biomass feedstock. All these data are listed in Table S6, which can be useful in replicating the results and becoming the basis of further researches.

 Table S6 Woody Biomass Feedstock Characterization Dataset

		]	Raw Data	a (dry ba	sis, wt%)	)	Triangle Method Result (dry basis, wt%)				
Feedstock	Type	C	Н	О	N	Ash	CELL	HEMI	LIGC	LIGH	LIGO
Data from Na	tional R	enewable		aborator	$v^{48}$						
Ailanthus	HW	50.77	6.36	42.05	0.31	0.51	42.87	30.71	6.27	1.22	18.43
Pistachio	HW	48.79	5.91	43.41	0.56	1.28	45.08	32.04	2.44	0.49	18.66
White Ash	HW	49.75	6.91	43.04	0.00	0.30	45.22	32.06	2.88	0.54	19.00
Manzanita	HW	48.27	5.95	44.77	0.17	0.82	47.03	33.28	0.66	0.20	18.02
Robinia	HW	50.86	5.72	42.04	0.57	0.80	42.07	29.63	7.90	1.20	18.40
Teak	HW	51.60	6.00	40.04	0.26	2.10	39.62	26.58	14.33	1.21	16.17
Almond	HW	48.31	6.00	42.73	0.68	2.24	48.56	32.37	2.23	0.00	14.59
Oak	HW	49.83	6.23	42.99	0.13	0.82	44.42	29.57	4.67	0.27	20.25
Almond	HW	47.12	5.97	40.07	1.19	5.55	43.14	28.23	0.06	11.70	11.30
Cherry tree	HW	50.03	5.87	42.41	0.31	1.36	43.32	27.94	6.93	0.25	20.19
Mixed	HW	49.09	5.93	42.49	0.33	2.10	44.23	27.89	5.32	0.09	20.38
Prune	HW	50.35	6.69	39.66	1.30	1.90	41.51	25.40	12.58	0.24	18.36
Spruce	SW	49.60	5.63	40.81	0.20	3.66	39.85	23.64	0.13	9.52	23.20
Eucalyptus	HW	48.20	5.30	42.20	0.00	4.30	44.03	26.11	5.83	0.00	19.73
Mixed	SW	50.30	5.80	40.65	0.42	2.80	37.87	21.77	0.18	6.82	30.57
Oak	HW	50.93	5.96	41.46	0.20	1.30	43.32	24.58	12.29	0.02	18.49
Spruce	SW	50.05	5.63	42.65	0.10	1.48	45.85	26.00	1.77	21.10	3.79
Olive	HW	51.38	6.32	40.02	0.45	1.69	39.01	22.06	4.29	31.71	1.25
Spruce	SW	50.90	6.40	42.00	0.00	0.70	44.95	25.07	2.99	21.57	4.72
Cedar	SW	48.80	6.40	44.40	0.00	0.40	53.77	29.55	0.00	11.95	4.33
Maple	HW	49.54	6.00	43.84	0.10	0.50	50.18	27.46	0.58	14.59	6.69
Larch	SW	50.67	6.38	42.51	0.00	0.45	46.46	25.18	2.99	17.77	7.16
Pine	SW	52.13	6.36	41.01	0.07	0.37	41.57	22.45	7.55	24.55	3.51
Douglas Fir	SW	52.30	6.30	40.32	0.10	0.98	39.97	21.35	9.67	26.08	1.94

Pine	SW	48.40	6.31	44.23	0.21	0.82	53.57	28.61	0.00	10.41	6.58
Olive	HW	45.15	5.63	37.56	1.55	10.01	41.45	22.09	3.66	15.70	7.10
Cotton	HW	48.48	6.12	41.48	0.97	2.85	46.80	24.91	2.14	14.66	8.64
Cotton	HW	48.48	6.12	41.48	0.97	2.85	46.80	24.91	2.14	14.66	8.64
Olive	HW	48.71	6.18	42.16	0.52	2.39	47.91	25.49	1.49	13.85	8.86
Pine	SW	50.10	6.00	38.17	0.10	5.63	37.33	19.84	10.39	26.02	0.80
Spruce	SW	48.82	5.84	42.44	0.17	2.73	47.44	24.95	1.85	13.46	9.57
Babassu	HW	50.38	5.38	42.35	0.26	1.59	44.75	23.44	5.31	16.83	8.08
Almond	HW	47.15	5.91	40.04	1.20	5.61	44.92	23.51	2.88	13.86	9.23
Cocoa	HW	46.31	5.57	36.12	3.21	8.60	38.30	19.99	9.70	20.21	3.20
Mulberry	HW	49.84	6.14	41.00	0.42	2.60	44.22	23.04	5.58	16.44	8.12
Ailanthus	HW	49.50	6.20	42.30	0.30	1.70	47.22	24.56	2.68	13.66	10.17
Birch	SW	48.74	6.26	44.09	0.19	0.54	52.28	26.98	0.00	9.83	10.38
Pine	SW	51.99	6.28	41.16	0.14	0.41	42.94	22.14	9.86	19.35	5.30
Olive	HW	50.77	5.90	37.07	1.36	4.61	34.30	17.53	13.78	29.78	0.00
Olive	HW	50.18	6.85	37.78	1.11	4.00	40.10	20.46	12.93	20.35	2.16
Willow	HW	49.29	5.98	42.72	0.57	1.38	48.03	24.39	2.42	11.89	11.89
Poplar	HW	50.19	6.06	40.43	0.60	2.70	43.33	21.81	8.95	15.67	7.54
Willow	HW	48.50	6.12	43.00	0.50	1.86	49.67	24.92	0.75	9.79	13.01
Douglas Fir	SW	50.63	6.23	42.54	0.12	0.47	46.78	23.38	5.02	12.79	11.56
Pine	SW	51.85	6.21	41.23	0.13	0.42	43.85	21.83	11.22	16.22	6.46
Pine	SW	51.48	6.16	41.14	0.16	0.97	43.97	21.75	10.86	15.29	7.16
Pistachio	HW	49.55	6.12	42.32	0.62	1.27	47.45	23.43	3.73	11.16	12.96
Peach	HW	51.21	6.14	41.14	0.40	1.07	44.27	21.78	10.43	14.56	7.89
Unidentified	SW	52.10	6.10	39.90	0.20	1.70	42.04	20.59	16.97	17.48	1.22
Cedar	SW	52.74	6.14	39.98	0.10	1.03	41.92	20.42	18.59	18.04	0.00
Almond	HW	48.60	5.70	37.51	0.62	7.46	40.05	19.49	15.30	15.39	2.31
Walnut	HW	51.00	6.04	40.31	0.78	1.78	43.46	21.13	13.01	14.68	5.94
Poplar	HW	49.93	6.10	42.26	0.29	1.36	46.94	22.76	4.97	10.80	13.18
Poplar	HW	47.67	6.15	45.29	0.20	0.68	56.36	27.22	0.00	5.04	10.70
Camphor	HW	50.30	6.10	42.50	0.10	0.80	47.24	22.38	5.72	9.90	13.96
Willow	HW	48.98	5.99	42.09	0.65	2.24	47.46	22.47	3.90	8.97	14.96
Palm	HW	47.28	6.25	38.82	2.83	4.59	41.83	33.02	3.91	2.92	13.73
Unidentified	HW	47.10	5.52	36.92	0.43	9.94	40.16	18.97	14.36	12.11	4.45
Fir	SW	50.35	6.14	43.18	0.05	0.28	48.30	22.74	4.32	9.02	15.35
Peanut	HW	45.77	5.46	39.56	1.63	7.46	45.05	21.20	3.60	8.17	14.52
Beech	SW	48.37	6.10	44.51	0.34	0.65	53.12	24.94	0.00	5.77	15.52
Spruce	SW	50.17	5.94	40.44	0.42	3.01	44.29	20.78	11.70	11.30	8.91
Eucalyptus	HW	50.43	6.01	41.53	0.17	1.76	45.85	21.24	9.33	9.87	11.95
Eucalyptus	HW	50.50	6.02	41.59	0.27	1.58	45.95	21.28	9.33	9.86	12.00
Maple	HW	50.64	6.02	41.74	0.25	1.35	46.16	21.25	9.44	9.58	12.23

Olive	HW	52.70	5.90	38.04	1.05	2.06	38.29	17.50	23.43	18.72	0.00
Oak	HW	48.82	6.06	44.17	0.15	0.78	51.25	23.37	0.04	5.80	18.75
Maple	HW	50.60	6.00	41.70	0.30	1.40	46.27	21.04	9.84	9.04	12.40
Walnut	HW	53.66	6.50	36.04	1.34	2.36	37.83	29.83	14.76	12.40	2.81
Unidentified	HW	50.48	6.04	42.43	0.17	0.78	47.34	21.51	7.31	8.35	14.71
Birch	SW	49.85	6.72	42.54	0.10	0.29	49.02	22.25	3.82	7.23	17.38
Kenaf (italy)	HW	46.60	5.80	42.62	1.00	3.67	50.74	23.00	0.00	4.97	17.62
Tan Oak	HW	48.50	6.08	44.98	0.05	0.35	53.86	24.40	0.00	4.49	16.90
Pine	SW	52.55	6.08	41.25	0.00	0.12	45.59	20.65	17.77	10.70	5.17
Oak	HW	48.78	6.09	44.98	0.00	0.15	53.41	24.19	0.00	4.75	17.50
Palm	HW	48.11	6.64	36.79	2.81	5.50	43.19	19.55	16.44	10.02	5.30
Peanut	HW	46.97	5.64	40.11	1.85	5.25	45.93	20.74	5.27	7.18	15.63
Spruce	SW	49.53	6.06	43.92	0.11	0.37	50.23	22.65	1.73	6.22	18.80
Birch	SW	48.89	6.04	44.43	0.22	0.35	51.81	23.19	0.00	5.12	19.53
Spruce	SW	50.20	5.90	41.14	0.20	2.56	45.79	20.46	11.01	8.34	11.84
Oak	HW	49.89	5.98	42.57	0.21	1.29	47.89	21.37	5.83	7.10	16.52
Mixed	HW	50.00	5.97	42.80	0.21	0.95	48.18	21.49	5.53	7.01	16.84
Casuarina	HW	48.59	5.94	43.37	0.45	1.62	50.00	22.14	1.30	5.38	19.56
Grape	HW	47.57	5.85	43.14	0.81	2.61	50.42	22.31	0.03	4.80	19.84
Spruce	SW	48.46	5.84	44.88	0.21	0.60	53.12	23.48	0.00	4.12	18.68
Cocoa	HW	49.21	5.34	33.87	3.04	8.42	31.42	13.87	23.88	22.41	0.00
Cocoa	HW	48.23	5.23	33.19	2.98	10.25	30.79	13.60	23.40	21.96	0.00
Oak	HW	49.74	5.96	42.56	0.23	1.47	48.04	21.17	5.67	6.54	17.11
Spruce	SW	48.39	5.55	41.67	0.10	4.19	46.73	20.59	5.47	6.35	16.67
Oak	HW	49.90	5.97	42.88	0.36	0.88	48.49	21.37	5.25	6.46	17.55
Fir	SW	49.00	5.98	43.91	0.05	1.04	50.52	22.22	1.03	5.11	20.07
Coconut	HW	50.29	5.05	39.63	0.45	4.14	36.26	15.91	5.79	0.27	37.62
Hazelnut	HW	51.00	5.40	40.50	1.30	1.80	31.13	13.66	7.08	0.32	46.01
Walnut	HW	53.52	6.52	35.37	1.53	2.95	34.14	14.98	6.18	40.81	0.94
Cypress	SW	54.98	6.54	38.08	0.00	0.40	33.42	14.66	6.65	42.56	2.31
Olive	HW	50.18	6.30	32.09	1.40	9.90	34.98	15.35	5.13	33.77	0.88
Grape	HW	54.01	6.83	35.00	1.46	2.50	39.85	17.48	5.18	34.95	0.04
Walnut	HW	47.86	5.75	34.60	1.07	10.62	32.77	14.38	5.44	36.56	0.23
Spruce	SW	51.10	5.50	42.30	0.10	1.00	38.88	17.06	5.71	0.23	37.12
Olive	HW	51.25	6.29	36.46	1.10	4.70	37.75	16.56	5.29	34.40	1.30
Almond	HW	48.55	5.33	40.74	0.81	4.50	37.73	16.55	5.46	0.19	35.56
Almond	HW	48.43	5.98	39.90	0.94	4.71	43.29	18.99	4.38	0.22	28.42
Grape	HW	45.72	5.05	38.95	1.07	9.13	38.46	16.87	4.71	0.24	30.58
Olive	HW	50.00	6.50	36.30	0.80	6.30	47.16	20.69	3.33	21.78	0.74
Peach	HW	53.15	7.19	35.86	0.60	3.20	55.60	24.39	2.17	14.59	0.06
Cherry	HW	53.41	7.04	38.05	0.30	0.90	52.35	22.97	3.07	20.07	0.64

Grape	HW	49.73	6.67	35.41	1.83	6.24	53.21	23.34	2.22	14.90	0.09
Pine	SW	52.60	7.02	40.07	0.00	0.31	56.99	25.00	2.28	15.31	0.11
Unidentified	SW	50.96	6.86	38.49	0.19	3.11	57.02	25.02	1.91	12.87	0.06
Olive	HW	49.85	6.59	39.06	0.70	3.40	54.14	23.75	2.41	15.91	0.39
Oak	HW	49.16	6.46	40.16	1.64	2.55	54.75	24.02	2.41	15.95	0.33
Elm	HW	50.35	6.57	42.34	0.00	0.74	55.07	24.16	2.58	17.45	0.00
Elm	HW	50.40	6.60	42.30	0.00	0.70	55.76	24.46	2.46	16.54	0.08
Oak	HW	50.44	6.59	42.73	0.00	0.24	55.91	24.53	2.49	16.29	0.54
Coconut	HW	50.64	5.09	39.91	0.45	3.75	40.33	31.54	8.13	5.05	11.21
Mixed	HW	50.09	5.94	42.30	0.26	1.31	47.63	20.87	7.48	6.76	15.95
Pistachio	HW	48.85	6.29	42.86	0.50	1.30	49.72	21.75	2.22	5.32	19.68
Poplar	HW	50.84	5.89	41.06	0.59	1.60	46.24	20.18	14.22	7.81	9.95
Peach	HW	53.00	5.90	39.14	0.32	1.59	42.36	18.43	25.69	11.93	0.00
Olive	HW	47.73	5.86	43.60	0.58	2.23	51.25	22.25	0.00	4.05	20.22
Fir	SW	51.36	5.99	42.20	0.06	0.36	47.35	20.52	11.79	7.17	12.82
Spruce	SW	50.25	5.99	43.36	0.10	0.30	49.09	21.24	5.11	5.77	18.49
Unidentified	SW	50.00	6.00	43.60	0.00	0.30	49.57	21.43	3.89	5.45	19.35
Almond	HW	48.04	5.79	42.32	0.72	3.06	48.66	21.04	2.75	5.03	19.47
Fir	SW	49.84	5.99	43.60	0.18	0.38	49.67	21.48	3.57	5.36	19.55
Eucalyptus	HW	48.29	5.93	44.28	0.39	1.10	52.18	22.53	0.00	3.81	20.37
Cotton	HW	44.88	5.54	41.57	1.04	6.66	50.16	21.64	0.00	3.20	18.34
Beech	SW	49.69	6.07	42.80	0.41	1.01	48.86	21.01	4.97	5.50	18.65
Peanut	HW	46.50	5.55	40.19	1.66	5.98	46.40	19.96	4.72	5.22	17.71
Prune	HW	49.47	6.25	42.67	0.58	0.96	49.13	21.12	4.31	5.33	19.15
Mixed	SW	49.73	5.95	43.40	0.22	0.67	49.45	21.25	3.89	5.23	19.50
Pine	SW	49.45	5.95	43.59	0.30	0.61	49.96	21.47	2.80	4.94	20.22
Madrone	HW	48.56	6.02	44.99	0.05	0.36	53.64	23.00	0.00	3.24	19.76
Unidentified	HW	50.52	5.80	40.35	0.40	2.86	45.80	19.63	16.51	7.19	8.01
Pine	SW	52.30	5.80	38.76	0.20	2.90	42.61	18.20	26.03	10.25	0.00
Sequoia	SW	52.30	5.90	40.30	0.20	1.30	46.45	19.82	24.01	7.72	0.71
Mixed	HW	50.49	5.95	42.83	0.16	0.54	48.47	20.61	7.60	5.65	17.14
Mixed	HW	50.48	5.94	42.80	0.16	0.54	48.46	20.59	7.66	5.63	17.11
Pine	SW	52.19	5.67	37.37	0.41	4.30	39.21	16.47	27.77	12.25	0.00
Sequoia	SW	50.67	5.98	42.91	0.05	0.36	48.68	20.44	7.95	5.26	17.32
Fir	SW	50.55	5.82	41.22	0.10	2.21	46.89	19.60	13.84	5.81	11.66
Poplar	HW	48.51	5.88	44.29	0.29	1.00	51.75	21.53	0.00	3.17	22.54
Eucalyptus	HW	48.50	5.89	44.43	0.28	0.75	52.22	21.72	0.00	3.05	22.26
Ecoblock	HW	51.48	5.92	42.03	0.14	0.43	47.87	19.88	14.08	5.66	12.08
Oak	HW	49.47	5.73	44.03	0.45	0.26	50.58	20.94	2.69	3.83	21.69
Coconut	HW	51.27	5.88	41.78	0.23	0.65	47.84	19.75	14.52	5.47	11.78
Fir	SW	50.40	5.80	41.40	0.10	2.20	47.23	19.49	12.96	5.22	12.90

Sequoia	SW	53.50	5.90	40.15	0.10	0.30	45.78	18.84	27.56	7.52	0.00
Eucalyptus	HW	49.04	5.88	44.01	0.30	0.76	50.95	20.95	1.48	3.35	22.51
Hazelnut	HW	47.79	5.78	43.79	0.76	1.43	51.86	21.31	0.00	2.77	22.64
Sequoia	SW	53.50	5.90	40.30	0.10	0.20	46.29	18.93	27.60	6.98	0.00
Eucalyptus	HW	48.32	5.89	45.12	0.15	0.52	54.18	22.10	0.00	1.97	21.24
Oak	HW	49.50	5.70	41.30	0.20	3.30	47.29	19.14	10.81	4.27	15.19
Cherry tree	HW	49.52	5.81	42.97	0.31	1.35	49.36	19.95	5.46	3.62	20.26
Unidentified	HW	49.00	6.00	44.60	0.00	0.30	52.14	20.90	0.10	2.42	24.14
Robinia	HW	48.73	5.66	41.71	1.00	2.90	48.28	19.28	7.36	3.49	18.68
Walnut	HW	49.86	5.83	43.30	0.22	0.78	49.80	19.88	5.57	3.30	20.68
Walnut	HW	49.80	5.82	43.25	0.22	0.85	49.76	19.87	5.56	3.29	20.66
Oak	HW	47.81	5.93	44.12	0.12	2.00	52.61	20.95	0.00	1.76	22.69
Fir	SW	48.52	5.81	44.66	0.25	0.72	52.72	20.73	0.00	1.75	24.08
Apricot	HW	51.39	6.29	41.82	0.20	0.20	49.07	19.26	14.29	3.65	13.53
Palm	HW	47.98	5.26	36.61	1.17	8.81	44.16	17.28	25.77	3.98	0.00
Olive	HW	49.20	5.40	37.90	0.70	6.60	46.06	17.90	25.99	3.45	0.00
Almond	HW	46.49	5.44	41.22	0.97	5.87	48.24	18.65	3.24	2.06	21.95
Spruce	SW	49.53	5.77	44.01	0.19	0.48	51.27	19.44	3.36	1.72	23.73
Vine	HW	48.15	5.61	42.84	0.81	2.59	50.23	19.05	3.14	1.67	23.33
Almond	HW	50.30	5.62	41.71	0.64	1.72	49.04	18.54	13.77	2.44	14.49
Almond	HW	48.85	5.51	40.94	0.80	3.90	48.30	18.01	11.73	1.95	16.10
Hazelnut	HW	52.90	5.60	38.70	1.40	1.40	45.44	16.82	32.09	4.25	0.00
Walnut	HW	49.98	5.71	43.35	0.21	0.71	50.68	18.75	6.85	1.50	21.51
Oak	HW	49.67	5.93	44.02	0.07	0.30	51.67	19.10	3.49	1.18	24.27
Spruce	SW	51.06	5.75	42.29	0.11	0.77	50.10	18.34	14.40	1.61	14.79
Cotton	HW	45.97	5.35	41.99	0.84	5.48	50.16	18.05	0.74	0.32	25.25
Oak	HW	49.76	5.40	39.29	0.15	5.30	48.48	17.44	23.89	1.00	3.89
Cherry tree	HW	46.93	5.97	39.29	1.11	6.63	47.74	17.12	9.47	0.92	18.12
Walnut	HW	49.74	5.63	43.16	0.37	1.08	50.93	18.25	7.25	0.81	21.69
Walnut	HW	49.72	5.63	43.14	0.37	1.07	50.94	18.25	7.25	0.81	21.69
Oak	HW	48.99	5.93	42.58	0.33	2.10	44.20	34.00	2.53	1.64	15.53
Kukui	HW	55.12	5.54	37.55	0.34	1.43	40.61	13.94	38.54	5.48	0.00
Leucaena	HW	47.89	5.84	43.29	0.41	2.50	50.29	21.72	0.43	4.30	20.78
Hickory	HW	49.70	6.50	43.10	0.00	0.70	45.14	34.61	2.22	1.47	15.86
Willow	HW	49.25	5.99	42.66	0.60	1.40	44.20	33.11	3.07	1.29	16.93
Maple	HW	49.88	6.09	43.26	0.14	0.60	44.59	33.22	3.09	1.21	17.30
Pine	SW	50.22	6.17	43.17	0.16	0.26	44.41	32.89	3.59	1.23	17.62
Data from Ida				41.00	6.22	1.22	20.00	11.00	0.07	7.50	20.16
Eucalyptus	HW	50.87	5.70	41.99	0.22	1.22	39.80	11.90	8.86	7.52	30.16
Hybrid Poplar	HW	49.95	6.12	41.98	0.31	1.64	52.24	15.87	8.08	22.16	0.00
Juniper	SW	52.67	6.08	37.83	0.55	2.87	34.79	8.91	7.77	45.66	0.00

Lodge Pole	SW	50.25	6.54	41.70	0.14	1.36	52.47	7.51	0.00	38.66	0.00
Pine Pine	SW	50.80	6.22	41.01	0.54	1.43	45.25	9.89	0.00	43.43	0.00
Pinyon	SW	50.98	5.89	38.61	0.27	4.25	34.44	11.94	6.98	39.19	3.16
Juniper											
Pinyon Pine	SW	52.62	6.27	38.69	0.55	1.87	37.79	8.96	2.85	48.53	0.00
Shrub Willow	HW	49.20	6.09	42.71	0.31	1.69	46.79	16.97	0.10	32.60	1.81
Data from Phy Bamboo	yllis2 <sup>50</sup> HW	48.04	6.11	42.57	0.58	2.70	47.46	21.89	0.20	27.74	0.00
Bamboo	HW	44.16	5.64	44.08	0.75	5.37	45.78	20.01	0.20	11.13	17.70
Bamboo	HW	46.06	5.75	46.18	0.73	1.83	43.78	28.03	0.00	1.13	24.86
Sawdust	пw	40.00	3.73	40.18	0.19	1.65	43.37	28.03	0.00	1.90	24.60
Pine Wood	SW	48.23	6.30	43.75	0.13	1.59	45.15	39.36	2.92	10.97	0.00
Douglas Fir Wood	SW	49.95	6.31	42.80	0.17	0.77	56.93	14.03	3.77	24.49	0.00
Pyrenean Oak Wood	HW	48.87	6.37	38.01	2.70	4.05	49.79	12.31	0.20	33.65	0.00
Pyrenean Oak Wood	HW	48.71	6.53	39.25	2.51	3.00	51.44	17.21	0.00	28.35	0.00
Literature Da	ta <sup>41,51,60</sup> –	-69,52,70-79,53	3,80–86,54–59	)							
Olive Branch	HW	48.77	6.08	40.59	1.06	3.50	34.67	24.02	0.00	37.81	0.00
Kiwi Branch	HW	49.01	5.59	42.42	0.78	2.20	32.98	34.24	14.30	0.00	16.27
Pine Bark	SW	51.00	5.19	42.02	0.69	1.10	32.81	14.46	12.69	0.00	38.94
Almond Tree Pruning	HW	50.63	6.42	40.82	0.79	1.34	42.19	25.17	2.88	28.42	0.00
Softwood bark	SW	51.87	5.85	39.39	0.39	2.50	22.40	22.28	7.13	31.92	13.52
Hardwood rich in fibres	HW	49.00	5.89	43.01	0.29	1.80	43.27	30.00	14.31	7.78	2.79
Softwood	SW	51.67	6.05	40.67	0.20	1.41	45.98	24.50	17.22	10.89	0.00
Hardwood	HW	49.11	6.27	41.53	0.39	2.70	44.79	31.01	4.48	17.02	0.00
Wood Bark	SW	52.25	6.00	39.95	0.19	1.60	24.80	29.80	13.60	30.20	0.00
Spruce Wood	SW	51.54	6.06	40.61	0.29	1.50	50.29	20.99	16.70	10.52	0.00
Beech Wood	HW	50.67	6.35	42.17	0.41	0.40	45.84	31.83	6.93	14.99	0.00
Beech Wood	HW	46.90	6.20	45.90	0.30	0.70	50.53	24.83	0.00	21.26	2.69
Spruce Wood	SW	48.30	6.30	44.60	0.40	0.40	47.59	22.89	0.00	29.12	0.00
Wood Chips	SW	46.17	5.87	47.39	0.08	0.48	38.31	38.31	0.00	2.47	20.42
Jatropha De- oiled Cake	SW	56.78	7.06	29.10	5.56	1.51	55.47	17.21	8.38	17.43	0.00
Willow	HW	49.55	6.45	39.62	2.68	1.70	57.90	16.91	3.53	19.96	0.00
Silver Fir	SW	50.96	6.37	42.00	0.20	0.47	53.46	15.39	5.07	25.61	0.00
Holm Oak	HW	46.78	5.75	44.44	0.49	2.54	40.32	27.56	0.00	8.14	21.43
Stone Pine	SW	50.01	5.95	42.96	0.30	0.78	44.08	21.61	9.38	15.06	8.93
Pyrenean Oak	HW	47.19	5.74	43.88	0.49	2.70	36.41	27.39	0.00	11.14	22.37
Bonbogori	HW	54.05	6.00	38.37	0.22	1.36	62.94	10.66	23.51	1.53	0.00
Moj	HW	51.35	6.09	40.58	0.30	1.68	63.48	7.56	15.55	11.73	0.00
Woody Waste	SW	48.09	6.68	44.80	0.10	0.33	41.42	31.96	0.00	26.29	0.00
Waste Square Timber	SW	46.94	6.56	45.85	0.10	0.55	44.17	24.26	0.00	31.03	0.00

Plywood	SW	42.55	5.81	43.68	1.69	6.27	40.77	24.58	0.00	21.37	7.01
Spruce Wood	SW	49.03	6.13	44.55	0.08	0.21	48.78	13.74	0.00	25.85	11.42
Pine	SW	48.55	5.76	44.37	0.02	1.30	48.15	22.20	9.04	0.00	19.31
Birch	HW	47.00	6.19	46.50	0.11	0.20	39.92	38.92	0.00	17.51	3.45
Spruce	SW	47.37	6.30	46.17	0.07	0.10	43.96	26.97	0.00	24.99	3.98
Pine	SW	46.87	6.30	46.67	0.07	0.10	42.96	26.97	0.00	24.03	5.94
Pine	SW	48.33	5.88	43.23	0.49	2.07	46.81	17.33	1.11	18.34	14.09
Beech	SW	49.73	6.29	43.04	0.40	0.53	46.15	31.53	5.39	16.39	0.00
Pinewood Sawdust	SW	49.19	6.10	44.08	0.08	0.56	53.70	21.88	8.82	15.05	0.00
Spruce	SW	48.76	6.23	44.60	0.15	0.26	49.38	22.66	0.00	27.71	0.00
Salix	HW	47.23	5.94	44.65	1.03	1.16	49.98	23.20	0.00	15.07	10.58
Poplar - Sapwood	HW	51.47	6.13	42.20	0.00	0.20	48.82	17.30	13.06	20.62	0.00
Poplar - Heartwood	HW	51.21	6.51	42.16	0.00	0.12	50.91	13.79	0.10	35.08	0.00
Norway Spruce	SW	50.28	6.20	43.19	0.10	0.23	42.33	26.20	4.86	26.38	0.00
Spruce Bark	SW	46.39	6.21	42.16	0.00	5.24	41.89	26.93	0.00	25.93	0.00
Eucalyptus Sawdust	HW	49.35	5.72	43.90	0.17	0.86	42.31	30.89	13.37	0.00	12.56
Pine	SW	49.33	6.39	43.44	0.20	0.63	38.77	24.21	0.00	36.38	0.00
Hybrid Poplar	HW	50.05	5.91	42.54	0.30	1.20	50.34	21.04	19.11	6.17	2.11
Subabul Wood	HW	48.16	5.89	45.06	0.00	0.89	44.57	26.88	2.51	7.00	17.83
Pine Chip	SW	47.19	6.64	45.74	0.17	0.27	53.87	16.85	0.00	29.01	0.00
Logging Residue Chip	SW	46.87	6.15	44.79	0.42	1.77	47.89	16.94	0.00	26.79	6.62
Fir Wood	SW	48.30	5.92	41.87	0.42	3.49	39.86	31.47	9.13	16.05	0.00
Pine Bark	SW	51.25	5.37	40.55	0.01	2.82	15.60	44.39	18.30	0.00	18.89
Bambusa vulgaris	HW	46.01	6.24	45.63	0.18	1.95	46.50	24.08	0.00	24.75	2.72
Bambusa vulgaris	HW	46.37	6.33	45.70	0.18	1.43	47.26	24.65	0.00	26.66	0.00
Bambusa vulgaris	HW	45.35	6.19	45.79	0.26	2.40	46.49	24.98	0.00	22.47	3.66
Lauan	HW	48.64	6.75	44.24	0.10	0.27	40.38	15.70	0.00	43.65	0.00
Patula Pine	SW	55.52	7.12	36.85	0.19	0.32	48.79	9.21	4.90	36.78	0.00

Note: db – dry basis; C – Carbon content; H – Hydrogen content; O – Oxygen content; N – Nitrogen content; Ash – Ash content; CELL – Cellulose content; HEMI – Hemicellulose content; LIGC – Lignin-C content; LIGH – Lignin-H content; LIGO – Lignin-O content.

## 4. Additional Results

## 4.1 Correlations between Simulation Results and Biomass Feedstock Properties

The correlations between different biomass characteristics and other indicators for AC production energy and carbon footprints are summarized in Figure S6-9. The biomass characteristics used in Figure S6-9 include the main elements of biomass ultimate analysis (Carbon, hydrogen and oxygen content), lignocellulosic components (cellulose, hemicellulose and lignin content), ash content and two other indicators derived from ultimate analysis (Hydrogen to carbon ratio (H/C) and oxygen to carbon ratio (O/C)). The value of all these variables can be found or deduced from the data given in Table S6. The indicators for Figure S6-9 are biogenic GHG emission, total GHG emission, primary energy demand and energy recovery ratio (ERR), respectively.

Besides the main insights that are concluded in the article, some additional findings can be summarized from Figure S6-9 with the given R-value (correlation coefficient) of each plot. Overall the correlation between most of the biomass characterization data and the proposed indicators are weak (with R-value < 0.2), except the hydrogen content, H/C ratio and ash content. In addition, the ash content is negatively correlated to all the proposed indicators, which is because ash has no reactions in the AC production process and retained in final AC production. However, the high ash content may reduce the quality of AC in some specific applications (e.g., adsorbent, supercapacitor.

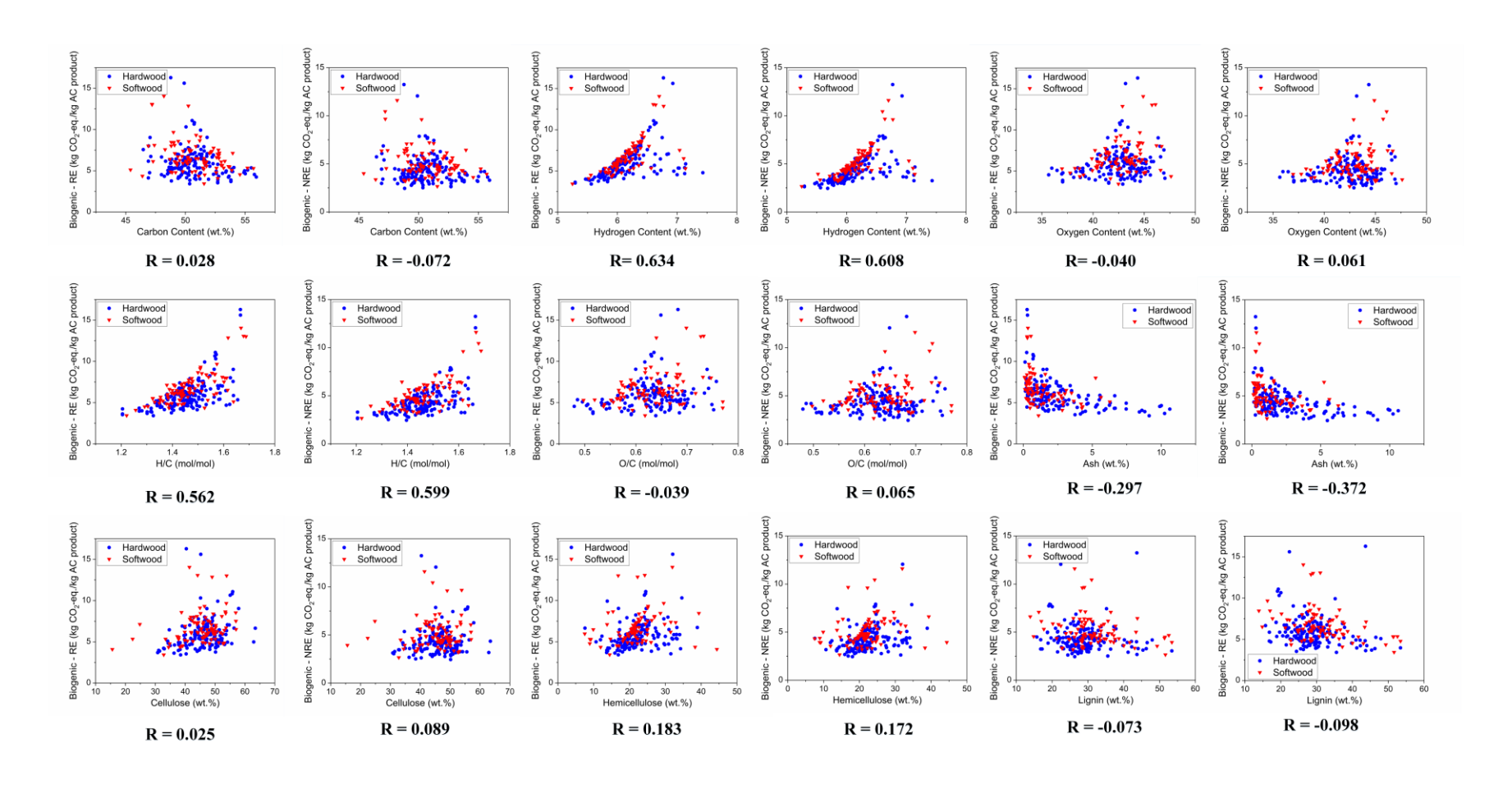


**Figure S6** Correlations between the Biogenic GHG Emission of Steam AC Production and Feedstock Composition (RE: Process with Energy Recovery; NRE: Process without Energy Recovery)

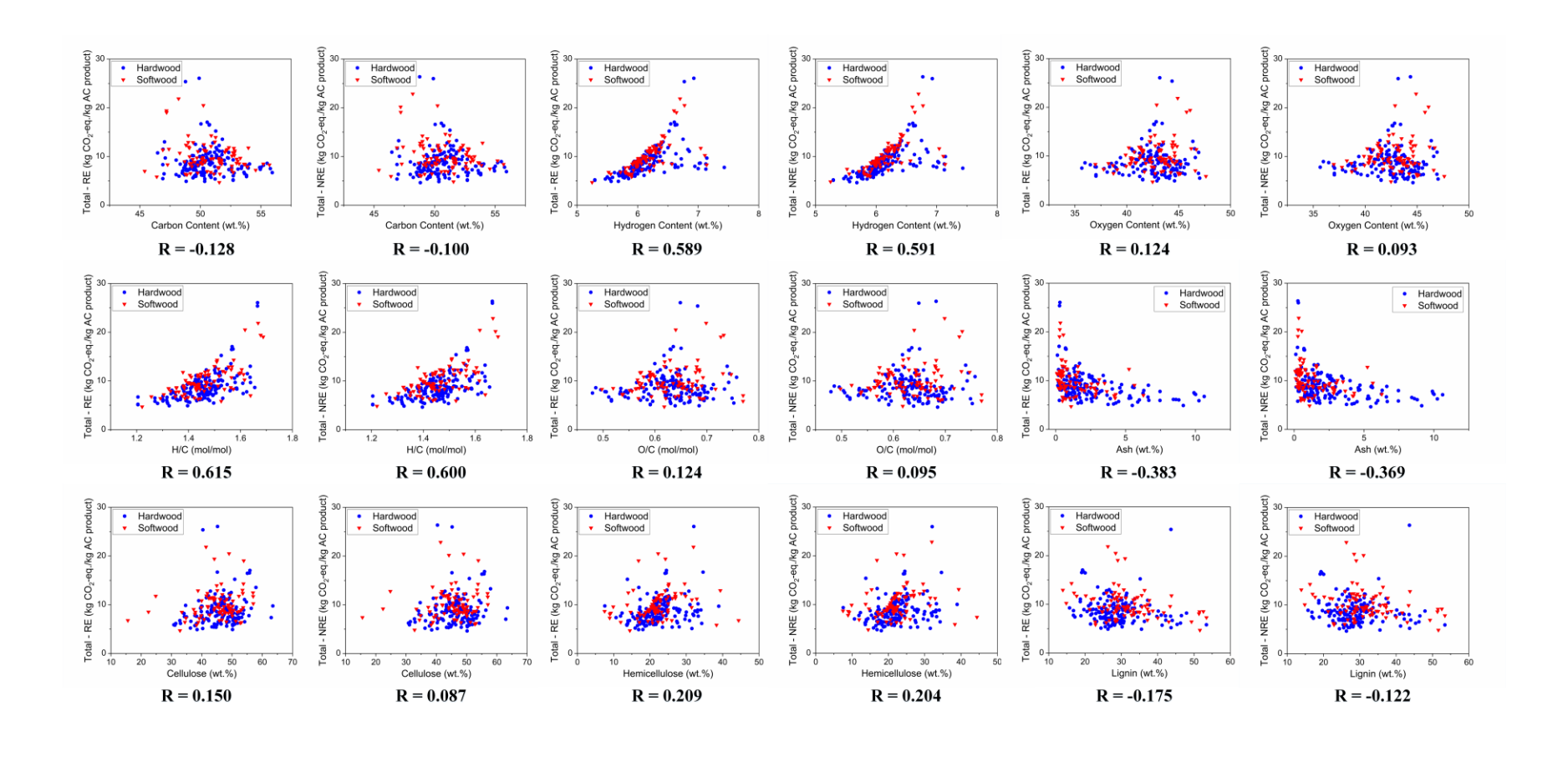


**Figure S7** Correlations between the Total GHG Emission of Steam AC Production and Biomass Feedstock Composition (RE: Process with Energy Recovery; NRE: Process without Energy Recovery)

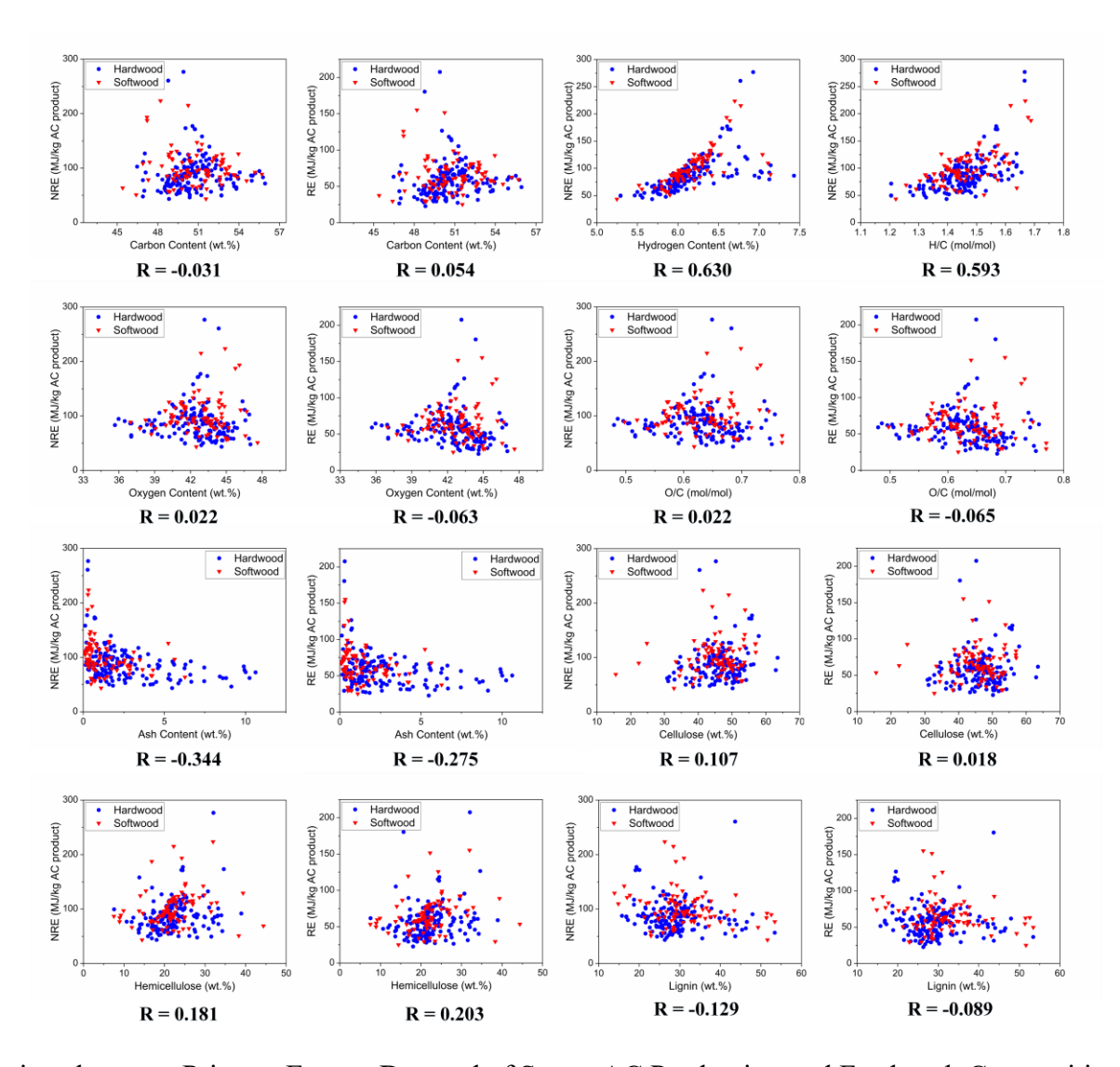


**Figure S8** Correlations between Primary Energy Demand of Steam AC Production and Feedstock Composition (RE: Process with Energy Recovery; NRE: Process without Energy Recovery)

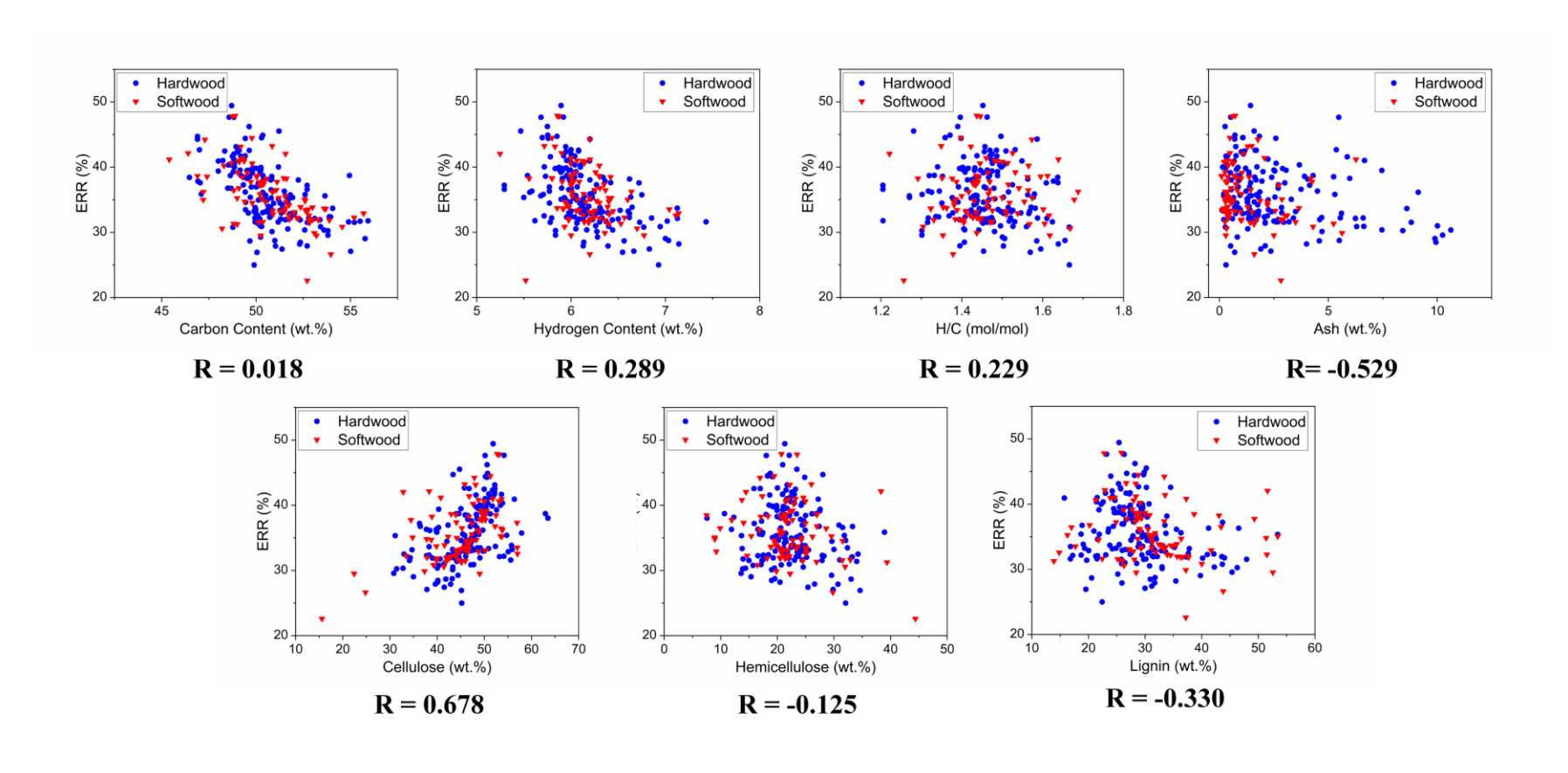
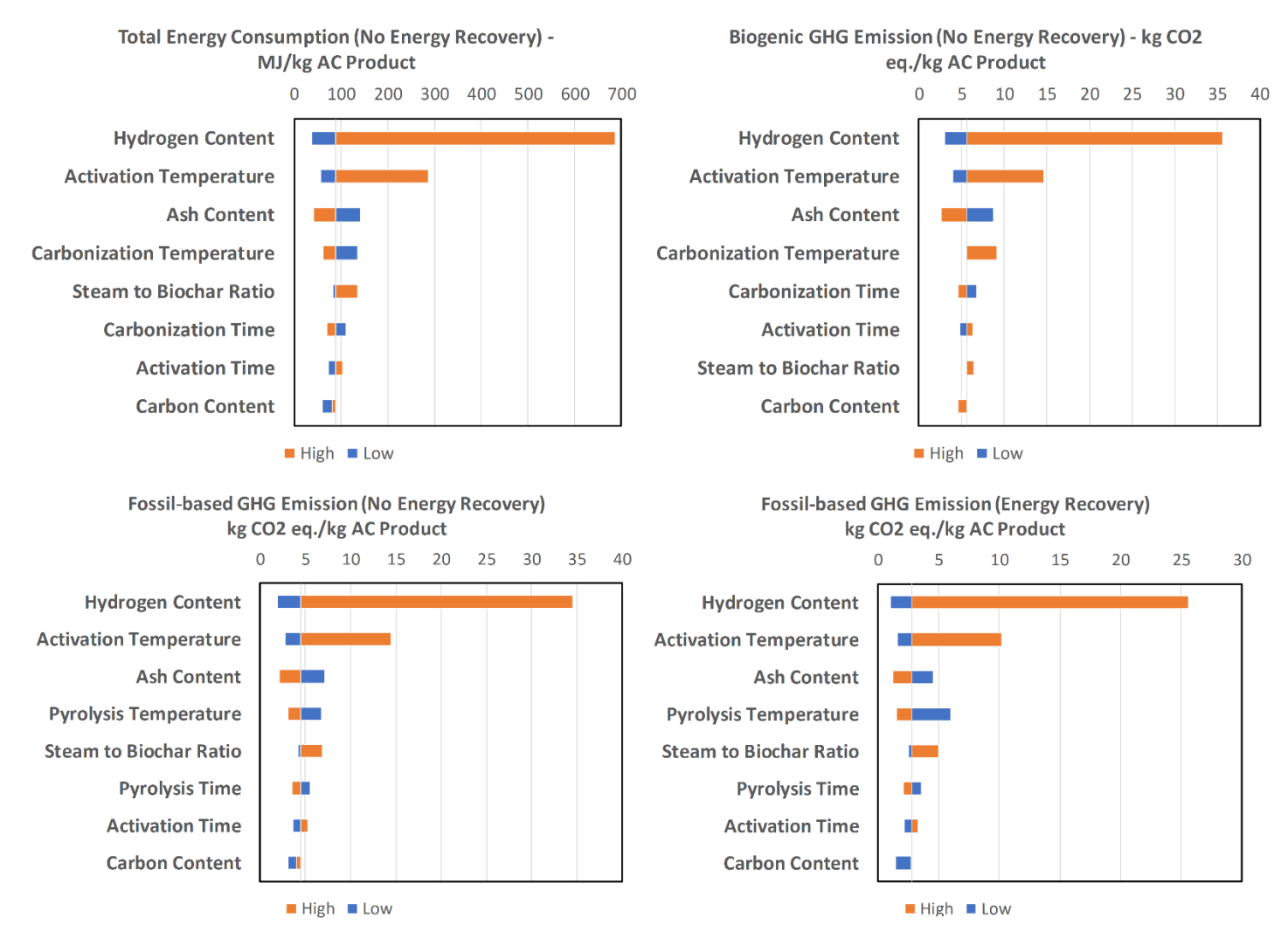


Figure S9 Correlations between Energy Recovery Ratio of Steam AC Production and Biomass Feedstock Composition

## 4.2 Additional Sensitivity Analysis Results



**Figure S10** Sensitivity Analysis for the Energy Consumption, Biogenic GHG Emission (without Energy Recovery) and Fossil-based GHG Emission (with/without Energy Recovery) of Steam AC Production Process

## 5. References

- (1) U.S. Energy Information Administration. *Annual Energy Review 2011*; Washington, DC, 2012.
- (2) Bayer, P.; Heuer, E.; Karl, U.; Finkel, M. Economical and Ecological Comparison of Granular Activated Carbon (GAC) Adsorber Refill Strategies. *Water Res.* **2005**, *39* (9), 1719–1728. https://doi.org/10.1016/j.watres.2005.02.005.
- (3) Markus Andreas, M. Eco-Efficiency Evaluation of Waste Gas Purification Systems in the Chemical Industry, Swiss Federal Institute of Technology Zurich, 1997.
- (4) Jeswani, H. K.; Gujba, H.; Brown, N. W.; Roberts, E. P. L.; Azapagic, A. Removal of Organic Compounds from Water: Life Cycle Environmental Impacts and Economic Costs of the Arvia Process Compared to Granulated Activated Carbon. *J. Clean. Prod.* **2015**, *89*, 203–213. https://doi.org/10.1016/j.jclepro.2014.11.017.
- (5) Gabarrell, X.; Font, M.; Vicent, T.; Caminal, G.; Sarrà, M.; Blánquez, P. A Comparative Life Cycle Assessment of Two Treatment Technologies for the Grey Lanaset G Textile Dye: Biodegradation by Trametes Versicolor and Granular Activated Carbon Adsorption. *Int. J. Life Cycle Assess.* **2012**, *17* (5), 613–624. https://doi.org/10.1007/s11367-012-0385-z.
- (6) Muñoz, I.; Peral, J.; Antonio Ayllón, J.; Malato, S.; José Martin, M.; Yves Perrot, J.; Vincent, M.; Domènech, X. Life-Cycle Assessment of a Coupled Advanced Oxidation-Biological Process for Wastewater Treatment: Comparison with Granular Activated Carbon Adsorption. *Environ. Eng. Sci.* 2007, 24 (5), 638–651. https://doi.org/10.1089/ees.2006.0134.
- (7) Manda, B. M. K.; Worrell, E.; Patel, M. K. Innovative Membrane Filtration System for Micropollutant Removal from Drinking Water - Prospective Environmental LCA and Its Integration in Business Decisions. *J. Clean. Prod.* 2014, 72, 153–166. https://doi.org/10.1016/j.jclepro.2014.02.045.
- (8) Hjaila, K.; Baccar, R.; Sarrà, M.; Gasol, C. M.; Blánquez, P. Environmental Impact Associated with Activated Carbon Preparation from Olive-Waste Cake via Life Cycle Assessment. *J. Environ. Manage.* **2013**, *130*, 242–247. https://doi.org/10.1016/j.jenvman.2013.08.061.
- (9) Arena, N.; Lee, J.; Clift, R. Life Cycle Assessment of Activated Carbon Production from Coconut Shells. *J. Clean. Prod.* **2016**, *125*, 68–77. https://doi.org/10.1016/j.jclepro.2016.03.073.
- (10) Sepúlveda-Cervantes, C. V.; Soto-Regalado, E.; Rivas-García, P.; Loredo-Cancino, M.; Cerino-Córdova, F. d. J.; García Reyes, R. B. Technical-Environmental Optimisation of the Activated Carbon Production of an Agroindustrial Waste by Means Response Surface and Life Cycle Assessment. *Waste Manag. Res.* **2018**, *36* (2), 121–130.

- https://doi.org/10.1177/0734242X17741680.
- (11) Kim, M. H.; Jeong, I. T.; Park, S. B.; Kim, J. W. Analysis of Environmental Impact of Activated Carbon Production from Wood Waste. *Environ. Eng. Res.* **2018**, *24* (1), 117–126. https://doi.org/10.4491/eer.2018.104.
- (12) Kim, M.; Kim, G. Life Cycle Assessment of Activated Carbon Production System by Using Poplar. *J. Korean Soc. Environ. Eng.* **2014**, *36* (11), 725–732.
- (13) Gu, H.; Bergman, R.; Anderson, N.; Alanya-Rosenbaum, S. Life Cycle Assessment of Activated Carbon From Woody Biomass. *Wood Fiber Sci.* **2018**, *50* (3), 1–15.
- (14) Sharifan, S. A Comparative Optimization Study of Activated Carbon Production from Hazelnut Shells by Thermal and Microwave Heating Methods, Imperial College London, 2013.
- (15) Hung, J. J. The Production of Activated Carbon from Coconut Shells Using Pyrolysis and Fluidized Bed Reactors, The University of Arizona, 2012.
- (16) Campo, B. G. Production of Activated Carbon from Fast Pyrolysis Biochar and the Detoxification of Pyrolytic Sugars for Ethanol Fermentation, Iowa State University, 2015.
- (17) Heidari, A.; Khaki, E.; Younesi, H.; Ray, H. Evaluation of Fast and Slow Pyrolysis Methods for Bio-Oil and Activated Carbon Production from Eucalyptus Wastes Using a Life Cycle Assessment Approach. *J. Clean. Prod.* **2019**, *241*, 118394. https://doi.org/10.1016/j.jclepro.2019.118394.
- (18) Azargohar, R. Production Of Activated Carbon And Its Catalytic Application For Oxidation Of Hydrogen Sulphide, University of Saskatchewan, 2009.
- (19) Fagbemi, L.; Khezami, L.; Capart, R. Pyrolysis Products from Different Biomasses: Application to the Thermal Cracking of Tar. *Appl. Energy* **2001**, *69* (4), 293–306. https://doi.org/10.1016/S0306-2619(01)00013-7.
- (20) Loya-González, D.; Loredo-Cancino, M.; Soto-Regalado, E.; Rivas-García, P.; Cerino-Córdova, F. de J.; García-Reyes, R. B.; Bustos-Martínez, D.; Estrada-Baltazar, A. Optimal Activated Carbon Production from Corn Pericarp: A Life Cycle Assessment Approach. *J. Clean. Prod.* **2019**, *219*, 316–325. https://doi.org/10.1016/j.jclepro.2019.02.068.
- (21) Suganya, S.; Senthil Kumar, P. Evaluation of Environmental Aspects of Brew Waste-Based Carbon Production and Its Disposal Scenario. *J. Clean. Prod.* **2018**, *202*, 244–252. https://doi.org/10.1016/j.jclepro.2018.08.143.
- (22) Dornburg, V.; Faaij, A. P. C. Efficiency and Economy of Wood-Fired Biomass Energy Systems in Relation to Scale Regarding Heat and Power Generation Using Combustion and Gasification Technologies. *Biomass and Bioenergy* **2001**, *21* (2), 91–108. https://doi.org/10.1016/S0961-9534(01)00030-7.
- (23) U.S. DOE-OIT. Steam System Opportunity Assessment for the Pulp and Paper, Chemical Manufacturing, and Petroleum Refining Industries. United States Department of Energy Office of Energy Efficiency and Renewable Energy: Washington, DC 2002, pp 1–87.

- (24) Ranzi, E.; Cuoci, A.; Faravelli, T.; Frassoldati, A.; Migliavacca, G.; Pierucci, S.; Sommariva, S. Chemical Kinetics of Biomass Pyrolysis. *Energy & Fuels* **2008**, *22* (6), 4292–4300. https://doi.org/10.1021/ef800551t.
- (25) Debiagi, P. E. A.; Pecchi, C.; Gentile, G.; Frassoldati, A.; Cuoci, A.; Faravelli, T.; Ranzi, E. Extractives Extend the Applicability of Multistep Kinetic Scheme of Biomass Pyrolysis. *Energy and Fuels* **2015**, *29* (10), 6544–6555. https://doi.org/10.1021/acs.energyfuels.5b01753.
- (26) Anca-Couce, A.; Scharler, R. Modelling Heat of Reaction in Biomass Pyrolysis with Detailed Reaction Schemes. *Fuel* **2017**, *206*, 572–579. https://doi.org/10.1016/j.fuel.2017.06.011.
- (27) Anca-Couce, A.; Sommersacher, P.; Scharler, R. Online Experiments and Modelling with a Detailed Reaction Scheme of Single Particle Biomass Pyrolysis. *J. Anal. Appl. Pyrolysis* **2017**, *127*, 411–425. https://doi.org/10.1016/j.jaap.2017.07.008.
- (28) Debiagi, P.; Gentile, G.; Cuoci, A.; Frassoldati, A.; Ranzi, E.; Faravelli, T. A Predictive Model of Biochar Formation and Characterization. *J. Anal. Appl. Pyrolysis* **2018**, *134* (June), 326–335. https://doi.org/10.1016/j.jaap.2018.06.022.
- (29) Nabavi-Pelesaraei, A.; Rafiee, S.; Mohtasebi, S. S.; Hosseinzadeh-Bandbafha, H.; Chau, K. wing. Integration of Artificial Intelligence Methods and Life Cycle Assessment to Predict Energy Output and Environmental Impacts of Paddy Production. *Sci. Total Environ.* **2018**, *631–632*, 1279–1294. https://doi.org/10.1016/j.scitotenv.2018.03.088.
- (30) Kaab, A.; Sharifi, M.; Mobli, H.; Nabavi-Pelesaraei, A.; Chau, K. wing. Combined Life Cycle Assessment and Artificial Intelligence for Prediction of Output Energy and Environmental Impacts of Sugarcane Production. *Sci. Total Environ.* **2019**, *664*, 1005–1019. https://doi.org/10.1016/j.scitotenv.2019.02.004.
- (31) Fahmi, I.; Cremaschi, S. Process Synthesis of Biodiesel Production Plant Using Artificial Neural Networks as the Surrogate Models. *Comput. Chem. Eng.* **2012**, *46*, 105–123. https://doi.org/10.1016/j.compchemeng.2012.06.006.
- (32) Liao, M.; Kelley, S. S.; Yao, Y. Artificial Neural Network Based Modeling for the Prediction of Yield and Surface Area of Activated Carbon from Biomass. *Biofuels, Bioprod. Biorefining* **2019**, *13*, 1015–1027. https://doi.org/10.1002/bbb.1991.
- (33) Aguda, R. Preparation and Characterization of Modified Biomass as Functional Carbon-Based Materials, North Carolina State University, 2017.
- (34) Martín-Gullón, I.; Asensio, M.; Marcilla, A.; Font, R. Steam Activation of a Bituminous Coal in a Multistage Fluidized Bed Pilot Plant: Operation and Simulation Model. *Ind. Eng. Chem. Res.* **1996**, *35* (11), 4139–4146. https://doi.org/10.1021/ie950759x.
- (35) AspenTech. Aspen Plus User Guide; Cambridge, 2000.
- (36) Peters, J. F.; Banks, S. W.; Bridgwater, A. V.; Dufour, J. A Kinetic Reaction Model for Biomass Pyrolysis Processes in Aspen Plus. *Appl. Energy* **2017**, *188*, 595–603. https://doi.org/10.1016/j.apenergy.2016.12.030.

- (37) AspenTech. Aspen Plus Getting Started Modeling Processes with Solids. **2013**, *128*, 594–601. https://doi.org/10.1016/j.jenvman.2013.06.008.
- (38) Wooley, R. J.; Putsche, V. Development of an ASPEN PLUS Physical Property Database for Biofuels Components; Golden, Colorado, 1996.
- (39) Atienza-Martínez, M.; Ábrego, J.; Mastral, J. F.; Ceamanos, J.; Gea, G. Energy and Exergy Analyses of Sewage Sludge Thermochemical Treatment. *Energy* **2018**, *144*, 723–735. https://doi.org/10.1016/j.energy.2017.12.007.
- (40) Yang, H.; Kudo, S.; Kuo, H. P.; Norinaga, K.; Mori, A.; Mašek, O.; Hayashi, J. I. Estimation of Enthalpy of Bio-Oil Vapor and Heat Required for Pyrolysis of Biomass. *Energy and Fuels* **2013**, *27* (5), 2675–2686. https://doi.org/10.1021/ef400199z.
- (41) Demirbaş, A. Calculation of Higher Heating Values. *Fuel* **1997**, 76 (5), 431–434. https://doi.org/10.1002/er.
- (42) Silva, H. S.; Ruiz, S. V; Granados, D. L.; Santángelo, J. M. Adsorption of Mercury (II) from Liquid Solutions Using Modified Activated Carbons. *Mater. Res.* 2010, 13 (2), 129–134. https://doi.org/10.1590/S1516-14392010000200003.
- (43) Ou, L.; Kim, H.; Kelley, S.; Park, S.; Biomaterials, F.; Carolina, N. Impacts of Feedstock Properties on the Process Economics of Fast-Pyrolysis Biorefineries. *Biofuels, Bioprod. Biorefining* **2018**, *12*, 442–452. https://doi.org/10.1002/bbb.1860.
- (44) Sajjadi, B.; Chen, W. Y.; Egiebor, N. O. A Comprehensive Review on Physical Activation of Biochar for Energy and Environmental Applications. *Rev. Chem. Eng.* **2018**. https://doi.org/10.1515/revce-2017-0113.
- (45) Demiral, H.; Demiral, I.; Karabacakoĝlu, B.; Tümsek, F. Production of Activated Carbon from Olive Bagasse by Physical Activation. *Chem. Eng. Res. Des.* **2011**, *89* (2), 206–213. https://doi.org/10.1016/j.cherd.2010.05.005.
- (46) Zheng, Z.; Xia, H.; Srinivasakannan, C.; Peng, J.; Zhang, L. Steam Activation of Eupatorium Adenophorum for the Production of Porous Carbon and Hydrogen Rich Fuel Gas. *J. Anal. Appl. Pyrolysis* **2014**, *110* (1), 113–121. https://doi.org/10.1016/j.jaap.2014.08.007.
- (47) Li, W.; Yang, K.; Peng, J.; Zhang, L.; Guo, S.; Xia, H. Effects of Carbonization Temperatures on Characteristics of Porosity in Coconut Shell Chars and Activated Carbons Derived from Carbonized Coconut Shell Chars. *Ind. Crops Prod.* 2008, 28 (2), 190–198. https://doi.org/10.1016/j.indcrop.2008.02.012.
- (48) National Renewable Energy Laboratory. Biomass Feedstock Composition and Property Database. 2015.
- (49) U.S. Department of Energy; Idaho National Laboratory. Bioenergy Feedstock Library bioenergylibrary.inl.gov (accessed Mar 13, 2019).
- (50) ECN.TNO. Phyllis2, database for biomass and waste https://phyllis.nl/ (accessed Mar 13, 2019).

- (51) Ferreiro, A. I.; Giudicianni, P.; Grottola, C. M.; Rabaçal, M.; Costa, M.; Ragucci, R. Unresolved Issues on the Kinetic Modeling of Pyrolysis of Woody and Nonwoody Biomass Fuels. *Energy and Fuels* **2017**, *31* (4), 4035–4044. https://doi.org/10.1021/acs.energyfuels.6b03445.
- (52) González, J. F.; Román, S.; Encinar, J. M.; Martínez, G. Pyrolysis of Various Biomass Residues and Char Utilization for the Production of Activated Carbons. *J. Anal. Appl. Pyrolysis* **2009**, *85* (1–2), 134–141. https://doi.org/10.1016/j.jaap.2008.11.035.
- (53) Garcia-Pérez, M.; Chaala, A.; Pakdel, H.; Kretschmer, D.; Roy, C. Vacuum Pyrolysis of Softwood and Hardwood Biomass. Comparison between Product Yields and Bio-Oil Properties. *J. Anal. Appl. Pyrolysis* **2007**, *78* (1), 104–116. https://doi.org/10.1016/j.jaap.2006.05.003.
- (54) Kataki, R.; Konwer, D. Fuelwood Characteristics of Some Indigenous Woody Species of North-East India. *Biomass and Bioenergy* **2001**, *20* (1), 17–23. https://doi.org/10.1016/S0961-9534(00)00060-X.
- (55) Azeez, A. M.; Meier, D.; Odermatt, J.; Willner, T. Fast Pyrolysis of African and European Lignocellulosic Biomasses Using Py-GC/MS and Fluidized Bed Reactor. *Energy and Fuels* **2010**, *24* (3), 2078–2085. https://doi.org/10.1021/ef9012856.
- (56) Jindal, M. K.; Jha, M. K. Catalytic Hydrothermal Liquefaction of Waste Furniture Sawdust to Bio-Oil. *Indian Chem. Eng.* **2016**, *58* (2), 157–171. https://doi.org/10.1080/00194506.2015.1006145.
- (57) Di Blasi, C.; Signorelli, G.; Di Russo, C.; Rea, G. Product Distribution from Pyrolysis of Wood and Agricultural Residues. *Ind. Eng. Chem. Res.* 1999, 38 (6), 2216–2224. https://doi.org/10.1021/ie980711u.
- (58) Luo, G.; Chandler, D. S.; Anjos, L. C. A.; Eng, R. J.; Jia, P.; Resende, F. L. P. Pyrolysis of Whole Wood Chips and Rods in a Novel Ablative Reactor. *Fuel* **2017**, *194*, 229–238. https://doi.org/10.1016/j.fuel.2017.01.010.
- (59) Sharma, R.; Sheth, P. N.; Gujrathi, A. M. Kinetic Modeling and Simulation: Pyrolysis of Jatropha Residue de-Oiled Cake. *Renew. Energy* **2016**, *86*, 554–562. https://doi.org/10.1016/j.renene.2015.08.066.
- (60) Bridgeman, T. G.; Jones, J. M.; Shield, I.; Williams, P. T. Torrefaction of Reed Canary Grass, Wheat Straw and Willow to Enhance Solid Fuel Qualities and Combustion Properties. *Fuel* **2008**, *87* (6), 844–856. https://doi.org/10.1016/j.fuel.2007.05.041.
- (61) López, F. A.; Centeno, T. A.; García-Díaz, I.; Alguacil, F. J. Textural and Fuel Characteristics of the Chars Produced by the Pyrolysis of Waste Wood, and the Properties of Activated Carbons Prepared from Them. *J. Anal. Appl. Pyrolysis* **2013**, *104*, 551–558. https://doi.org/10.1016/j.jaap.2013.05.014.
- (62) Salinas-Martínez de Lecea, C.; Linares-Solano, A.; Garcia, P.; Molina, A.; Ruiz-Colorado, A. A.; Romero-Anaya, A. J. Phosphoric Acid Activation of Recalcitrant Biomass Originated in Ethanol Production from Banana Plants. *Biomass and Bioenergy* **2010**, *35* (3), 1196–1204. https://doi.org/10.1016/j.biombioe.2010.12.007.

- (63) Gueye, M.; Richardson, Y.; Kafack, F. T.; Blin, J. High Efficiency Activated Carbons from African Biomass Residues for the Removal of Chromium(VI) from Wastewater. *J. Environ. Chem. Eng.* **2014**, *2* (1), 273–281. https://doi.org/10.1016/j.jece.2013.12.014.
- (64) Güngör, A.; Önenç, S.; Uçar, S.; Yanik, J. Comparison between the "One-Step" and "Two-Step" Catalytic Pyrolysis of Pine Bark. *J. Anal. Appl. Pyrolysis* **2012**, *97*, 39–48. https://doi.org/10.1016/j.jaap.2012.06.011.
- (65) Rambo, M. K. D.; Schmidt, F. L.; Ferreira, M. M. C. Analysis of the Lignocellulosic Components of Biomass Residues for Biorefinery Opportunities. *Talanta* **2015**, *144*, 696–703. https://doi.org/10.1016/j.talanta.2015.06.045.
- (66) Sasmal, S.; Goud, V. V.; Mohanty, K. Characterization of Biomasses Available in the Region of North-East India for Production of Biofuels. *Biomass and Bioenergy* **2012**, *45*, 212–220. https://doi.org/10.1016/j.biombioe.2012.06.008.
- (67) Wei, L.; Xu, S.; Zhang, L.; Zhang, H.; Liu, C.; Zhu, H.; Liu, S. Characteristics of Fast Pyrolysis of Biomass in a Free Fall Reactor. *Fuel Process. Technol.* **2006**, *87* (10), 863–871. https://doi.org/10.1016/j.fuproc.2006.06.002.
- (68) Mun, T. Y.; Seon, P. G.; Kim, J. S. Production of a Producer Gas from Woody Waste via Air Gasification Using Activated Carbon and a Two-Stage Gasifier and Characterization of Tar. *Fuel* **2010**, *89* (11), 3226–3234. https://doi.org/10.1016/j.fuel.2010.05.042.
- (69) Jung, S. H.; Kim, S. J.; Kim, J. S. Characteristics of Products from Fast Pyrolysis of Fractions of Waste Square Timber and Ordinary Plywood Using a Fluidized Bed Reactor. *Bioresour. Technol.* **2012**, *114*, 670–676. https://doi.org/10.1016/j.biortech.2012.03.044.
- (70) Lyu, G.; Wu, S.; Zhang, H. Estimation and Comparison of Bio-Oil Components from Different Pyrolysis Conditions. *Front. Energy Res.* **2015**, *3* (June), 1–11. https://doi.org/10.3389/fenrg.2015.00028.
- (71) Grnli, M. A Theoretical and Experimental Study of the Thermal Degradation of Biomass, The Norwegian University of Science and Technology, 1996.
- (72) Janković, B. The Pyrolysis Process of Wood Biomass Samples under Isothermal Experimental Conditions-Energy Density Considerations: Application of the Distributed Apparent Activation Energy Model with a Mixture of Distribution Functions. *Cellulose* **2014**, *21* (4), 2285–2314. https://doi.org/10.1007/s10570-014-0263-x.
- (73) Shen, D. K.; Gu, S.; Luo, K. H.; Bridgwater, A. V.; Fang, M. X. Kinetic Study on Thermal Decomposition of Woods in Oxidative Environment. *Fuel* **2009**, *88* (6), 1024–1030. https://doi.org/10.1016/j.fuel.2008.10.034.
- (74) Chen, Z.; Hu, M.; Zhu, X.; Guo, D.; Liu, S.; Hu, Z.; Xiao, B.; Wang, J.; Laghari, M. Characteristics and Kinetic Study on Pyrolysis of Five Lignocellulosic Biomass via Thermogravimetric Analysis. *Bioresour. Technol.* **2015**, *192*, 441–450. https://doi.org/10.1016/j.biortech.2015.05.062.
- (75) Butler, E.; Devlin, G.; Meier, D.; McDonnell, K. Characterisation of Spruce, Salix, Miscanthus and Wheat Straw for Pyrolysis Applications. *Bioresour. Technol.* **2013**, *131*, 202–209. https://doi.org/10.1016/j.biortech.2012.12.013.

- (76) Burhenne, L.; Messmer, J.; Aicher, T.; Laborie, M. P. The Effect of the Biomass Components Lignin, Cellulose and Hemicellulose on TGA and Fixed Bed Pyrolysis. *J. Anal. Appl. Pyrolysis* **2013**, *101*, 177–184. https://doi.org/10.1016/j.jaap.2013.01.012.
- (77) Xu, J.; Elkamel, A.; Taqvi, S. T. H.; Liu, C.-G.; Rahimuddin, S. A.; Gull, M.; Mehmood, M. A.; Ahmad, M. S. Pyrolysis, Kinetics Analysis, Thermodynamics Parameters and Reaction Mechanism of Typha Latifolia to Evaluate Its Bioenergy Potential. *Bioresour. Technol.* **2017**, *245* (August), 491–501. https://doi.org/10.1016/j.biortech.2017.08.162.
- (78) Chen, Z.; Zhu, Q.; Wang, X.; Xiao, B.; Liu, S. Pyrolysis Behaviors and Kinetic Studies on Eucalyptus Residues Using Thermogravimetric Analysis. *Energy Convers. Manag.* **2015**, *105*, 251–259. https://doi.org/10.1016/j.enconman.2015.07.077.
- (79) Williams, C. L.; Westover, T. L.; Emerson, R. M.; Tumuluru, J. S.; Li, C. Sources of Biomass Feedstock Variability and the Potential Impact on Biofuels Production. *Bioenergy Res.* **2016**, *9* (1), 1–14. https://doi.org/10.1007/s12155-015-9694-y.
- (80) Raveendran, K.; Ganesh, A.; Khilar, K. C. Influence of Mineral Matter on Biomass Pyrolysis Characteristics. *Fuel* 1995, 74 (12), 1812–1822. https://doi.org/10.1016/0016-2361(95)80013-8.
- (81) Phanphanich, M.; Mani, S. Impact of Torrefaction on the Grindability and Fuel Characteristics of Forest Biomass. *Bioresour. Technol.* **2011**, *102* (2), 1246–1253. https://doi.org/10.1016/j.biortech.2010.08.028.
- (82) López-González, D.; Fernandez-Lopez, M.; Valverde, J. L.; Sanchez-Silva, L. Thermogravimetric-Mass Spectrometric Analysis on Combustion of Lignocellulosic Biomass. *Bioresour. Technol.* **2013**, *143*, 562–574. https://doi.org/10.1016/j.biortech.2013.06.052.
- (83) Rousset, P.; Aguiar, C.; Labbé, N.; Commandré, J. M. Enhancing the Combustible Properties of Bamboo by Torrefaction. *Bioresour. Technol.* **2011**, *102* (17), 8225–8231. https://doi.org/10.1016/j.biortech.2011.05.093.
- (84) Chen, W. H.; Hsu, H. C.; Lu, K. M.; Lee, W. J.; Lin, T. C. Thermal Pretreatment of Wood (Lauan) Block by Torrefaction and Its Influence on the Properties of the Biomass. *Energy* **2011**, *36* (5), 3012–3021. https://doi.org/10.1016/j.energy.2011.02.045.
- (85) Ramos-Carmona, S.; Martínez, J. D.; Pérez, J. F. Torrefaction of Patula Pine under Air Conditions: A Chemical and Structural Characterization. *Ind. Crops Prod.* **2018**, *118* (March), 302–310. https://doi.org/10.1016/j.indcrop.2018.03.062.
- (86) Zhou, C.; Liu, G.; Wang, X.; Qi, C. Co-Combustion of Bituminous Coal and Biomass Fuel Blends: Thermochemical Characterization, Potential Utilization and Environmental Advantage. *Bioresour. Technol.* 2016, 218, 418–427. https://doi.org/10.1016/j.biortech.2016.06.134.